



**TECHNISCHE  
UNIVERSITÄT  
WIEN**

Vienna University of Technology

## DIPLOMARBEIT

# **Sociohydrology: An Optimal Control Approach of Human-Flood Interactions**

Ausgeführt am Institut für  
Wirtschaftsmathematik  
der Technischen Universität Wien

unter der Anleitung von  
Ao.Univ.Prof. Dipl.-Ing. Dr.techn. Gernot Tragler

und der Mithilfe von  
Univ.Prof. Dipl.-Ing. Dr.techn. Alexia Fürnkranz-Prskawetz

durch  
Siegfried Langer  
Obkirchergasse 17/10  
1190 Wien

Wien, November 9, 2014

---



## Abstract

This thesis deals with the interplay between people and nature, especially with the mutual dependences and implications of people and rivers. Using a hypothetical city, which settles near a river due to economic advantages, a mathematical model is developed. This model is used to constitute the dynamics in this sociohydrological interplay.

The following work consists of three parts. Firstly, we look at a model of Di Baldassarre et al. in *Socio-hydrology: conceptualising human-flood interactions*, of which we provide an overview and reproduce the simulations. The model contains the damage due to flooding and the distance to the river. Additionally, it deals with the height of levees, which people can build, and the psychological aspect of flooding events, which is incorporated in the awareness of flood risk.

Based on this work, the second part describes the development of an optimal control model with two control and three state variables. The distance to the river, the awareness of floods, and the height of the levees are used as state variables. The control variables are the additional height of the levees and a parameter measuring the risk preference of people living in this community. We give different specifications of the functional forms and dynamics, and step by step we try to improve the model and make it more realistic.

Moreover, some preliminary steps to optimal control theory are taken. We look at a situation, where a social planner has to choose constant control variables over a finite time horizon. Additionally, we give an overview, on how this decision depends on initial conditions. Finally, we consider relative differences of the objective function, if not the best constant control is chosen.

## Zusammenfassung

Die vorliegende Diplomarbeit beschäftigt sich mit dem Zusammenspiel von Mensch und Natur, im speziellen mit den gegenseitigen Abhängigkeiten und Einflüssen der Faktoren Mensch und Wasser. Anhand einer fiktiven Stadt, welche sich aufgrund ökonomischer Vorteile in der Nähe eines Flusses ansiedelt, wird ein mathematisches Modell entwickelt. Dieses soll dazu dienen, die dynamischen Entwicklungen in diesem sogenannten soziohydrologischen Zusammenspiel möglichst gut abzubilden.

Die Arbeit besteht aus drei Teilen. Als erster Schritt wird ein Modell von Di Baldassarre et al. aus *Socio-hydrology: conceptualising human-flood interactions* erläutert, und die Simulationen aus dieser Studie werden reproduziert. Zu diesem Zweck werden Schäden durch Hochwasser modelliert sowie die Reaktion der Bewohner, die Hochwasserschutz bauen und erhöhen können. Die Stadt hat die Möglichkeit, die Distanz zum Fluss zu verändern, um den Trade-Off zwischen ökonomischen Vorteilen und dem monetären Nachteil aufgrund der Schäden durch Hochwasser entsprechend zu gestalten. Schlussendlich modellieren die Autoren hier auch eine psychologische Komponente, welche in der Erinnerung an vergangene Überflutungen enthalten ist.

Aufbauend auf diesem Modell behandelt der zweite Teil der vorliegenden Diplomarbeit die Entwicklung eines optimalen Kontrollmodells. Als Zustandsvariablen dienen die Distanz zum Fluss, die Erinnerung an vergangene Schäden und die Höhe der Dämme. Die beiden Kontrollen sind die Erhöhung der Dämme und ein Parameter, der die Risikopräferenz dieser Stadt misst. Dementsprechend handelt es sich um ein Modell mit zwei Kontrollvariablen und drei Zustandsvariablen. Es werden verschiedene Ansätze für die Dynamiken und funktionalen Zusammenhänge entwickelt und schrittweise verbessert.

Der letzte Teil der Diplomarbeit stellt eine Vorstufe zur optimalen Kontrolltheorie dar. Es wird die beste konstante Kontrolle für einen endlichen Zeithorizont bestimmt. Darauf aufbauend wird einerseits dargestellt, wie diese Entscheidungen von der Wahl der Startwerte abhängen. Andererseits geben wir einen Überblick, wie stark sich Unterschiede zum optimalen Zielfunktionswert ergeben, wenn man geringfügige Abweichungen von der optimalen Kontrolle zulässt.

## **Acknowledgements**

I want to thank my supervisor Prof. Dr. Gernot Tragler for the support and sharing his experience during this thesis. Furthermore I want to thank Prof. Dr. Alexia Fürnkranz-Prskawetz for her inputs concerning the subject and this thesis in general.

Finally I want to thank three friends of mine, Mag. Magdalena Hampl, Dipl.-Ing. Johanna Grames, and Dipl.-Ing. Lukas Richter. Each of them was very helpful for this thesis in their own way.

# Contents

<b>1</b>	<b>Introduction</b>	<b>1</b>
<b>2</b>	<b>The Model of Di Baldassarre et al.</b>	<b>3</b>
2.1	Introduction . . . . .	3
2.2	The Model . . . . .	4
2.3	Simulations . . . . .	8
<b>3</b>	<b>An Optimal Control Model</b>	<b>13</b>
3.1	Introduction . . . . .	13
3.2	The Model . . . . .	13
3.2.1	Water Levels . . . . .	13
3.2.2	Damage . . . . .	15
3.2.3	Output . . . . .	16
3.2.4	Costs . . . . .	16
3.2.5	Objective Function and Dynamics . . . . .	20
3.3	Analytical Calculations in the Uncontrolled Model . . . . .	21
3.3.1	Evolution of the State Variables . . . . .	21
3.3.2	Possible Paths of the Height $H$ . . . . .	22
3.3.3	The Jacobian of the System . . . . .	23
3.4	Simulations of the Dynamics . . . . .	25
3.4.1	The Combination of the Two Models . . . . .	25
3.4.2	Simulations of the Uncontrolled Model . . . . .	29
3.5	Summary . . . . .	35
<b>4</b>	<b>Adaptations of the Optimal Control Model</b>	<b>36</b>
4.1	Functional Forms . . . . .	36
4.1.1	Water Levels . . . . .	36
4.1.2	Damage Function . . . . .	38
4.2	Results and Simulations . . . . .	39

4.2.1	Simulations of Di Baldassarre et al. . . . .	39
4.2.2	Simulations of the Optimal Control Model . . . . .	44
<b>5</b>	<b>Preliminary Steps for Optimal Control</b>	<b>55</b>
<b>6</b>	<b>Summary and Possible Extensions</b>	<b>66</b>
6.1	Summary . . . . .	66
6.2	Possible Extensions . . . . .	67
	<b>List of Figures</b>	<b>70</b>
	<b>List of Tables</b>	<b>71</b>
	<b>References</b>	<b>72</b>

# Chapter 1

## Introduction

People have always tried to settle along rivers. There is a great number of examples of this observed behaviour. One of the best is the river Nile in Egypt, which you can see in Figure (1.1). Obviously, there is great attraction to settle along the river. A second example is the region of former Mesopotamia, where ancient cities like Babylon arose long time ago in the area of the Tigris-Euphrates river system.



Figure 1.1: The river Nile at night with Cairo at the top, see [http://commons.wikimedia.org/wiki/File:Nile\\_River\\_Delta\\_at\\_Night.JPG](http://commons.wikimedia.org/wiki/File:Nile_River_Delta_at_Night.JPG) (last accessed on 7 November 2014)

One advantage of this behaviour is the possibility to transport produced goods and commodities on the water. It also influences agriculture in a good way, because the soil close



Figure 1.2: Levees for high water levels in Grein (Austria) in 2013, see <http://images.derstandard.at/t/12/2013/06/05/1369406555724-wall.jpg> (last accessed on 7 November 2014)

to rivers tends to be more fertile. However, living in a floodplain implies the disadvantage of more or less regular flooding events, which can bring great or even total destruction of the infrastructure. So people always have to live with the trade-off between taking the risk of flooding and the will to settle near rivers for economic reasons. A possible response to lower the risk is the construction of levees, which entails negative effects as well. First of all, there are costs to build them, but more important, they make flooding events rarer, but in case of such an event more damage is caused. There are even countries, which remove at least parts of levees because of this situation.

An Austrian example can be seen in Figure (1.2), where safety can be guaranteed up to a pretty high level of water. Fortunately, in this case of 2013 the river did not get over this threshold level, but the destruction would have been enormous.

In this thesis, we want to incorporate these dynamics and dependences into a mathematical model. Di Baldassarre et al. present such a model in [1], which we summarize in Chapter 2. Based on their approach, in Chapter 3 we develop an optimal control model, which we will gradually improve in Chapter 4 in order to increase the closeness to reality. In Chapter 5 we give some preliminary steps to optimal control. The final Chapter 6 concludes by summarizing the obtained results and suggesting possible extensions of this thesis.

# Chapter 2

## The Model of Di Baldassarre et al.

### 2.1 Introduction

In the past, much effort has been put on the study of humans' reaction to flooding events, for example in [2] or even going back to 1945 in [3]. Scientists have gained good insights into the impact of these human interventions on the frequency and magnitude of flooding, as documented in [4], [5], and in [6]. Only very recently, M. Sivapalan et al. created the term *sociohydrology* in [7], which establishes a link between the mutual influences between flooding and socioeconomic conditions. In what follows, we will take a closer look at the dynamics of this socio-hydrological interplay between people and nature and how Di Baldassarre et al. investigated them mathematically in [1].

The idea is to get insights by the use of a hypothetical community, which settles down close to a river realizing economic benefits due to the location until a first flooding event occurs. At that moment, a certain awareness of the the risk of flooding emerges, people move the centre of the settlement away from the river and build levees, as illustrated in Figure (2.1). A greater distance to the river lowers the magnitude of destruction in future flooding events, the higher levees lead to a decreased frequency of such events, but with more damage once a flooding occurs. The community suffers from negative economic effects because of the greater distance, but also due to the costs caused by the construction of levees. Over time the awareness declines because people forget about past flooding events. Overall, we have many impacts on and interplay between the different parameters and variables, which are presented in a mathematical way in what follows.

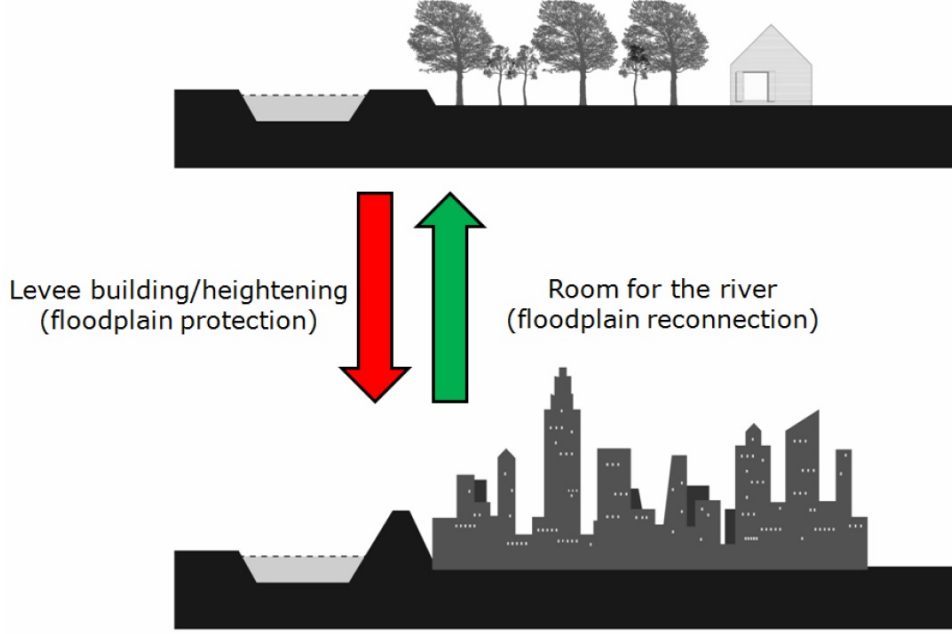


Figure 2.1: Levee building (from [8])

## 2.2 The Model

In the model of Di Baldassarre et al. there are five main variables, which can also be seen in the overview in Figure (2.3) on Page 7. There is the distance between the settlement and the river  $D$ , the size or wealth of the hypothetical community  $G$ , the height of the levees  $H$ , and the awareness of flood risk,  $M$ . In the centre of the figure, as well as of the model, there is the intensity of flooding  $F$ . The arrows in the figure show the influences of these variables on each other. The definitions and dynamics of the model in the mathematical sense will be outlined first, and then each of the arrows in Figure (2.3) will be discussed in detail.

The proportion of the damage due to flooding is defined as

$$F = \begin{cases} 1 - e^{-\frac{W + \xi_H H_-}{\alpha_H D}} & \text{if } W + \xi_H H_- > H_- , \\ 0 & \text{otherwise ,} \end{cases} \quad (2.1)$$

which takes values between 0 (no destruction) and 1 (total destruction). The water level  $W$  is exogenously given as time series in this model. In general, we will denote variables with a '-' as subscript as the values immediately before the flooding event. The height of the levees influences the actual water level  $W + \xi_H H$ , where  $\xi_H$  indicates the proportion of additional water levels because of the levees. As you can see in Figure (2.2), the river is wedged between the levees and therefore gets higher, which describes this

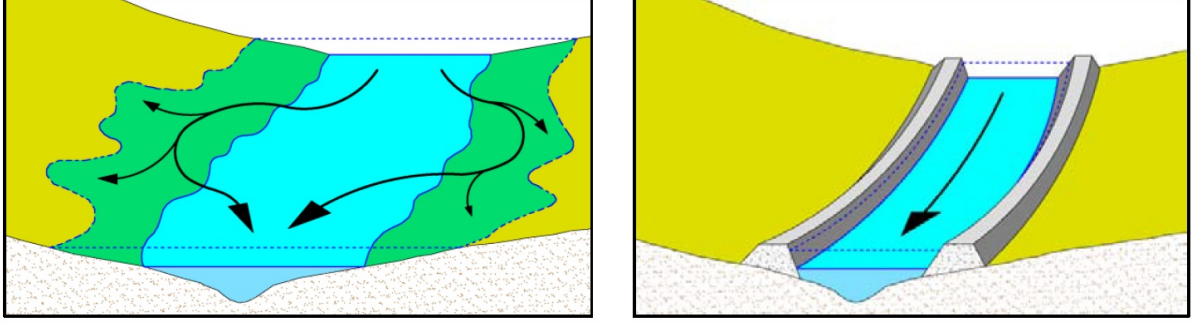


Figure 2.2: Additional height due to levees (from [8])

assumption technically. Finally, we have a topographical parameter  $\alpha_H$ , which measures the decrease in damage with increasing distance. There is no damage, if the actual water level  $W + \xi_H H_-$  is lower than the height of the levees  $H_-$ .

Now the reaction of the community in the case of flooding is investigated. Let

$$R = \begin{cases} \epsilon_T(W + \xi_H H_- - H_-) & \text{if } (F > 0) \wedge (FG_- > \gamma_E R \sqrt{G_-}) \\ & \wedge (G_- - FG_- > \gamma_E R \sqrt{G_-}), \\ 0 & \text{otherwise} \end{cases} \quad (2.2)$$

denote the additional height of levees. It depends on how much the real water was above the levees, which is the difference between  $W + \xi_H H_-$  and  $H_-$ . For example, in [9] it is shown that people take into account some safety measures, described by a safety factor  $\epsilon_T$ , which we set to 1.1.

Equation (2.2) states that we assume that people only react if three constraints are fulfilled. First, there actually has to be damage  $F > 0$  because of a flooding event. Next, in  $FG_- > \gamma_E R \sqrt{G_-}$  the right-hand side describes the costs to build levees. If the size or wealth of the economy is  $G$ , then  $\sqrt{G}$  is used as measure for the length of the border of this community. So  $R\sqrt{G_-}$  gives the vertical area of additional levees. We assume costs of  $\gamma_E$  for one unit of this area. Since  $F$  describes the proportional damage, the term  $FG_-$  denotes the damage in absolute terms due to flooding. So people only build new levees if the total construction costs are lower than the damage  $FG_-$  of the flooding event. Finally, the third condition  $G_- - FG_- > \gamma_E R \sqrt{G_-}$  indicates the fact that it has to be financially feasible for the community to build higher levees, where  $G_- - FG_-$  is the remaining wealth after the flooding event.

The next variable in the model to be discussed is the awareness of flood risk  $M$ . The

main influencing factor for awareness is the shock

$$S = \begin{cases} \alpha_S F & \text{if } R > 0, \\ F & \text{otherwise,} \end{cases} \quad (2.3)$$

which people suffer from in the case of flooding. It is assumed that if additional levees are built, the shock is dampened with a factor  $\alpha_S$  between 0, where the shock is completely removed due to building new levees, and 1, where the shock is not reduced at all. In case of no additional levees, people suffer from psychological shock of the full size of the damage  $F$ .

The dynamics of the system are described in form of four differential equations:

$$\dot{G}(t) = \rho_E \left(1 - \frac{D(t)}{\lambda_E}\right) G(t) - \Delta(\gamma(t)) \left(F(t)G(t) + \gamma_E R(t)\sqrt{G(t)}\right), \quad (2.4a)$$

$$\dot{D}(t) = \left(M(t) - \frac{D(t)}{\lambda_P}\right) \frac{\varphi_P}{\sqrt{G(t)}}, \quad (2.4b)$$

$$\dot{H}(t) = \Delta(\gamma(t))R(t) - \kappa_T H(t), \quad (2.4c)$$

$$\dot{M}(t) = \Delta(\gamma(t))S(t) - \mu_S M(t), \quad (2.4d)$$

where  $\Delta(\gamma(t))$  is 0 in times of no flooding and 1 when a flooding event happens. Note that from now on the time argument  $t$  will often be omitted for the sake of convenience.

The dynamics of  $G$  (describing the economy) in (2.4a) depends on a maximum relative growth rate  $\rho_E$ , which is lowered by the factor  $\left(1 - \frac{D}{\lambda_E}\right)$ , representing the influence of the distance on economic growth. There is a critical distance  $\lambda_E$  where the growth is exactly 0. Moving further away, even negative growth can occur. This continuous dynamic evolution is instantaneously reduced by  $FG + \gamma_E R\sqrt{G}$  in the case of flooding, which denotes the decline of  $G$  because of the damage on the one hand, and the costs to build the higher levees on the other hand.

In (2.4b) the evolution of  $D$  (describing the politics) positively depends on the awareness of the risk of flood  $M$ . Feeling more unsafe, represented by a higher value of  $M$ , people move further away from the river. However, they are also aware of the economic benefits from the river, which is contained in  $\frac{D}{\lambda_P}$ . The parameter  $\lambda_P$  can be seen as perception of risk, as it describes people's attitude in the trade-off between gaining economic benefits and avoiding damage. The remaining parameter  $\varphi_P$  is a technical one to incorporate how fast new houses can be built. Finally,  $\sqrt{G}$  in the denominator should represent the fact

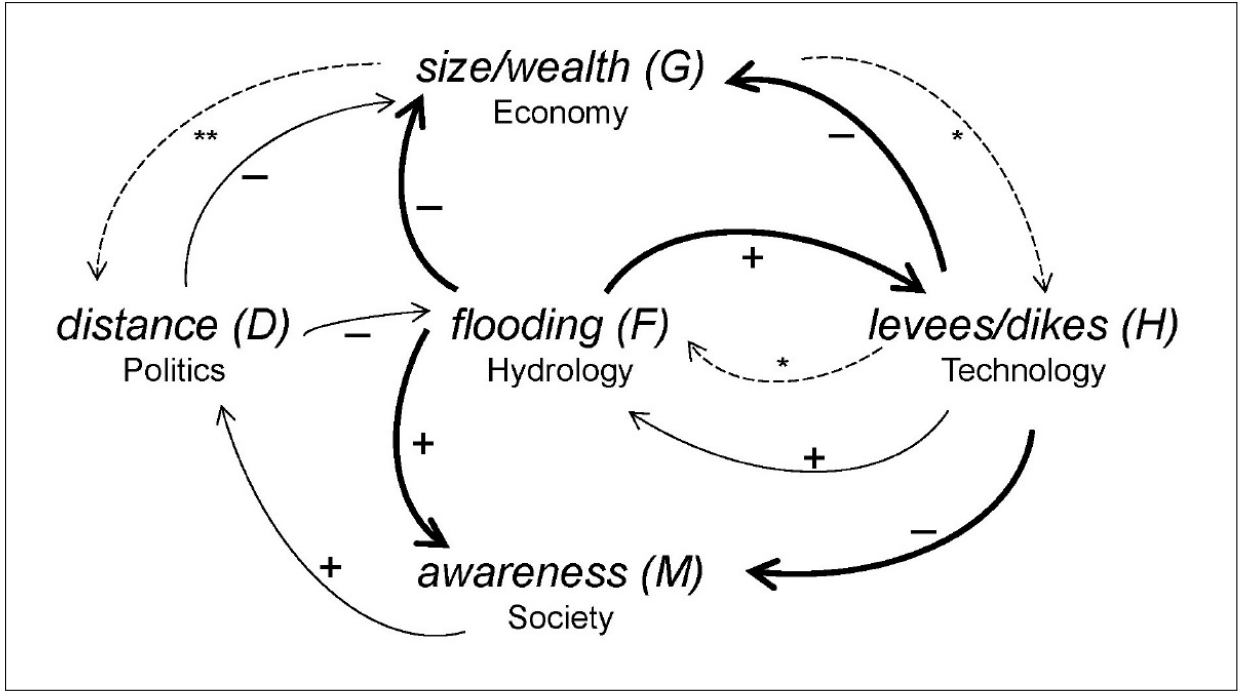


Figure 2.3: Loop diagram of the dynamics of the model in [1]

that a big economy takes longer time to be moved than a smaller one.

The height  $H$  (describing the technology) in (2.4c) is continuously lowered through decay, represented by the rate of decay  $\kappa_T$ . In case of flooding, the additional height  $R$  is added. In (2.4d), the awareness of risk  $M$  (describing the society) is on the one hand lowered by the memory loss rate  $\mu_S$ , but on the other hand instantaneously soared in the amount of the shock  $S$  in case of a flooding event.

Having presented all variables and dynamics we now can obtain a further understanding referring to Figure (2.3). Firstly, the solid thin arrows will be explained. Distance  $D$  has two outgoing arrows with '-'. One of them goes to size  $G$ , incorporating the negative connection between distance and economic growth. This can be seen in the differential equation in (2.4a). The other one goes to flooding  $F$ , because we assumed lower damage with greater distance in (2.1). The arrow from awareness  $M$  to distance  $D$  comes from (2.4b), representing the willingness to move further away with higher awareness of risk. Finally, there is one arrow with '+' from height  $H$  of the levees to flooding  $F$ , because higher levees imply higher damage in the case of flooding.

The bold solid arrows show the effects, which occur instantaneously in case of flooding. The three arrows pointing away from  $F$  illustrate that the damage through flooding

lowers the size or wealth  $G$ , but raises both the awareness  $M$  and the height of levees  $H$ . These three effects are all incorporated in the differential equations (2.4a), (2.4c), and (2.4d). A greater level of  $H$  lowers the wealth of the economy  $G$  because of the costs due to  $R$ , but it has also a reducing effect on the awareness  $M$  due to the diminished shock  $S$ .

Finally, it is harder to settle away a big community than a small one. Therefore we have a dashed arrow from size  $G$  to distance  $D$ , which can also be seen in (2.4b). A greater size of the wealth influences the height as well, because costs of  $R$  depend on  $G$ , see (2.2). The last arrow, the dashed one from height to flooding, represents, as seen in the definition of  $F$  in (2.1), that we have less flooding events, when the levees are higher.

Summing up, the model of Di Baldassare et al. in [1] contains the following functions and dynamics:

$$F = \begin{cases} 1 - e^{-\frac{W + \xi_H H_-}{\alpha_H D}} & \text{if } W + \xi_H H_- > H_- , \\ 0 & \text{otherwise ,} \end{cases}$$

$$R = \begin{cases} \epsilon_T(W + \xi_H H_- - H_-) & \text{if } (F > 0) \wedge (FG_- > \gamma_E R \sqrt{G_-}) \\ & \wedge (G_- - FG_- > \gamma_E R \sqrt{G_-}) , \\ 0 & \text{otherwise ,} \end{cases}$$

$$S = \begin{cases} \alpha_S F & \text{if } R > 0 , \\ F & \text{otherwise ,} \end{cases}$$

$$\begin{aligned} \dot{G} &= \rho_E \left(1 - \frac{D}{\lambda_E}\right) G - \Delta(\gamma(t)) (FG + \gamma_E R \sqrt{G}) , \\ \dot{D} &= \left(M - \frac{D}{\lambda_P}\right) \frac{\varphi_P}{\sqrt{G}} , \\ \dot{H} &= \Delta(\gamma(t)) R - \kappa_T H , \\ \dot{M} &= \Delta(\gamma(t)) S - \mu_S M . \end{aligned}$$

## 2.3 Simulations

In [1] the authors present a few simulations to illustrate the dynamics and outcome of their model. For this purpose they consider a hypothetical community called *Wet-*

*Town* which settles near the river *WildWaters*. At the beginning, the town has a size of  $G(0) = 10000 \text{ m}^2$  and is settled  $D(0) = 2000 \text{ m}$  away from the river. No experience of flooding events has been gained so far, nor have levees been built, which implies  $M(0) = 0$  and  $H(0) = 0$ .

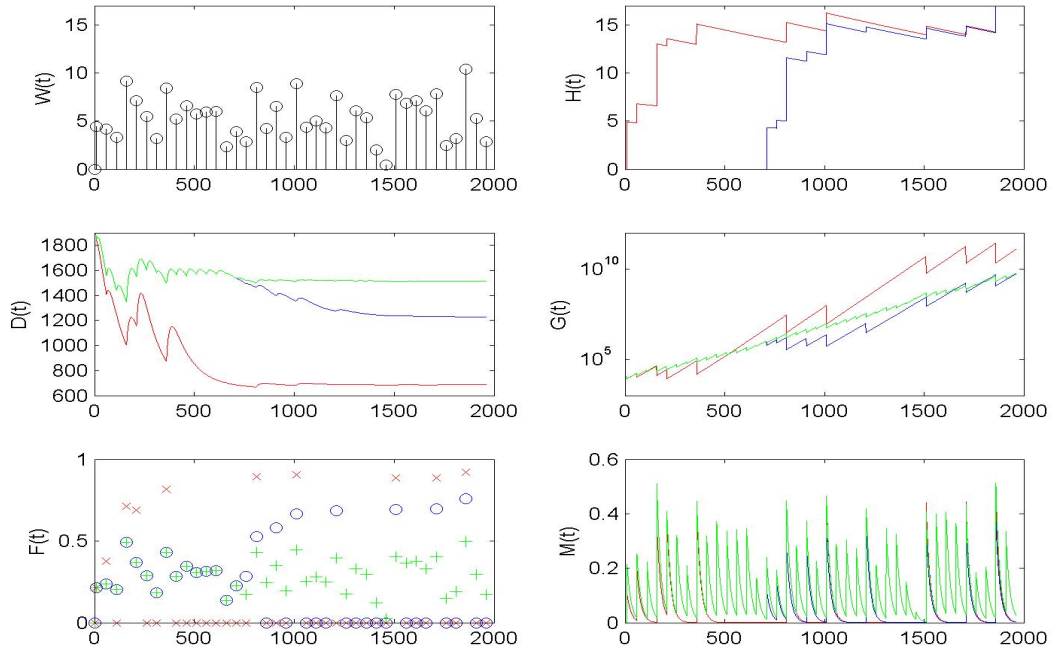
We look at both a situation with fast decay of levees ( $\kappa_T = 0.003$ ) and slow decay ( $\kappa_T = 0.0003$ ). In each of the two cases we use three values for  $\gamma_E$ , which incorporate different cost scenarios for the building of levees. All the parameters are summarized in Table (2.1). The simulations were made with the software R for statistical computing (see <http://www.r-project.org> for further information), which we reproduced with MATLAB. The data-set for the water levels  $W$  can be found in Table (2.2) and the results are shown in Figure (2.4). In Figure (2.4a) the results for low decay are shown and in Figure (2.4b) those for high decay, respectively. In each we present the three cost scenarios  $\gamma_E = 0.5$  (red),  $\gamma_E = 50$  (blue), and  $\gamma_E = 5000$  (green).

Table 2.1: Model parameters in [1]

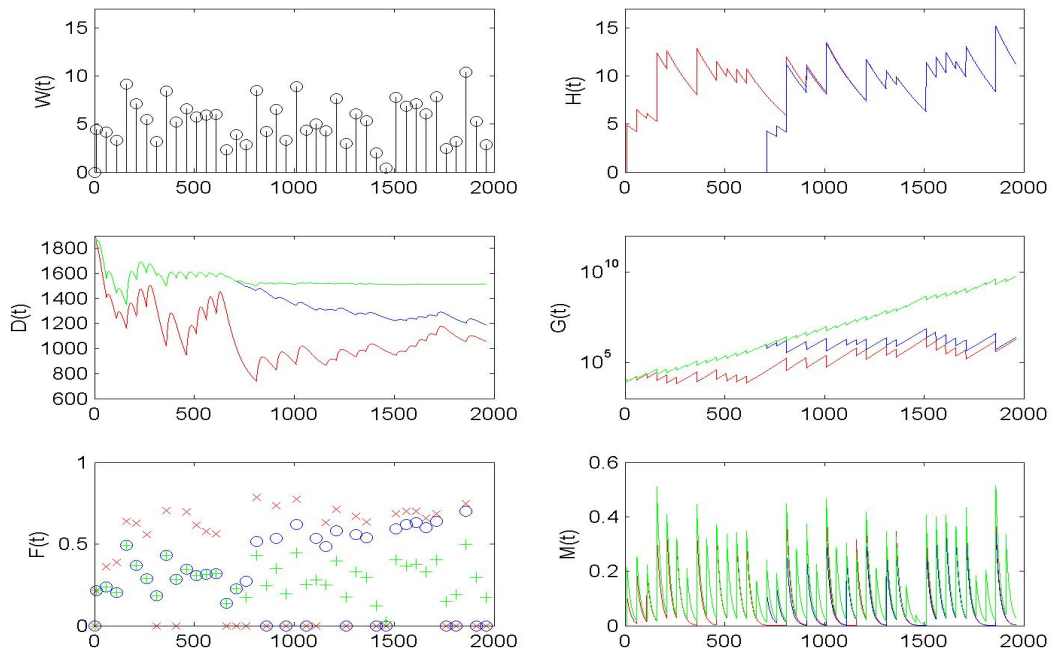
Parameter	Value
$\zeta_H$	0.5
$\alpha_H$	0.01
$\rho_E$	0.02
$\gamma_E$	0.5, 50, 5000
$\lambda_P$	12000
$\varphi_P$	10000
$\epsilon_T$	1.1
$\kappa_T$	0.0003, 0.003
$\alpha_S$	0.5
$\mu_S$	0.05
$\lambda_E$	5000

The six figures contain the water levels  $W$ , the height of the levees  $H$ , the distance  $D$ , the size  $G$ , the intensity of flooding  $F$ , and finally the awareness of risk  $M$ . The data-set contains 40 flooding events. Obviously at the given points of time we see the instantaneous changes in the graphs. Concerning the cost scenarios, in both graphs one can find the same behaviour. When the costs for levees are small (red), from the beginning on people start to build levees and settle closer to the river. The size of the community  $G$  increases continuously during periods with no flooding, but it is disturbed by the sudden setbacks due to flooding events. Because of the high levees, the town only suffers from a few flooding events, and therefore the awareness of risk  $M$  stays at a fairly moderate level.

With increased costs (blue), the starting point for building levees occurs later. This is



(a) The case of  $\kappa_T = 0.0003$



(b) The case of  $\kappa_T = 0.003$

Figure 2.4: The simulations in [1] with data set *Wevents.txt*

Table 2.2: Data-set *Wevents.txt*

$t$	10	60	110	160	210
$W(t)$	4.4513	4.2012	3.2881	9.1504	7.0966
$t$	260	310	360	410	460
$W(t)$	5.4519	3.1900	8.4174	5.1970	6.5924
$t$	510	560	610	660	710
$W(t)$	5.7604	5.9216	5.9977	2.2996	3.9348
$t$	760	810	860	910	960
$W(t)$	2.8799	8.4838	4.2616	6.5402	3.3003
$t$	1010	1060	1110	1160	1210
$W(t)$	8.8951	4.3969	4.9934	4.3163	7.6233
$t$	1260	1310	1360	1410	1460
$W(t)$	2.9636	6.0565	5.3243	1.9834	0.4061
$t$	1510	1560	1610	1660	1710
$W(t)$	7.8053	6.8754	7.1046	6.0855	7.8367
$t$	1760	1810	1860	1910	1960
$W(t)$	2.4323	3.1908	10.3746	5.2563	2.8682

the result from the fact that people cannot afford levees earlier. The decrease in distance because of the higher security due to levees starts later and it converges to a comparably higher value. Wealth  $G$  increases at a slower rate with more flooding events than in the case of lower costs. Consequently,  $M$  rises more often.

In the last case (green), where  $\gamma_E = 5000$ , we assume extremely high costs to build levees. So people do not even start to build them, therefore  $F > 0$  holds in every single point covered by the data set. As a consequence,  $D$  converges to a distance of about 1500 m (compared to 1200 m and 700 m in the other cases with relatively lower costs). When we look at the size  $G$ , there is no unique effect due to higher costs. A possible explanation is that the negative effect by the greater distance is compensated by the savings of the absence of levees. This simulation illustrates the assumption that lower levees (blue) or even no levees (green) lead to flooding more often, but with lower intensity than in the red case of high levees.

In Figure (2.4b), where greater decay of the levees is assumed, we can gain two further insights. Firstly, levees are not built up to such a high level as in Figure (2.4a) for a smaller decay. The evolution of  $G$  in the high-cost scenario seems to be relatively better compared to the other cost-scenarios. One reason could be that with the higher decay of the levees it becomes even more expensive to keep them at a certain height. So the effect

of the savings due to absence of levees is higher than before.

# Chapter 3

## An Optimal Control Model

### 3.1 Introduction

The model presented in the previous chapter is the basis for an optimization model. Different to Di Baldassarre et al. in [1], where  $W$  enters the model as an input factor in a stochastic way, in the following, the water levels will be modelled as a deterministic function. Some of the other functions and dynamics will be rather similar to that in [1]. Where mathematically necessary, new variables and functions will be introduced. The goal of this chapter is to build up an optimal control problem, where the stream of the sum of damages and the costs of building levees is minimized over some planning horizon. For that purpose, two control variables will be used. Firstly, it is assumed that people are able to choose the additional height of levees, which is defined as  $v$ . As a second control variable we use the perception of risk  $\lambda_P$  in (2.4b), in the following denoted by  $u$ .

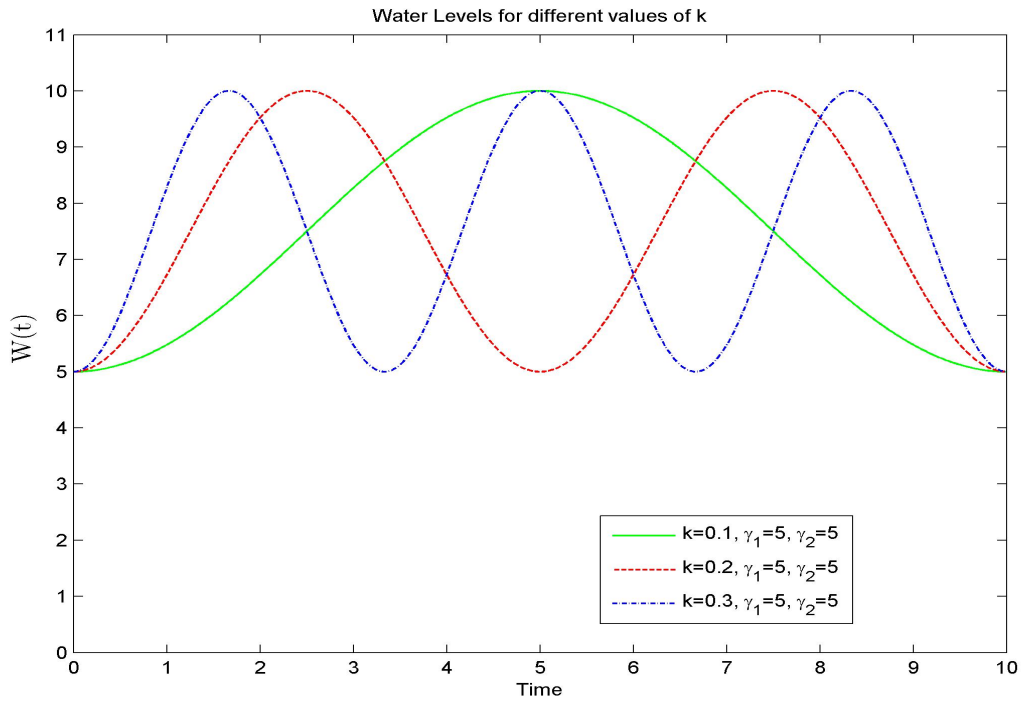
### 3.2 The Model

#### 3.2.1 Water Levels

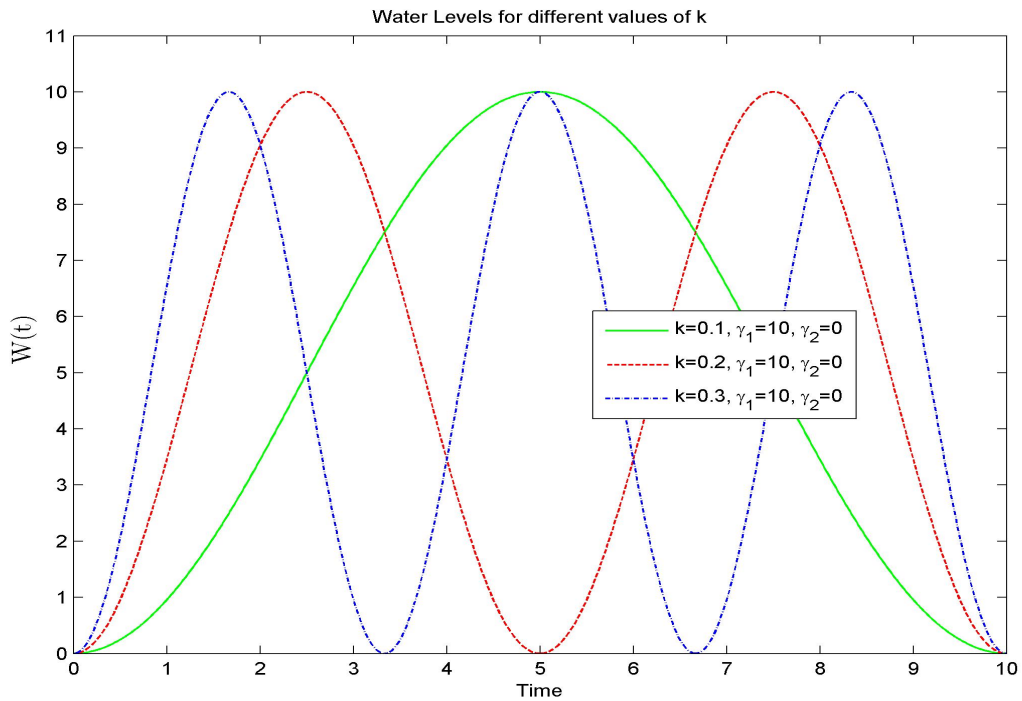
Let  $W$  be the exogenously given fluctuating water levels that are assumed to follow the deterministic time-dependent function

$$W(t) = \gamma_1 \sin^2(kt\pi) + \gamma_2. \quad (3.1)$$

The period length of the fluctuations is described by  $k$ , the minimum water level is  $\gamma_2$ , and the maximum level is  $\gamma_1 + \gamma_2$ . Two examples for this function are illustrated in Figure (3.1).



(a)  $(\gamma_1, \gamma_2) = (5, 5)$



(b)  $(\gamma_1, \gamma_2) = (10, 0)$

Figure 3.1: Water levels  $W(t)$  for  $k = 0.1, 0.2, 0.3$  for two different sets of minimum and maximum water levels

### 3.2.2 Damage

Di Baldassarre et al. defined the damage in [1] by

$$F = \begin{cases} 1 - e^{-\frac{W + \xi_H H_-}{\alpha_H D}} & \text{if } W + \xi_H H_- > H_-, \\ 0 & \text{otherwise} \end{cases}$$

with the height of the levees  $H_-$  immediately before a flooding event and the distance of the settlement to the river  $D$  (cf. (2.1)). The actual water level is  $W + \xi_H H_-$  and therefore higher than the water level  $W$  due to the presence of levees, where  $\xi_H$  is the exacerbation parameter. The parameter  $\alpha_H$  measures the decrease in damage for increasing distance. On the one hand, we want to maintain the fact that there is only damage if  $W + \xi_H H_- > H_-$  holds. On the other hand, for the analysis afterwards continuity and differentiability are required. So the idea is to define a continuous and differentiable function which has its inflection point at  $(1 - \xi_H)H$  and is convex before and concave after this inflection point.

We adopt the approach

$$f(x) = \frac{x^2}{ax^2 + b}$$

with the derivatives  $f'(x) = \frac{2bx}{(ax^2 + b)^2}$  and  $f''(x) = \frac{2b(b - 3ax^2)}{(ax^2 + b)^3}$ , implying  $f(0) = f'(0) = 0$ . For the (positive) inflection point  $\tilde{x}$  we conclude that

$$f''(\tilde{x}) = 0 \Leftrightarrow \tilde{x} = \sqrt{\frac{b}{3a}}.$$

This implies  $f(\tilde{x}) = \frac{1}{4a}$ ,  $f'(\tilde{x}) = \frac{3\sqrt{3}}{8\sqrt{ab}}$ , and  $\lim_{x \rightarrow \infty} f(x) = \frac{1}{a}$ .

With this approach,  $f(x)$  is a continuous S-shaped function, which convexly approaches its inflection point and then converges concavely to its asymptote at  $\frac{1}{a}$ . Keeping in mind the fact that  $(1 - \xi_H)H$  should be the inflection point,  $\sqrt{\frac{b}{3a}} = (1 - \xi_H)H$  has to hold, which leads to  $b = 3a(1 - \xi_H)^2 H^2$ .

Inserting all this information into the initial approach for  $f(x)$  and renaming the variables, the result is

$$\tilde{F}(W, H) = \frac{W^2}{aW^2 + b} = \frac{W^2}{a[W^2 + 3(1 - \xi_H)^2 H^2]}.$$

For simplicity, but also for the asymptote to be 1, we set  $a = 1$ . Assuming exponentially decreasing damage  $F$  in distance  $D$  we define

$$F(W, H, D) = \frac{W^2}{W^2 + 3(1 - \xi_H)^2 H^2} \cdot \exp(-\alpha_H D), \quad (3.2)$$

which is a both continuous and differentiable approximation for the damage function used by Di Baldassarre et al. in [1]. We provide examples of  $F(W, H, D)$  expressing them as functions of the water levels  $W$  in Figure (3.2) and of time  $t$  in Figure (3.3), for several parameter sets.

### 3.2.3 Output

We define the output of the economy as

$$Y = (1 - \beta F) \left( \frac{D}{\lambda_E} \right)^{-\alpha_Y}, \quad (3.3)$$

which is qualitatively different to the formulation of [1]. While Di Baldassarre et al. modelled the change of the size  $G$  by

$$\dot{G} = \rho_E \left( 1 - \frac{D}{\lambda_E} \right) G - \Delta(\gamma(t)) (FG + \gamma_E R \sqrt{G})$$

in the form of a differential equation, see (2.4a), here we use a function for the output  $Y$ . We assume that the distance  $D$  is the input factor for the production function and  $\lambda_E$  measures the importance of the river for the economy. A higher  $\lambda_E$ , therefore, means that the river is more important for the settlement than otherwise. Moreover, the production is lowered due to the damages of flooding events, which is contained in the factor  $(1 - \beta F)$ . Here  $\beta$  is a parameter between 0 and 1, which describes the intensity of the influence of flooding events on production. If the economy was more service-orientated, there would be a lower  $\beta$  than for an economy which mainly produces, for example, agricultural goods.

### 3.2.4 Costs

We present three different specifications for the cost function. The first two are proposed by Chahim et al. in [10], where the authors use an impulse control approach to dike height optimization. Depending on the actual height  $h$  and the additional height  $v$ , an

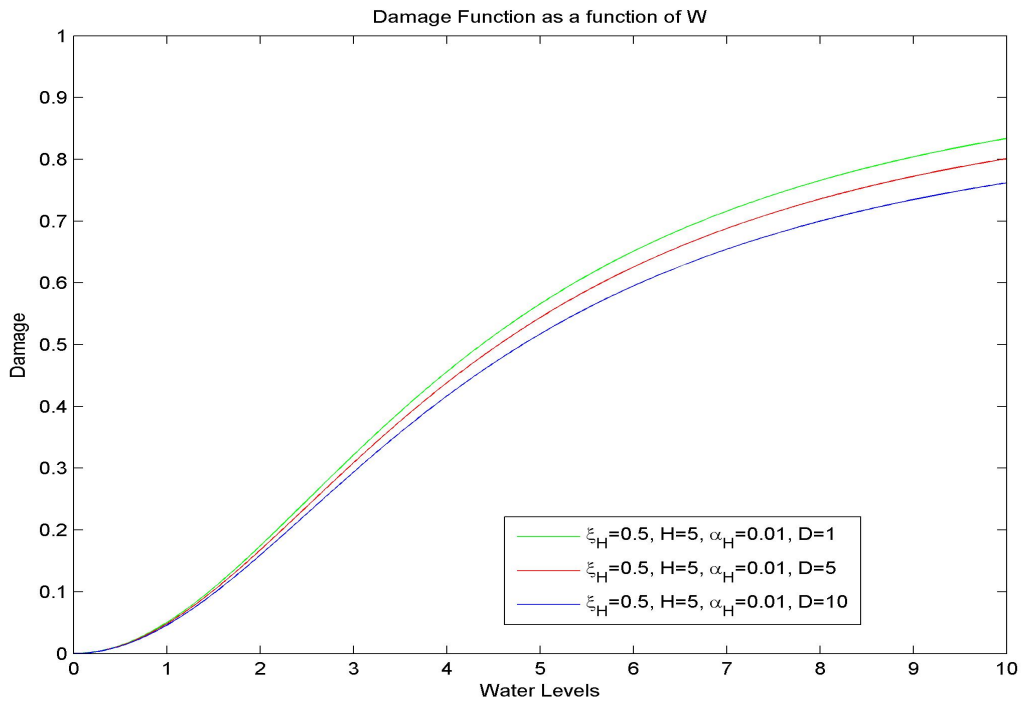
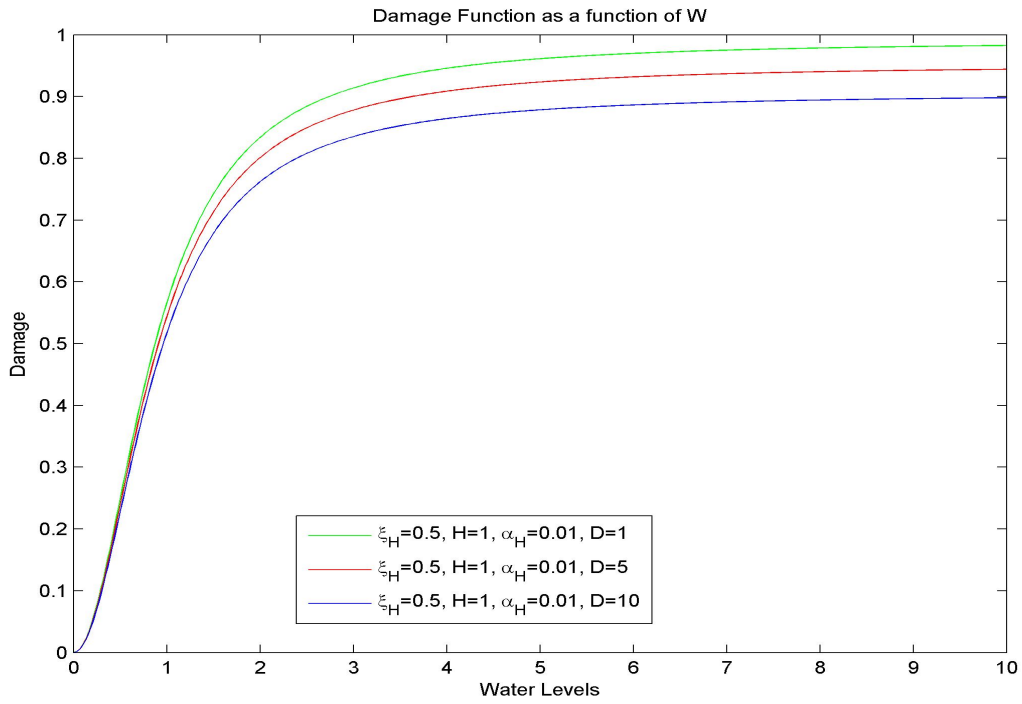
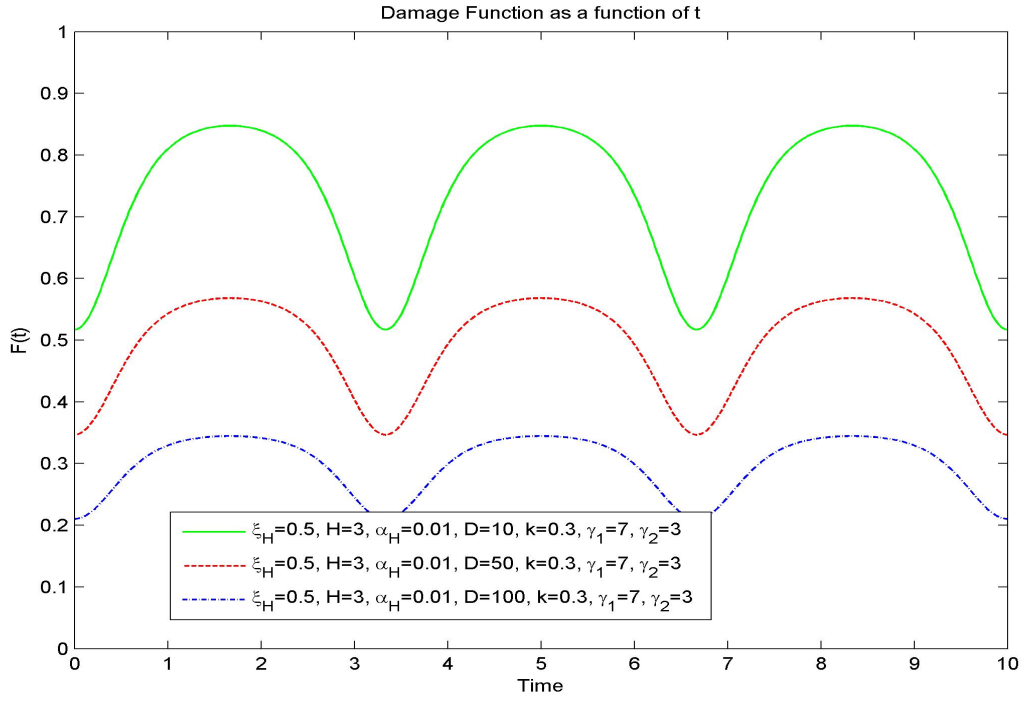
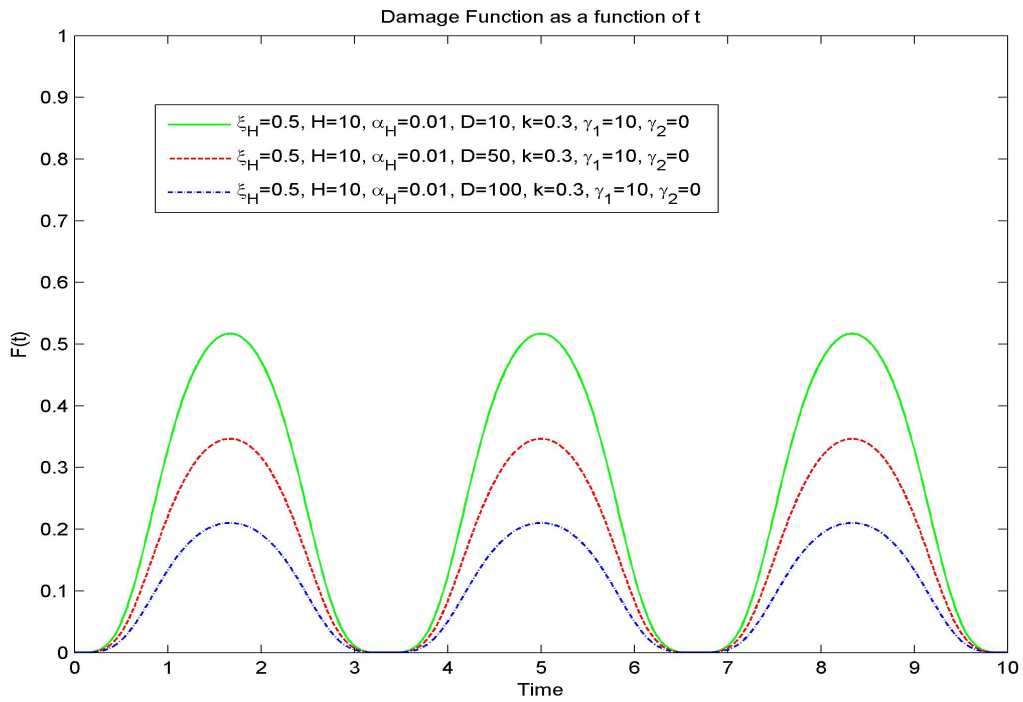


Figure 3.2: Damage  $F(W)$  for  $(\alpha_H, \zeta_H) = (0.01, 0.5)$  for  $H = 1$  and  $H = 5$  for different values of  $D$



(a)  $(\gamma_1, \gamma_2, H) = (7, 3, 3)$



(b)  $(\gamma_1, \gamma_2, H) = (10, 0, 10)$

Figure 3.3: Damage  $F(t)$  for different sets of parameters

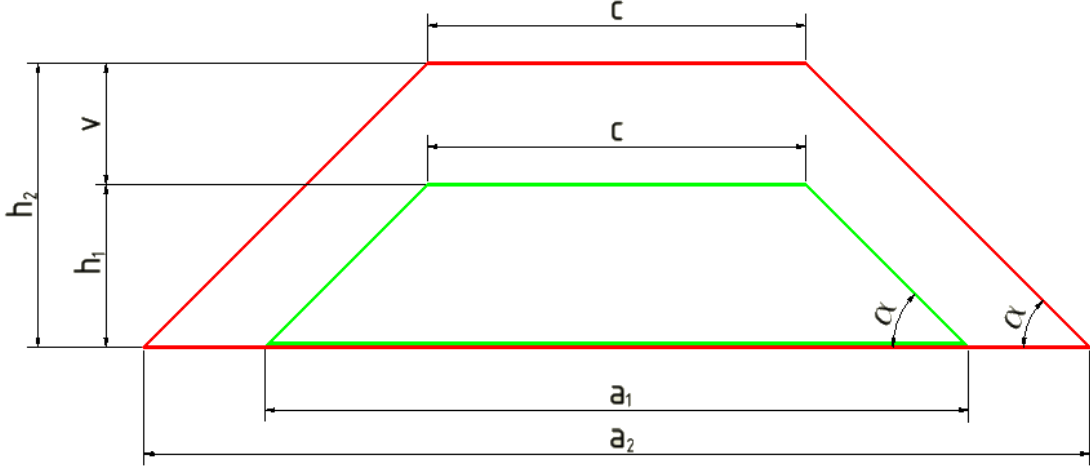


Figure 3.4: Adding height  $v$  to the levees

exponential form

$$C_1(h, v) = \begin{cases} (c_0 + b_0 v) e^{a_0(h+v)} & \text{for } v > 0, \\ 0 & \text{for } v = 0 \end{cases} \quad (3.4)$$

with positive constants  $a_0$ ,  $b_0$ ,  $c_0$ , and quadratic costs in the form of

$$C_2(h, v) = \begin{cases} a_1(h+v)^2 + b_1 v + c_1 & \text{for } v > 0, \\ 0 & \text{for } v = 0 \end{cases} \quad (3.5)$$

are considered, where again  $a_1$ ,  $b_1$ ,  $c_1$  are positive constants.

Later on, when we formulate the optimal control model where the costs are contained in the objective function, we will better understand the disadvantage of these two formulations because of the inherent discontinuity in  $v$ . Therefore we consider a third form based on the geometrical representation in Figure (3.4).

Assuming that the costs are proportional to the cross sectional area of the levees, we calculate the difference between the green trapezoid before and the red one after the heightening of the levees. We assume that the angle  $\alpha$  at the bottom and the length at the top of the levees  $c$  stay constant because of technical issues. Focusing on the triangles in the right corner of the two trapezoids, we get  $\tan(\alpha) = \frac{2h_1}{a_1 - c}$  and  $\tan(\alpha) = \frac{2h_2}{a_2 - c}$ ,

respectively. As a result we obtain

$$a_2 = \frac{(h_1 + v)(a_1 - c)}{h_1} + c,$$

$$a_1 = \frac{2h_1}{\tan(\alpha)} + c.$$

The difference of the cross sectional areas,  $A_1$  and  $A_2$ , used as a measure for the costs, is then calculated by

$$\begin{aligned} A_2 - A_1 &= \frac{(a_2 + c)h_2}{2} - \frac{(a_1 + c)h_1}{2} \\ &= \frac{\left(\frac{(h_1+v)(a_1-c)}{h_1} + c + c\right)(h_1 + v)}{2} - \frac{a_1 h_1 + c h_1}{2} \\ &= \frac{(h_1 a_1 - h_1 c + v a_1 - c v + 2 c h_1)(h_1 + v) - a_1 h_1^2 - c h_1^2}{2 h_1} \\ &= \frac{1}{2 h_1} (2 a_1 h_1 v + a_1 v^2 - c v^2) \\ &= \left(\frac{2 h_1}{\tan(\alpha)} + c\right) v + \frac{v^2}{2 h_1} \left(\frac{2 h_1}{\tan(\alpha)} + c - c\right) \\ &= \left(\frac{2 h_1}{\tan(\alpha)} + c\right) v + \frac{v^2}{\tan(\alpha)}. \end{aligned}$$

For convenience, we assume  $\alpha = 45^\circ$ , which implies  $\tan(\alpha) = 1$ , which finally leads to the cost function

$$C_3(h, v) = 2 h v + c v + v^2. \quad (3.6)$$

Contrary to (3.4) and (3.5), this cost function is continuous and differentiable, which is necessary for solving an optimal control problem.

### 3.2.5 Objective Function and Dynamics

Finally, we formulate an optimal control model by

$$\min_{u, v} \int_0^\infty e^{-rt} (\rho F(W, H, D) + C(H, v)) dt \quad (3.7)$$

$$\text{s.t.} \quad \dot{D} = \left(M - \frac{D}{u}\right) \frac{\varphi_p}{\sqrt{Y}}, \quad (3.8)$$

$$\dot{M} = \alpha F - \mu_M M, \quad (3.9)$$

$$\dot{H} = v - \mu_H H. \quad (3.10)$$

The objective function (3.7) contains the damage  $F(W, H, D)$  and the costs  $C(H, v)$  to build new levees. Costs do not only depend on the additional height  $v$ , but also on the actual height  $H$ . Technically, a bigger basement is needed for the levees if they already have a greater height. Mathematically, not only  $\frac{\partial C(H, v)}{\partial v} > 0$  but also  $\frac{\partial C(H, v)}{\partial H} > 0$  holds. The parameter  $\rho$  represents the weight of damage in the objective function, and finally we use a discount rate  $r$ . People have to decide about risk-taking  $u$  and how much to increase the height of the levees  $v$  to maximize the discounted present value of future damage and costs.

Distance depends on the awareness of floods  $M$ , reduced by  $\frac{D}{u}$ , where  $u$  is a control parameter representing the risk attitude of society. A higher value of  $u$  implies less risk taking of the economy, since the distance to the river will be reduced to a lesser extent. With  $\varphi_P$ , we again include a technical parameter to measure how fast new houses can be built. We also take into account that a larger economy is harder to move, so we have  $\sqrt{Y}$  in the denominator. The change in memory or awareness  $M$  depends positively on the damage  $F$ , where  $\alpha$  is the same reducing parameter as in the shock function of [1], lowered by forgetting at the rate  $\mu_M$ . Finally, the height  $H$  increases by the control variable  $v$ , which is the additional height, and decreases by the decay rate  $\mu_H$ , respectively.

### 3.3 Analytical Calculations in the Uncontrolled Model

#### 3.3.1 Evolution of the State Variables

In this section we take a closer look at the system of differential equations (3.8)-(3.10), which is given by

$$\begin{aligned}\dot{D} &= \left(M - \frac{D}{u}\right) \frac{\varphi_p}{\sqrt{Y}}, \\ \dot{M} &= \alpha F - \mu_M M, \\ \dot{H} &= v - \mu_H H.\end{aligned}$$

Taking into account the definitions of  $W$ ,  $Y$ , and  $F$ , we obtain the system

$$\begin{aligned}\dot{D} &= \left(M - \frac{D}{u}\right) \frac{\varphi_p}{\sqrt{\left[1 - \beta \frac{W^2}{W^2 + 3(1 - \xi_H)^2 H^2} \cdot \exp(-\alpha_H D)\right] \left(\frac{D}{\lambda_E}\right)^{-\alpha}}}, \\ \dot{M} &= \alpha \frac{W^2}{W^2 + 3(1 - \xi_H)^2 H^2} \cdot \exp(-\alpha_H D) - \mu_M M, \\ \dot{H} &= v - \mu_H H.\end{aligned}$$

To get a first insight, we will consider the uncontrolled model. For that purpose, we let the two control variables, namely the additional height of levees  $v$  and the social risk parameter  $u$ , be exogenously given and constant, and we set the three differential equations to zero to get equilibrium points. From the third equation we then easily get  $H^* = \frac{v}{\mu_H}$ , which we can insert into the other two equations. Since  $\varphi_P \neq 0$ , obviously  $D = uM$  is necessary for  $\dot{D} = 0$  to hold. Putting all these expressions together into the second equation, we get

$$0 = \alpha \frac{W^2}{W^2 + 3(1 - \xi_H)^2 \left(\frac{v}{\mu_h}\right)^2} \cdot \exp(-\alpha_H u M) - \mu_M M.$$

It is important to notice that the water level  $W$  depends on time  $t$ . Hence, in general the solution  $M^*$  will be no equilibrium point, because it fluctuates over time. We could speak of an equilibrium function  $M^*(t)$ , and since  $D^*(t) = uM^*(t)$ , also  $D^*(t)$  will behave in a similar manner.

Thus, in the uncontrolled model an equilibrium will be represented by a triple  $(D^*(t), M^*(t), H^*)$ , where  $H^*$  is an equilibrium point and both  $D^*$  and  $M^*$  are some kind of equilibrium functions. This behaviour can be seen in the simulations in the following section.

### 3.3.2 Possible Paths of the Height $H$

Now we look at Equation (3.10), which is the linear differential equation

$$\dot{H} = v - \mu_H H$$

with constant coefficients. Reformulating to  $\dot{H} + \mu_H H = v$  yields the standard form. The general solution of the homogeneous equation and the particular integral are, respectively,

$$\begin{aligned} H_{hom}(t) &= C \cdot e^{-\mu_H t}, \text{ where } C \in \mathbb{R}^+, \\ H_{part}(t) &= \frac{v}{\mu_H}, \end{aligned}$$

where the latter is computed with the method of variation of parameters. Therefore the general solution  $H(t) = H_{hom}(t) + H_{part}(t)$ , after inserting  $H(0) = H_0$ , is

$$H(t) = \frac{v}{\mu_H} + \left(H_0 - \frac{v}{\mu_H}\right) e^{-\mu_H t}.$$

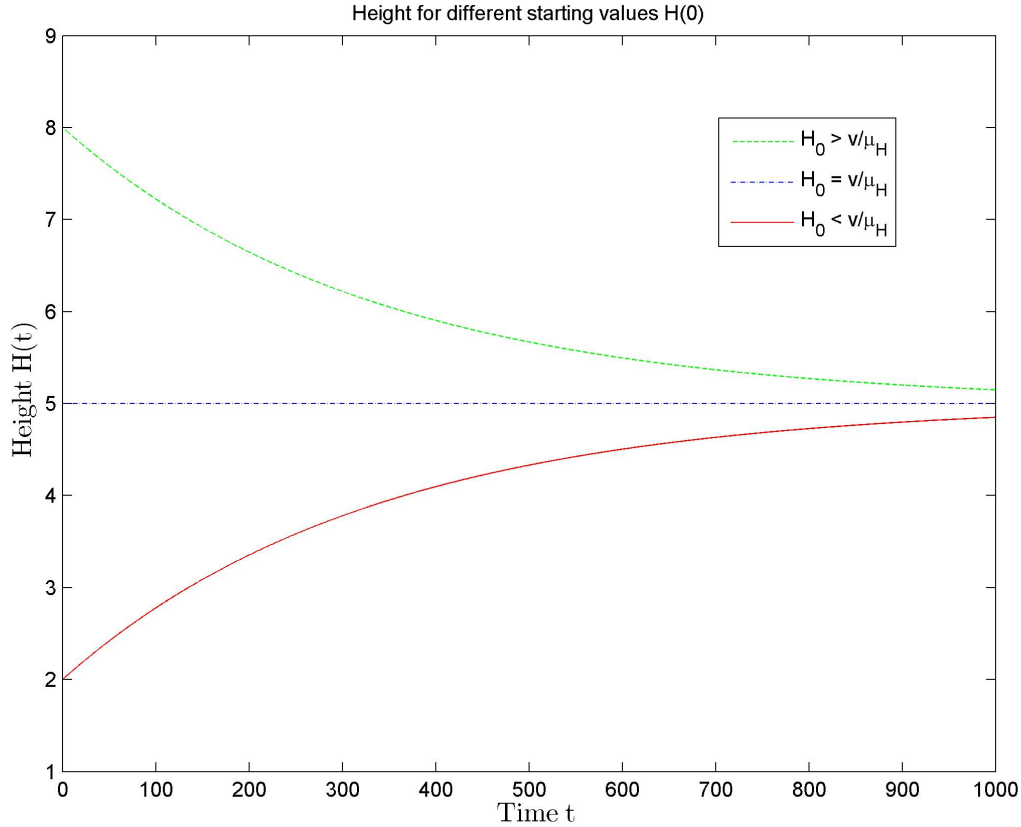


Figure 3.5: The evolution of  $H(t)$

In general,  $H(t)$  converges to  $\frac{v}{\mu_H}$ , and there are three cases for the evolution of  $H(t)$ :

$$\begin{aligned}
 H_0 > \frac{v}{\mu_H} &\Rightarrow \text{exponentially decreasing to } \frac{v}{\mu_H}, \\
 H_0 = \frac{v}{\mu_H} &\Rightarrow \text{constant at } \frac{v}{\mu_H}, \\
 H_0 < \frac{v}{\mu_H} &\Rightarrow \text{exponentially increasing to } \frac{v}{\mu_H}.
 \end{aligned}$$

Graphical presentations of these functions with  $v = 0.015$  and  $\mu_H = 0.003$  (these values are also used for simulations in the following chapters) are given in Figure (3.5).

### 3.3.3 The Jacobian of the System

For future work, the calculations of the Jacobian for the system of differential equations are outlined. Using the notation  $Y = Y(F) = Y(F(W, H, D))$  in Equations (3.8)-(3.10), the system of differential equations

$$\begin{aligned}
\dot{D} &= \left(M - \frac{D}{u}\right) \frac{\varphi_P}{\sqrt{Y(F(W, H, D))}}, \\
\dot{M} &= \alpha F(W, H, D) - \mu_M M, \\
\dot{H} &= v - \mu_H H
\end{aligned}$$

is given in a more compact way. The components of the Jacobian

$$J = \begin{pmatrix} \frac{\partial \dot{D}}{\partial D} & \frac{\partial \dot{D}}{\partial M} & \frac{\partial \dot{D}}{\partial H} \\ \frac{\partial \dot{M}}{\partial D} & \frac{\partial \dot{M}}{\partial M} & \frac{\partial \dot{M}}{\partial H} \\ \frac{\partial \dot{H}}{\partial D} & \frac{\partial \dot{H}}{\partial M} & \frac{\partial \dot{H}}{\partial H} \end{pmatrix}$$

are calculated as

$$\begin{aligned}
\frac{\partial \dot{D}}{\partial D} &= -\left(M - \frac{D}{u}\right) \cdot \frac{\varphi_P}{2 \cdot \sqrt{Y(F(W, H, D))}^3} \cdot \frac{\partial Y(F(W, H, D))}{\partial F(W, H, D)} \cdot \frac{\partial F(W, H, D)}{\partial D} \\
&\quad - \frac{\varphi_P}{u \cdot \sqrt{Y(F(W, H, D))}}, \\
\frac{\partial \dot{D}}{\partial M} &= \frac{\varphi_P}{\sqrt{Y(F(W, H, D))}}, \\
\frac{\partial \dot{D}}{\partial H} &= -\left(M - \frac{D}{u}\right) \cdot \frac{\varphi_P}{2 \cdot \sqrt{Y(F(W, H, D))}^3} \cdot \frac{\partial Y(F(W, H, D))}{\partial F(W, H, D)} \cdot \frac{\partial F(W, H, D)}{\partial H}, \\
\frac{\partial \dot{M}}{\partial D} &= \alpha \cdot \frac{\partial F(W, H, D)}{\partial D}, \\
\frac{\partial \dot{M}}{\partial M} &= -\mu_M, \\
\frac{\partial \dot{M}}{\partial H} &= \alpha \cdot \frac{\partial F(W, H, D)}{\partial H}, \\
\frac{\partial \dot{H}}{\partial D} &= 0, \\
\frac{\partial \dot{H}}{\partial M} &= 0, \\
\frac{\partial \dot{H}}{\partial H} &= -\mu_H.
\end{aligned}$$

In an equilibrium with  $\dot{H} = 0$  we have  $H^* = \frac{v}{\mu_H}$ . Using  $\dot{D} = 0$  it follows that  $D^* = u \cdot M^*$ . In this case  $(M - \frac{D}{u}) = 0$  holds and for the remaining Jacobian

$$J_{equ} = \begin{pmatrix} -\frac{\varphi_P}{u \cdot \sqrt{Y(F(W,H,D))}} & \frac{\varphi_P}{\sqrt{Y(F(W,H,D))}} & 0 \\ \alpha \cdot \frac{\partial F(W,H,D)}{\partial D} & -\mu_M & \alpha \cdot \frac{\partial F(W,H,D)}{\partial H} \\ 0 & 0 & -\mu_H \end{pmatrix}$$

we can compute the leading principal minors

$$\begin{aligned} \Delta_1 &= -\frac{\varphi_P}{u \cdot \sqrt{Y(F(W,H,D))}} < 0, \\ \Delta_2 &= \frac{\varphi_P}{u \cdot \sqrt{Y(F(W,H,D))}} \cdot \mu_M - \frac{\varphi_P}{\sqrt{Y(F(W,H,D))}} \cdot \alpha \cdot \frac{\partial F(W,H,D)}{\partial D} > 0, \\ \Delta_3 &= \Delta_2 \cdot (-\mu_H) < 0. \end{aligned}$$

Because of the fact that  $\frac{\partial F(W,H,D)}{\partial D} < 0$ , these leading principal minors are alternating with  $\Delta_1 < 0$ , and hence the Jacobian is negative definite. As the trace of the Jacobian is negative, all the eigenvalues are negative, too. As a result, all equilibria of this system are stable.

## 3.4 Simulations of the Dynamics

### 3.4.1 The Combination of the Two Models

In this section we want to find out, how the model of Di Baldassarre et al. in [1] reacts if we use (3.1) as water function. So we look at

$$\begin{aligned} F &= \begin{cases} 1 - e^{-\frac{W + \xi_H H_-}{\alpha_H D}} & \text{if } W + \xi_H H_- > H_-, \\ 0 & \text{otherwise,} \end{cases} \\ R &= \begin{cases} \epsilon_T (W + \xi_H H_- - H_-) & \text{if } (F > 0) \wedge (FG_- > \gamma_E R \sqrt{G_-}) \\ & \wedge (G_- - FG_- > \gamma_E R \sqrt{G_-}), \\ 0 & \text{otherwise,} \end{cases} \\ S &= \begin{cases} \alpha_S F & \text{if } R > 0, \\ F & \text{otherwise,} \end{cases} \end{aligned}$$

$$\begin{aligned}
\dot{G} &= \rho_E \left(1 - \frac{D}{\lambda_E}\right) G - \Delta(\gamma(t)) (FG + \gamma_E R \sqrt{G}), \\
\dot{D} &= \left(M - \frac{D}{\lambda_P}\right) \frac{\varphi_P}{\sqrt{G}}, \\
\dot{H} &= \Delta(\gamma(t)) R - \kappa_T H, \\
\dot{M} &= \Delta(\gamma(t)) S - \mu_S M,
\end{aligned}$$

with

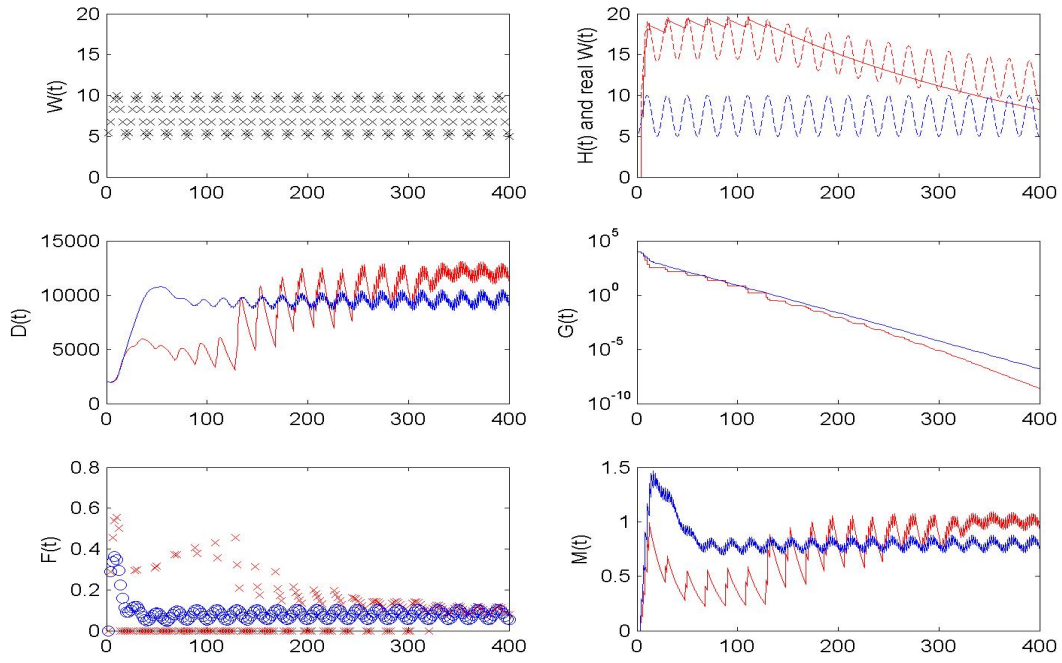
$$W(t) = \gamma_1 \sin^2(kt\pi) + \gamma_2,$$

and run the simulations as in [1].

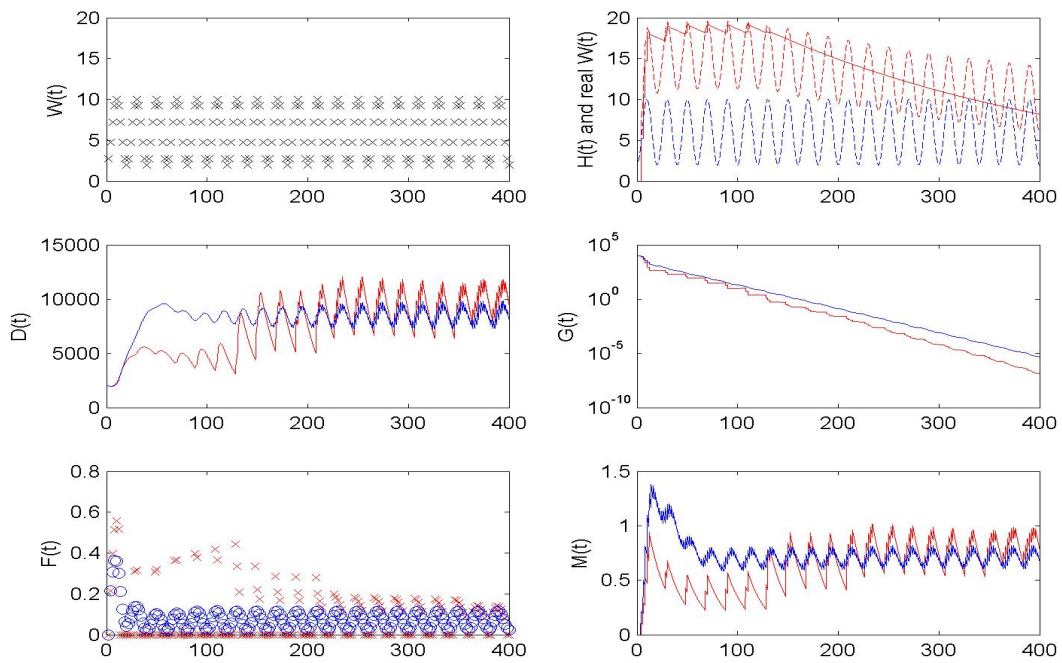
For a few different sets of  $(\gamma_1, \gamma_2, k)$  the results are shown in what follows. To get a better understanding we additionally plot the real water levels  $W + \zeta_H H$  as dashed lines in the top right figure with the height of the levees. We omit the green case, because it gives exactly the same results as the blue case. So the only difference to the parameter set before is that we only look at  $\gamma_E = 0.5$  in red and  $\gamma_E = 50$  in blue. In Figure (3.6) and Figure (3.7) we present results for fast ( $\kappa_T = 0.003$ ) and slow decay ( $\kappa_T = 0.0003$ ), respectively. In both cases the water levels fluctuate between 5 and 10 at the top and between 2 and 10 at the bottom.

Firstly, we examine the case in blue, which represents the case with high costs at  $\gamma_E = 50$ . In all of the four plots, the line for the height does not even move a single time, so there are never levees built. As a consequence, the real water levels  $W + \zeta_H \cdot H$  behave exactly like the water levels  $W$ . After a period of adaption in the beginning the distance oscillates around 10000 m, while  $M$  fluctuates around 0.75. Since no levees are built and therefore  $W + \zeta_H \cdot H > H$  always holds,  $F$  shows qualitatively the same behaviour as the water levels and is positive all the time. The economy decreases continuously with the same rate, since  $G$  is approximately a line in the plot with logarithmic scale.

The red case shows a few differences. People begin to build levees from the beginning on, and after a short period of adaption, the height reaches its peak at nearly 20 m. In the case of high  $\kappa_T$  in Figure (3.6), after about 100 years the height begins to fall. One possible reason could be that people cannot afford the maintaining costs of the levees due to the falling wealth  $G$ . In consequence, they move away from the river and  $D$  rises. Lower levees lead to more regular but less intensive flooding events, which is seen in the evolution of  $F$ . Almost the same happens if we switch to a lower rate of decay in

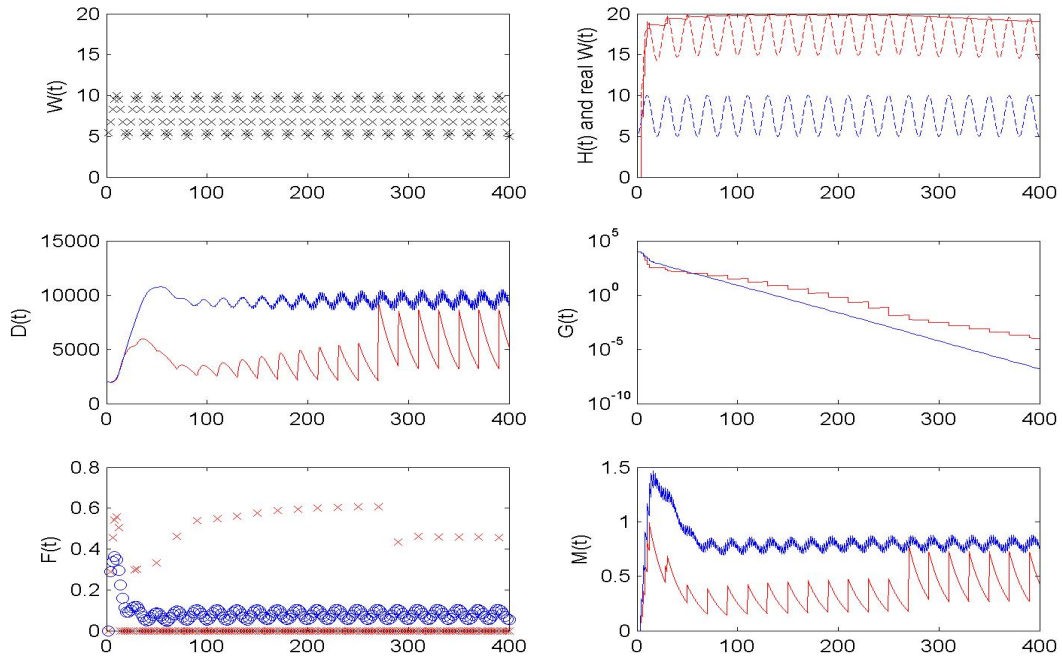


(a)  $(\gamma_1, \gamma_2, k) = (5, 5, 0.05)$

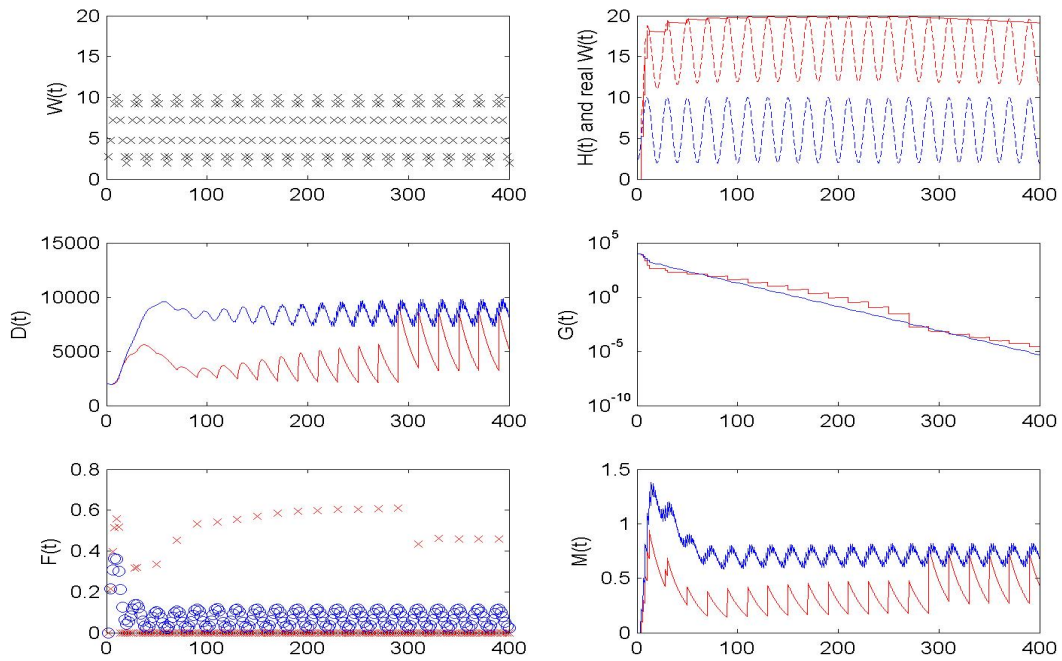


(b)  $(\gamma_1, \gamma_2, k) = (8, 2, 0.05)$

Figure 3.6: The simulations with  $W(t) = \gamma_1 \sin^2(kt\pi) + \gamma_2$  and  $\kappa_T = 0.003$



(a)  $(\gamma_1, \gamma_2, k) = (5, 5, 0.05)$



(b)  $(\gamma_1, \gamma_2, k) = (8, 2, 0.05)$

Figure 3.7: The simulations with  $W(t) = \gamma_1 \sin^2(kt\pi) + \gamma_2$  and  $\kappa_T = 0.0003$

Figure (3.7). The only difference is the timing. As levees do not decay so fast, people can afford the maintaining for a longer time, so all the consequences described above are qualitatively the same but begin later in time.

### 3.4.2 Simulations of the Uncontrolled Model

In this chapter we present simulations of the dynamics of the optimal control model. So we simulate the system of functions

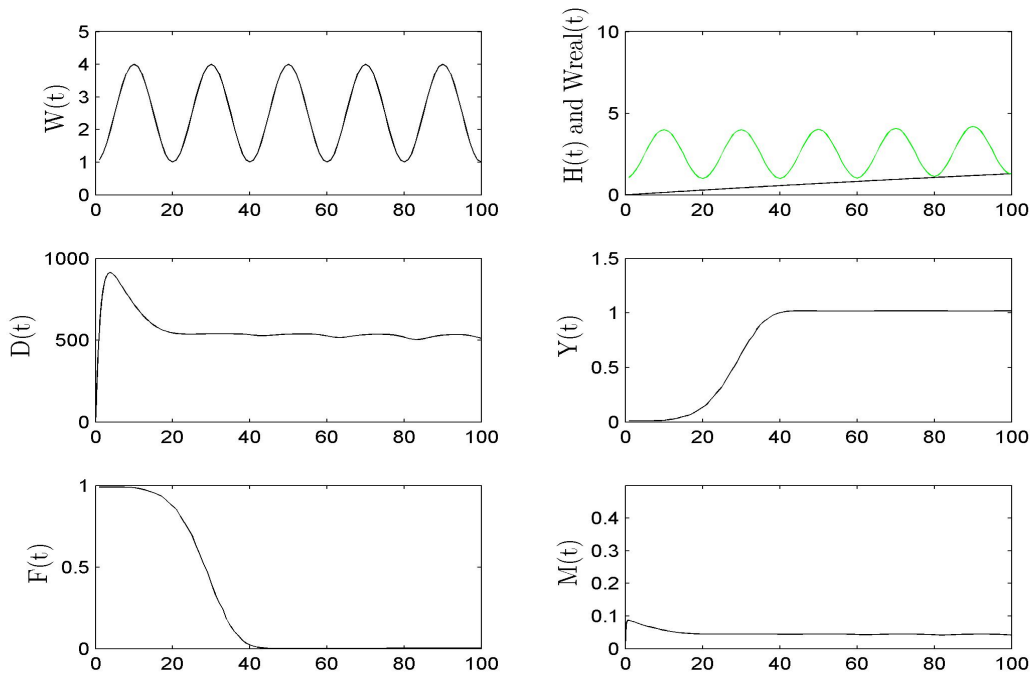
$$\begin{aligned} W(t) &= \gamma_1 \sin^2(kt\pi) + \gamma_2, \\ F(W, H, D) &= \frac{W^2}{W^2 + 3(1 - \xi_H)^2 H^2} \cdot \exp(-\alpha_H D), \\ Y &= (1 - \beta F) \left( \frac{D}{\lambda_E} \right)^{-\alpha_Y} \end{aligned}$$

with the dynamics

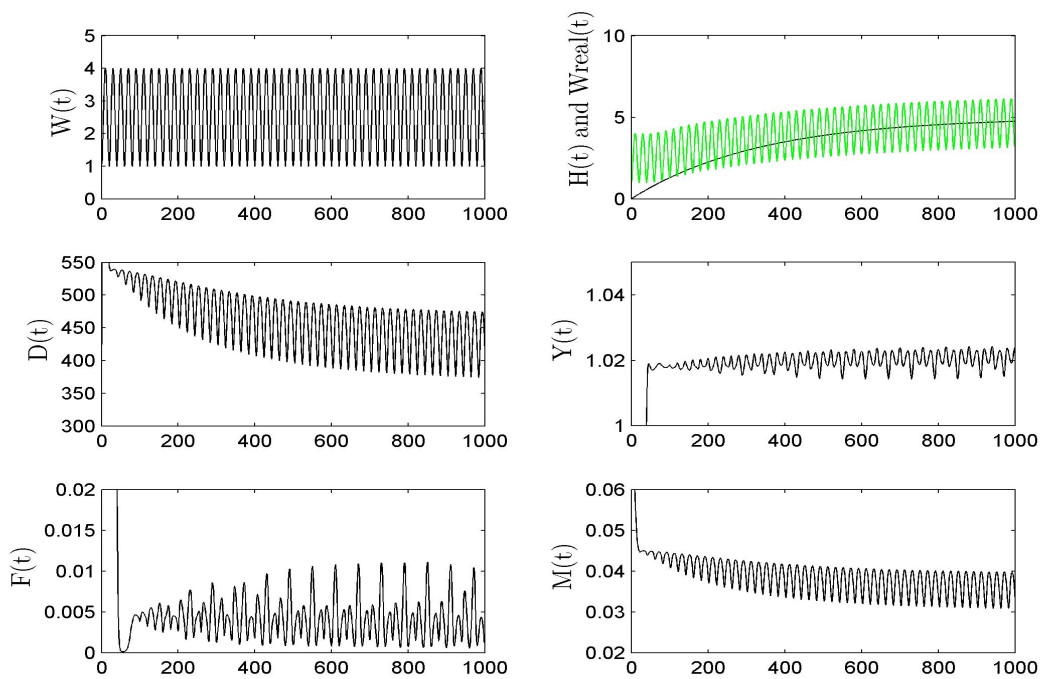
$$\begin{aligned} \dot{D} &= \left( M - \frac{D}{u} \right) \frac{\varphi_p}{\sqrt{Y}}, \\ \dot{M} &= \alpha F - \mu_M M, \\ \dot{H} &= v - \mu_H H. \end{aligned}$$

The parameters we used in this simulation are summarized in Table (3.1). To get a first insight, these are the same as in the other simulations before for the purpose of getting comparable results. We want to emphasize that the additional height of the levees  $v$  and the risk parameter  $u$  are set to constant values in these simulations. Therefore, the following results show the dynamics for given and constant pairs of  $(u, v)$ , while there is no optimization involved.

With the parameter set from Table (3.1),  $\frac{v}{\mu_H} = 5$  holds and therefore, we distinguish between four cases with  $H_0 = 0, 3, 5,$  and  $10$ . This allows us to consider the three different situations with exponentially falling, constant, and exponentially growing height  $H$ , see Chapter 3. The case  $H(0) = 0$  is interesting to compare the results with the former simulations. In each case we plotted the graphs in the short run for 100 years at the top, and in the long run for 1000 years on the bottom. The six small figures are always the same. In the top left we plot the function  $W(t) = \gamma_1 \sin^2(kt\pi) + \gamma_2$ , which is the same for all examples. At the top right, the different cases for the evolution of the height  $H$  are given. Distance  $D$ , Output  $Y$ , flood intensity  $F$ , and finally the awareness of risk  $M$  follow in the remaining figures.

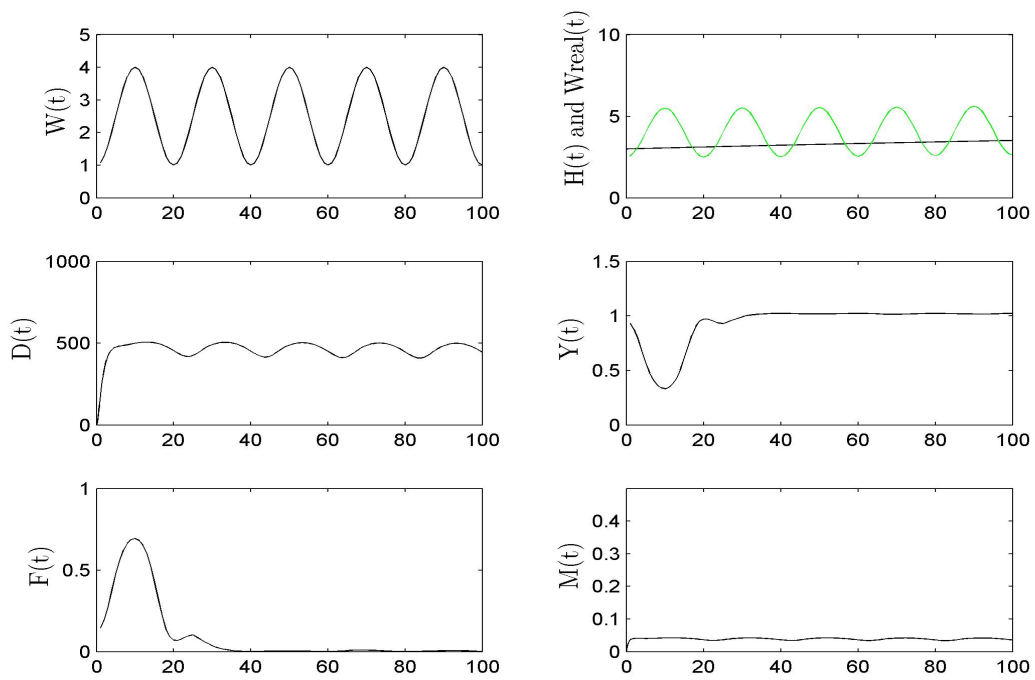


(a) Short run  $t \in (0, 100)$

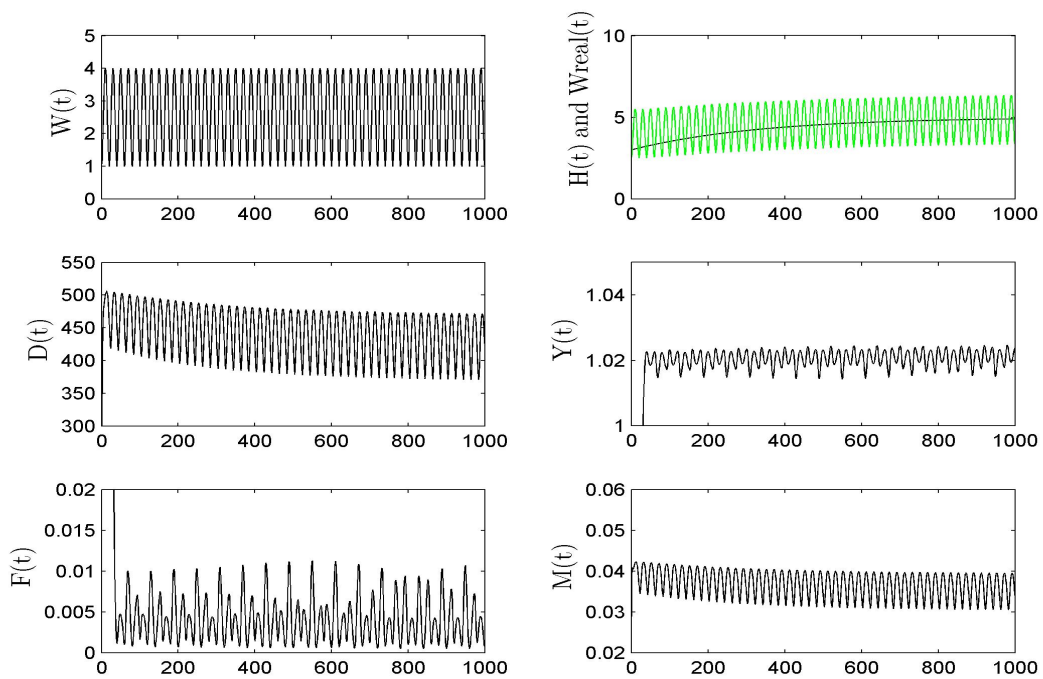


(b) Long run  $t \in (0, 1000)$

Figure 3.8: Simulations of the system of differential equations for  $(D_0, M_0, H_0) = (1, 0, 0)$

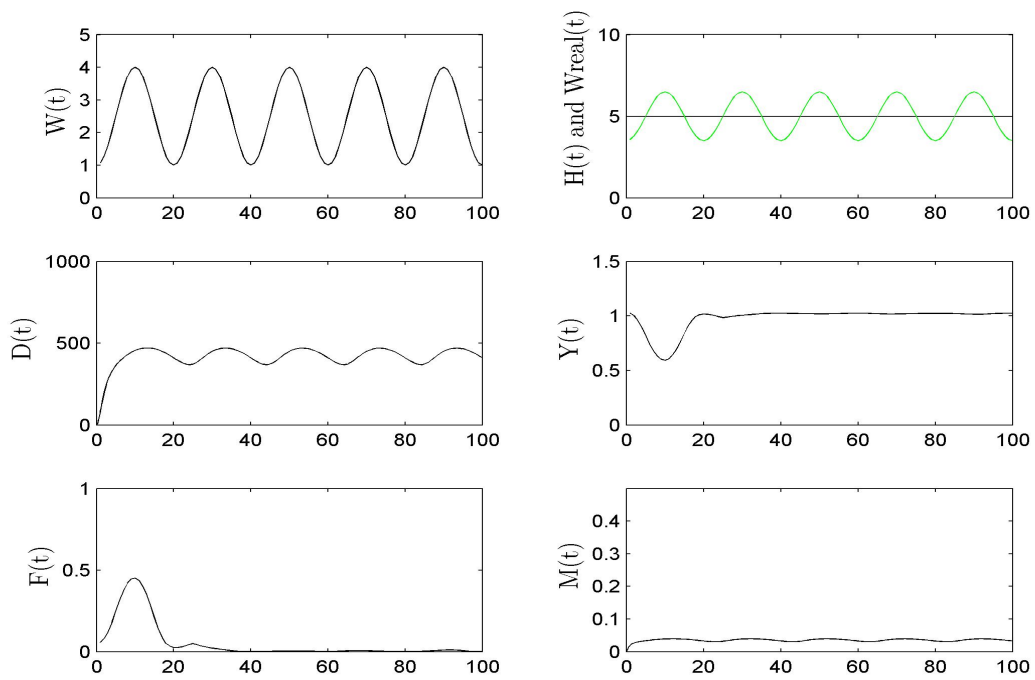


(a) Short run  $t \in (0, 100)$

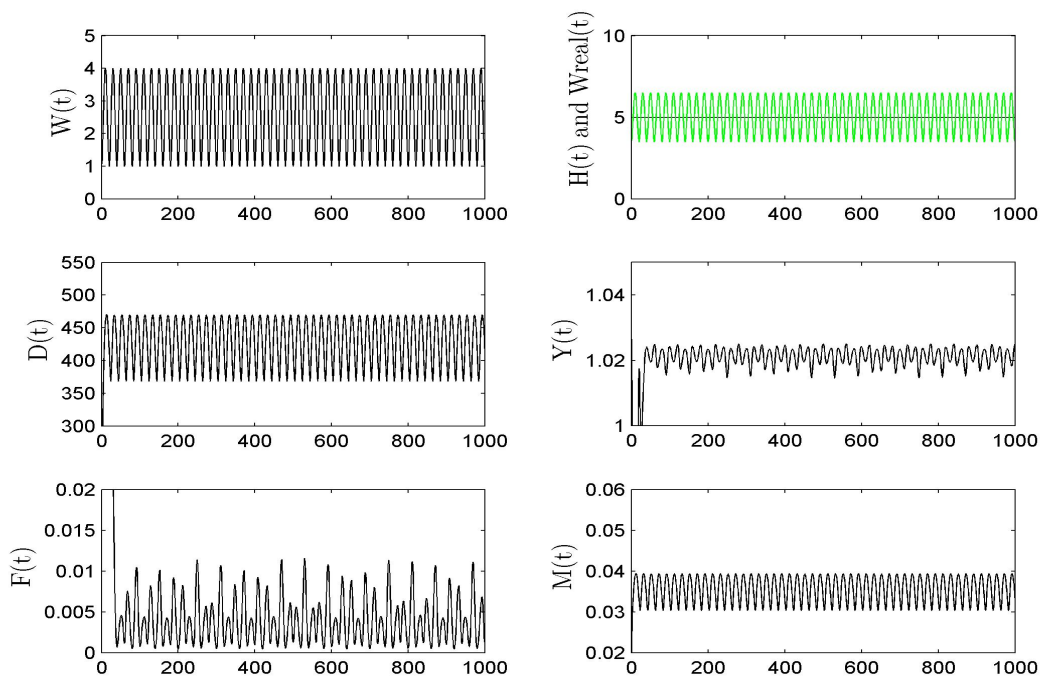


(b) Long run  $t \in (0, 1000)$

Figure 3.9: Simulations of the system of differential equations for  $(D_0, M_0, H_0) = (1, 0, 3)$

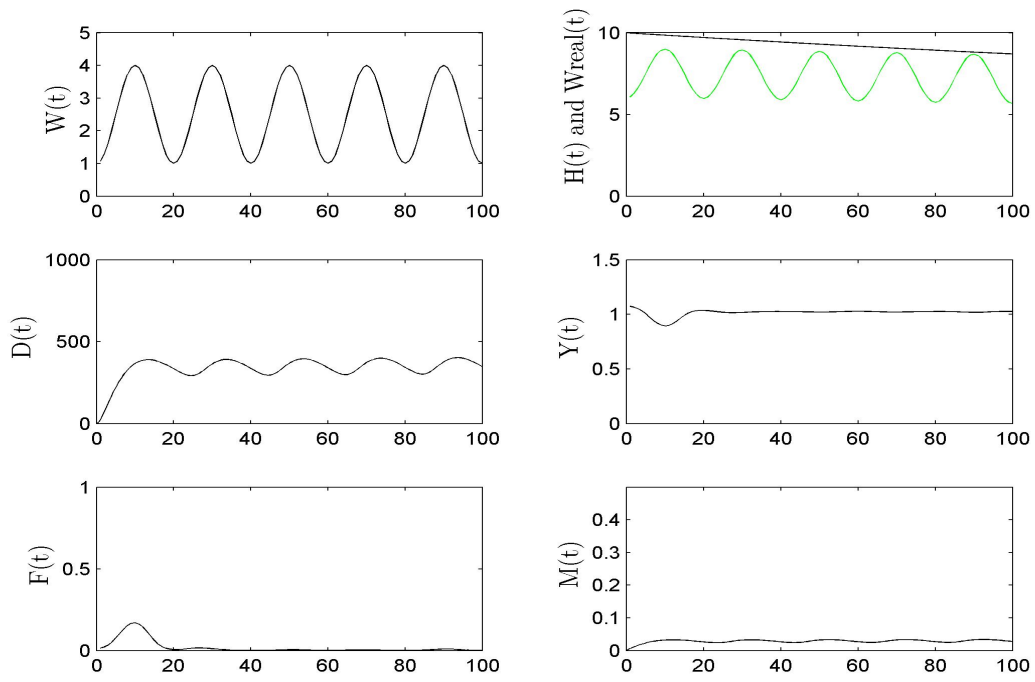


(a) Short run  $t \in (0, 100)$

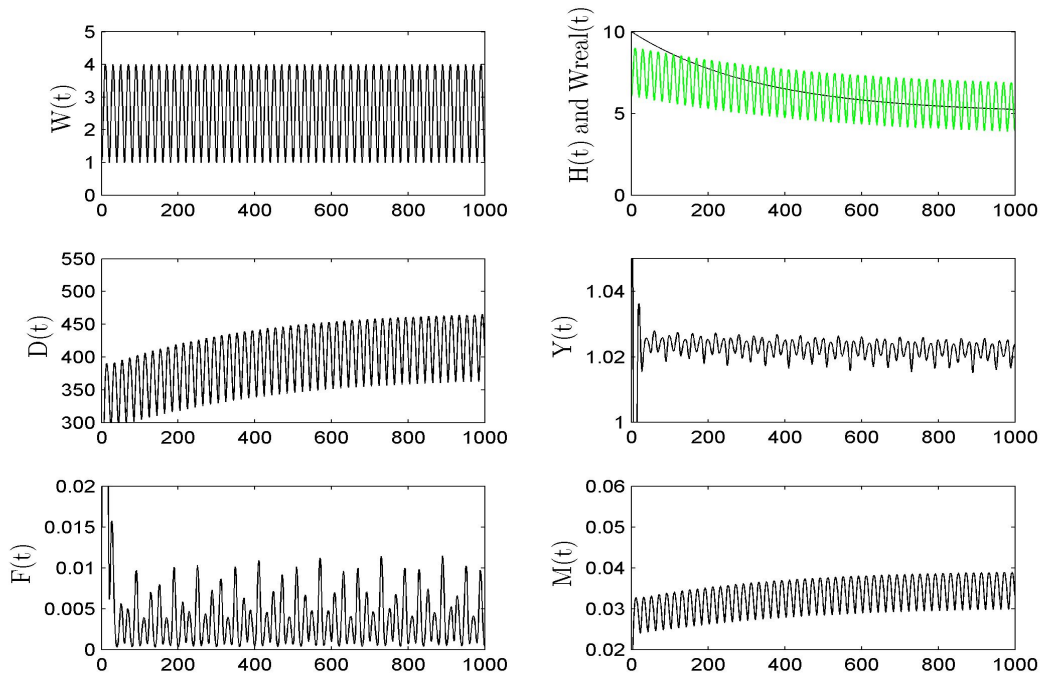


(b) Long run  $t \in (0, 1000)$

Figure 3.10: Simulations of the system of differential equations for  $(D_0, M_0, H_0) = (1, 0, 5)$



(a) Short run  $t \in (0, 100)$



(b) Long run  $t \in (0, 1000)$

Figure 3.11: Simulations of the system of differential equations for  $(D_0, M_0, H_0) = (1, 0, 10)$

Table 3.1: Model parameters for Chapter 3

Parameter	Value
$u$	12000
$v$	0.015
$\varphi_P$	10000
$\beta$	1
$\zeta_H$	0.5
$\lambda_E$	5000
$\alpha_Y$	0.1
$\alpha$	0.5
$\alpha_H$	0.01
$\mu_M$	0.05
$\mu_H$	0.003
$\gamma_1$	3
$\gamma_2$	1
$k$	0.05

Even in the short run, in all four cases very fast convergence to a state is seen, where the variables oscillate around a certain level. In the long run, the height of the levees rises over time in Figure (3.8) and Figure (3.9). Distance  $D$  and awareness  $M$  show the opposite reaction, both fall. Lower distance leads to higher flood intensities  $F$ . But these flooding events seem to be less frequent, so that the risk awareness  $M$  also goes down. We do not see a big reaction in size  $Y$ . There are oscillations due to the periodicity in the whole system, but neither the amplitude nor the frequency change remarkably.

The third case, with constant height  $H$  is rather unspectacular. After a few changes in the short run, all variables come to a state of oscillations with constant amplitude and frequency. In the last Figure (3.11), with falling height, exactly the opposite of the first two cases appears in the long run. The distance and awareness of risk increase and  $Y$  again shows no reaction in the long run.

Overall it can be said, that independent of the starting value  $H_0$ , the fluctuation of the water levels seems to have only a small effect, if we take the same parameters as in the model of [1]. Especially the small units in the  $y$ -axis are notable in the long run to make the fluctuations in the variables even observable.

## 3.5 Summary

In this chapter we introduced an optimal control model based on the model of Di Baldassarre et al. in [1]. Their model consists of three main variables, namely the damage through flooding  $F$ , the additional height of levees after flooding  $R$ , and the shock due to the damage  $S$ . The dynamics are given by four differential equations, which describe the evolutions of the size of the economy  $G$ , the distance to the river  $D$ , the height of the levees  $H$ , and the memory of past flooding events  $M$ . Additionally, they present a few simulations in the programme R with different cost scenarios. We reproduced these simulations using MATLAB.

The next step was to take this model as a starting point and introduce an optimal control model. After redefining the functions for the water levels and the damage in a continuous and differentiable deterministic way, the most important aspect for an optimal control model is to formulate an objective function, which we introduced in (3.7) as the discounted present value of future damage and costs.

Another difference to the model of Di Baldassarre et al. in [1] concerns the dynamics of the system. We changed the differential equation for the size  $G$  and modelled this variable by defining the output  $Y$  explicitly. Our dynamics therefore consist of the remaining three differential equations, except for some notational conventions. So finally we stated an optimal control model with two control variables, namely the additional height of levees  $v$  and the risk parameter  $u$ , and three state variables  $D$ ,  $M$ , and  $H$ .

To combine the two models, we simulated the dynamics of Di Baldassarre et al. in [1] using the deterministic function for the water levels, which we defined in this chapter. Finally we provided a few simulations of the uncontrolled dynamics of the optimal control model.

# Chapter 4

## Adaptations of the Optimal Control Model

In this chapter we make a few adaptations in the functions defined in the previous chapters. On the one hand, we present two other formulations for the water levels and a second function for the damage. On the other hand, we repeat the simulations we carried out in the previous chapters and compare the results.

### 4.1 Functional Forms

#### 4.1.1 Water Levels

Previously, the water levels were modelled in Equation (3.1) as a deterministic time-dependent function

$$W_1(t) = \gamma_1 \sin^2(kt\pi) + \gamma_2,$$

where  $k$  represents the length of the fluctuations, while the minimum and maximum water levels are given by  $\gamma_2$  and  $\gamma_1 + \gamma_2$ , respectively. Since water levels always have to be non-negative, we had to choose the parameters appropriately. Except for 40 points of time with positive values, all the water levels were zero in the model of Di Baldassarre et al. in [1]. In our formulation,  $W_1(t) > 0$  always holds, so there is flooding all the time. As a result, in all simulations the size of the economy fell dramatically. A possible way to deal with this is to reformulate the function of the water levels as

$$W_2(t) = \max \{0, \gamma_1 \sin^2(kt\pi) + \gamma_2\} \quad (4.1)$$

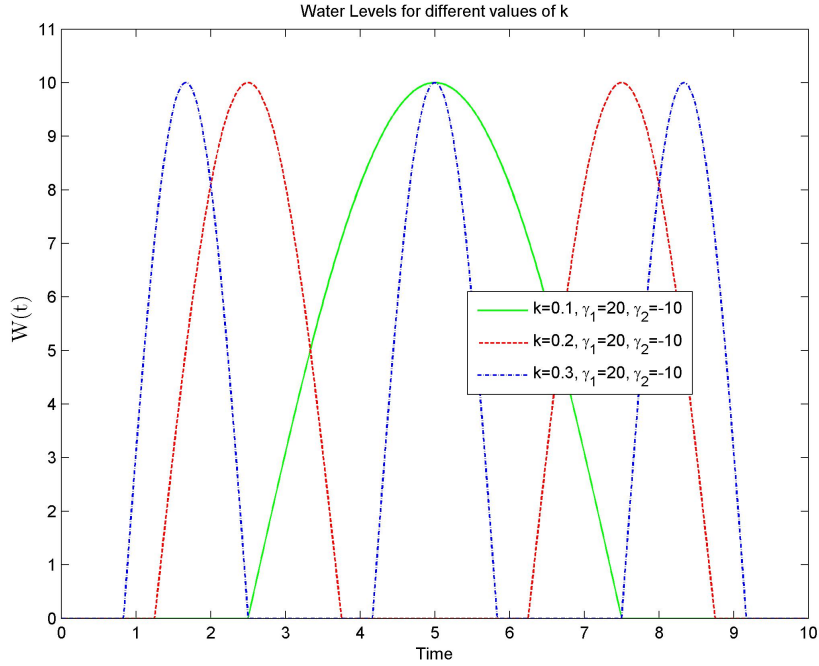


Figure 4.1:  $W_2(t) = \max \{0, \gamma_1 \sin^2(kt\pi) + \gamma_2\}$

and to choose other values for  $\gamma_1$  and  $\gamma_2$ . A few examples of the new formulation are given in Figure (4.1). In this case periods with  $W(t) = 0$  occur, which can give the economy the chance to build up some size without the disturbance of flooding events.

Additionally, we also investigate a third formulation of the form

$$W_3(t) = a \sum_{j=1}^k \cos(jt) + b \text{ with } k \in 2\mathbb{N}, \quad (4.2)$$

and choose  $a$ ,  $k$ , and  $b$  appropriately, so that the values of this function do not exceed a certain value. An example can be seen in Figure (4.2) with  $a = 0.5$ ,  $k = 10$ , and  $b = 1.5$ . This formulation can be interpreted as follows. Naturally there are always some fluctuations in the water levels due to rainy days. In some periods the water reaches high values, which is represented in the three peaks in Figure (4.2). With this formulation, the economy has the chance to recover during periods with lower water levels to withstand times with higher water levels.

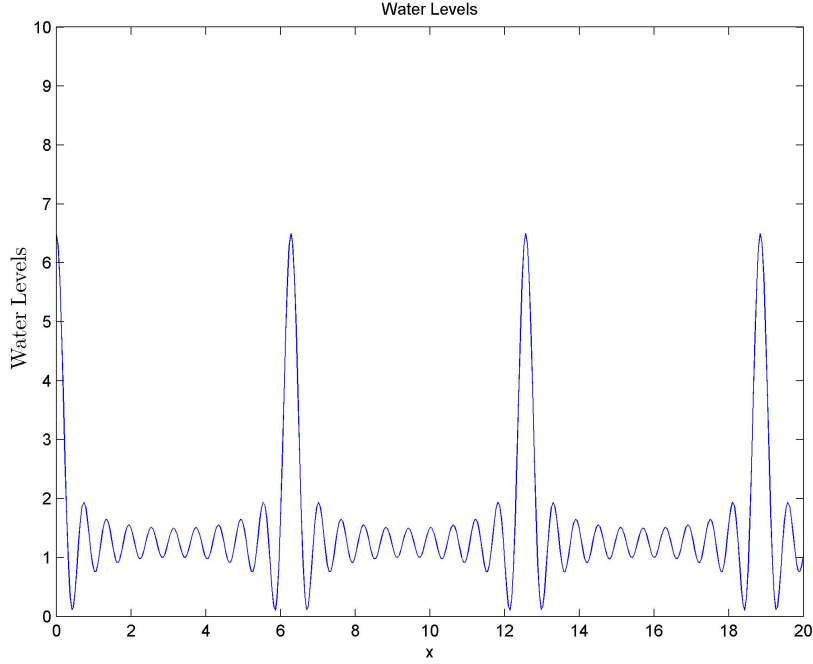


Figure 4.2:  $W_3(t) = 0.5 \sum_{j=1}^{10} \cos(jt) + 1.5$

### 4.1.2 Damage Function

In (3.2) the function

$$F_1(W, H, D) = \frac{W^2}{W^2 + 3(1 - \xi_H)^2 H^2} \cdot \exp(-\alpha_H D)$$

fulfilled the condition that the inflection point should be at  $(1 - \xi_H)H$ . This function was a first approximation for the step function from Di Baldassarre et al. in [1]. As compared to the old damage function, see Figures (3.2) and (3.3), we want to improve the approximation of the jump discontinuity.

For that purpose, we make use of the approach

$$f(x) = a + b \arctan(cx + d).$$

Since  $\arctan(x) \in (-\frac{\pi}{2}, \frac{\pi}{2})$  we choose  $a := \frac{1}{2}$  and  $b := \frac{1}{\pi}$  to obtain  $\frac{1}{2} + \frac{1}{\pi} \arctan(x) \in (0, 1)$ . The inflection point of  $\arctan(cx + d)$  is at  $cx + d = 0$ , which yields to  $x = -\frac{d}{c}$ .

Analogously to the approach in Section (3.2.2) we set  $-\frac{d}{c} = (1 - \xi_H)H$  to get  $d =$

$-c(1 - \xi_H)H$ . Inserting all these expressions and taking into account that with higher distance to the river the damage should exponentially decrease we define

$$F_2(W, H, D) = \left( \frac{1}{2} + \frac{1}{\pi} \arctan(c(W - (1 - \xi_H)H)) \right) \exp(-\alpha_H D). \quad (4.3)$$

The parameter  $c$  is a measure for the slope in the inflection point. If we set  $c$  sufficiently high, we get a good approximation for the damage function used by Di Baldassarre et al. in [1]. Two illustrations are given in Figure (4.3).

Starting with  $c = 1$ , the quality of the approximation improves pretty fast, and already  $c = 20$  yields a very good approximation. The two figures were produced for heights of the levees of 3 and 9, therefore different inflection points occur in the two figures.

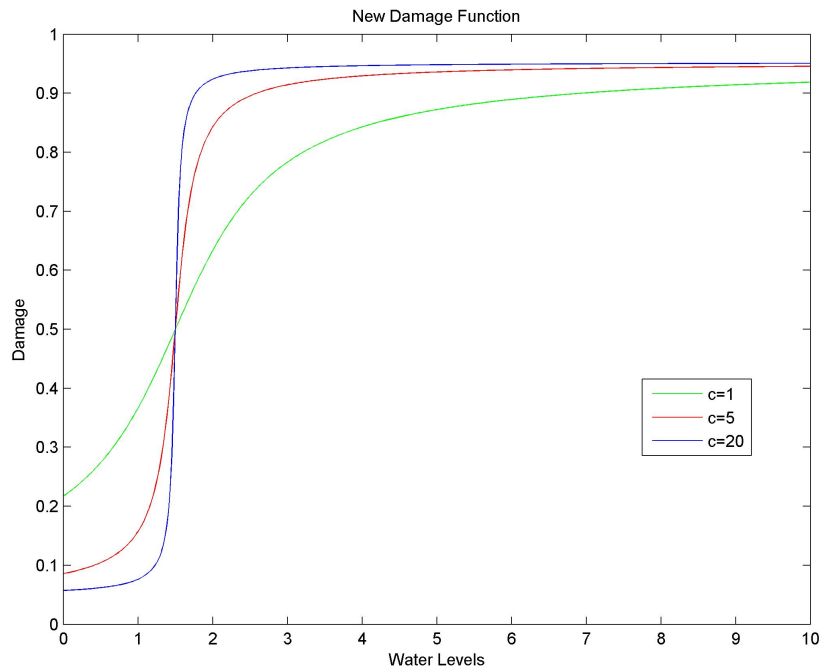
## 4.2 Results and Simulations

Finally, we repeat the simulations of Di Baldassarre et al. in [1] using the two new functions for the water levels. Then we simulate the uncontrolled dynamics of the optimal control model with the new functions.

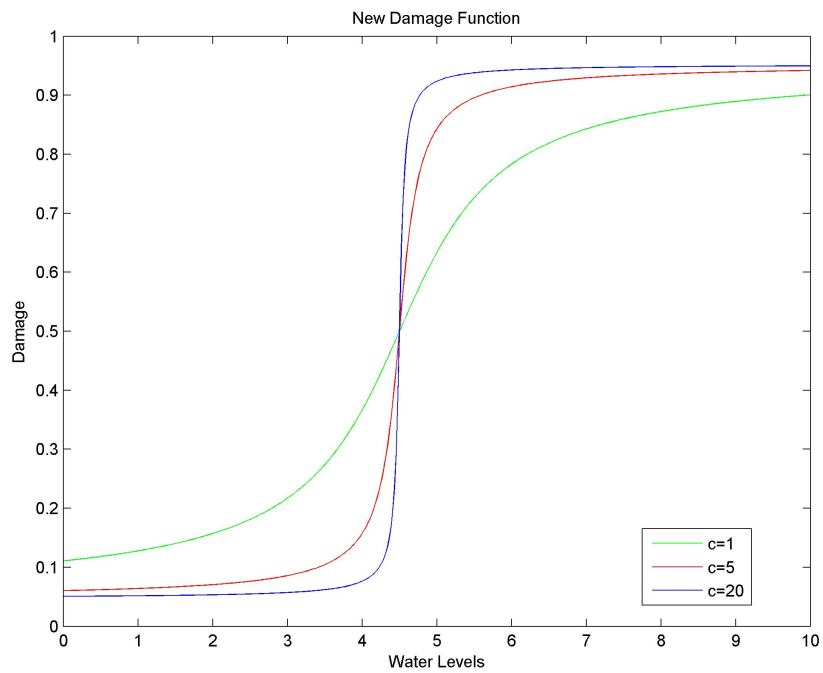
### 4.2.1 Simulations of Di Baldassarre et al.

We look at the system of Di Baldassarre et al., which is described by

$$\begin{aligned} F &= \begin{cases} 1 - e^{-\frac{W + \xi_H H_-}{\alpha_H D}} & \text{if } W + \xi_H H_- > H_-, \\ 0 & \text{otherwise,} \end{cases} \\ R &= \begin{cases} \epsilon_T(W + \xi_H H_- - H_-) & \text{if } (F > 0) \wedge (FG_- > \gamma_E R \sqrt{G_-}) \\ & \wedge (G_- - FG_- > \gamma_E R \sqrt{G_-}), \\ 0 & \text{otherwise,} \end{cases} \\ S &= \begin{cases} \alpha_S F & \text{if } R > 0, \\ F & \text{otherwise,} \end{cases} \end{aligned}$$



(a) Damage at  $H = 3$



(b) Damage at  $H = 9$

Figure 4.3: Damage function  $F_2(W, H, D)$  for  $\zeta_H = 0.5$ ,  $\alpha_H = 0.01$ ,  $D = 10$ , and different values for  $c$  and  $H$

$$\begin{aligned}
\dot{G} &= \rho_E \left(1 - \frac{D}{\lambda_E}\right) G - \Delta(\gamma(t)) (FG + \gamma_E R \sqrt{G}), \\
\dot{D} &= \left(M - \frac{D}{\lambda_P}\right) \frac{\varphi_P}{\sqrt{G}}, \\
\dot{H} &= \Delta(\gamma(t)) R - \kappa_T H, \\
\dot{M} &= \Delta(\gamma(t)) S - \mu_S M,
\end{aligned}$$

using

$$W_2(t) = \max \left\{ 0, \gamma_1 \sin^2(kt\pi) + \gamma_2 \right\}$$

as well as

$$W_3(t) = a \sum_{j=1}^k \cos(jt) + b \text{ with } k \in 2\mathbb{N}$$

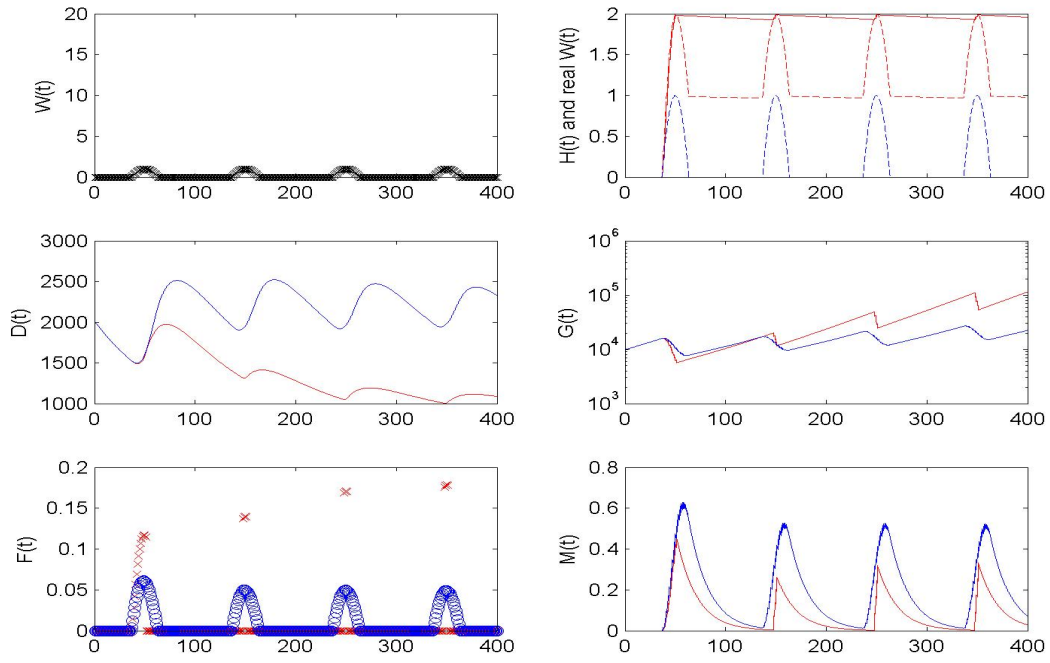
as functions for the water levels.

Starting with  $W_2(t)$  we get the results in Figures (4.4) and (4.5) for  $\kappa_T = 0.0003$  and  $\kappa_T = 0.003$ , respectively, corresponding to different rates of decay of the levees. In both figures we look at the case with  $(\gamma_1, \gamma_2, k) = (6, -5, 0.01)$  at the top and  $(\gamma_1, \gamma_2, k) = (8, -5, 0.01)$  at the bottom. Qualitatively the same things happen for both high and low values of  $\kappa_T$ .

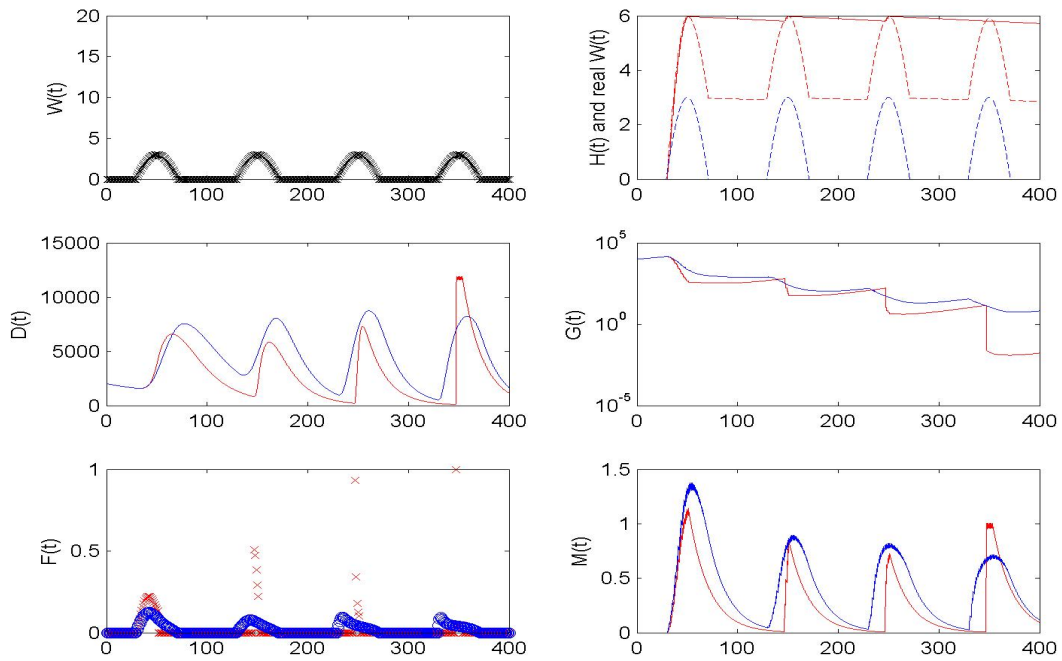
If the water levels are rather low, like in Figures (4.4a) and (4.5a), the size of the economy increases, since there is less money required when building lower levees. People can settle closer to the river and the damage by floods is lower, which therefore yields more moderate levels of risk awareness  $M$ .

Using  $W_3(t) = 0.5 \sum_{j=1}^{10} \cos(jt) + 1.5$  we get the results in Figure (4.6), where we again distinguished between low and high decay  $\kappa_T$ . Since there are qualitatively the same results in these two cases, we concentrate on Figure (4.6a). Most of the time, the water levels remain at a low level, but peaks occur regularly. In all figures, the red line corresponds to low costs, whereas the blue line indicates high costs, respectively. Higher levees are built if the costs are lower. Together with the higher levees, people are not forced to move away from the river as far as in the blue case with higher costs. This smaller distance avoids a rapid decrease of the size of the economy as observed in the blue case.

A lower distance combined with higher levees, has implications concerning the dam-

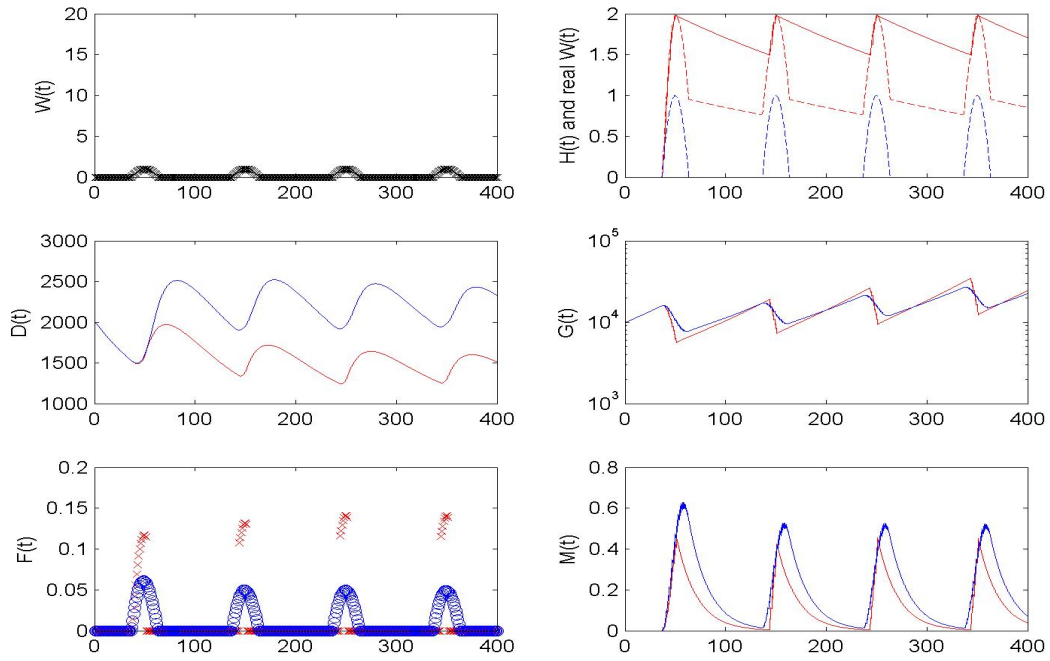


(a)  $(\gamma_1, \gamma_2, k) = (6, -5, 0.01)$

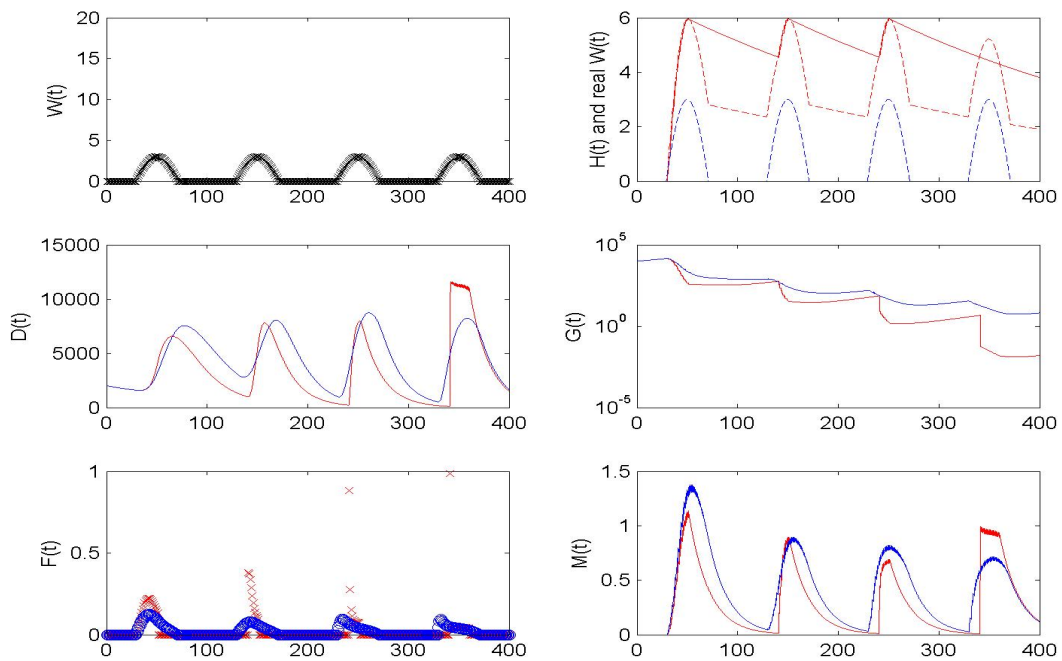


(b)  $(\gamma_1, \gamma_2, k) = (8, -5, 0.01)$

Figure 4.4: The simulations with  $W_2(t) = \max \{0, \gamma_1 \sin^2(kt\pi) + \gamma_2\}$  and  $\kappa_T = 0.0003$



(a)  $(\gamma_1, \gamma_2, k) = (6, -5, 0.01)$



(b)  $(\gamma_1, \gamma_2, k) = (8, -5, 0.01)$

Figure 4.5: The simulations with  $W_2(t) = \max \{0, \gamma_1 \sin^2(kt\pi) + \gamma_2\}$  and  $\kappa_T = 0.003$

age due to flooding events. In the red case, there are less often flooding events but with higher damage. As a result the awareness  $M$  stays at a lower level, but jumps in the case of flooding events are higher than in the blue case.

## 4.2.2 Simulations of the Optimal Control Model

Finally, we look at the dynamics of the optimal control model using the two new functions for the water levels  $W_2$  and  $W_3$  together with the newly defined damage function  $F_2$ . So we simulate the system

$$\begin{aligned}\dot{D} &= \left(M - \frac{D}{u}\right) \frac{\varphi_p}{\sqrt{Y}}, \\ \dot{M} &= \alpha F - \mu_M M, \\ \dot{H} &= v - \mu_H H\end{aligned}$$

with

$$\begin{aligned}F_2(W, H, D) &= \left(\frac{1}{2} + \frac{1}{\pi} \arctan(c(W - (1 - \xi_H)H))\right) \exp(-\alpha_H D), \\ Y &= (1 - \beta F) \left(\frac{D}{\lambda_E}\right)^{-\alpha_Y}\end{aligned}$$

using each of the water level functions

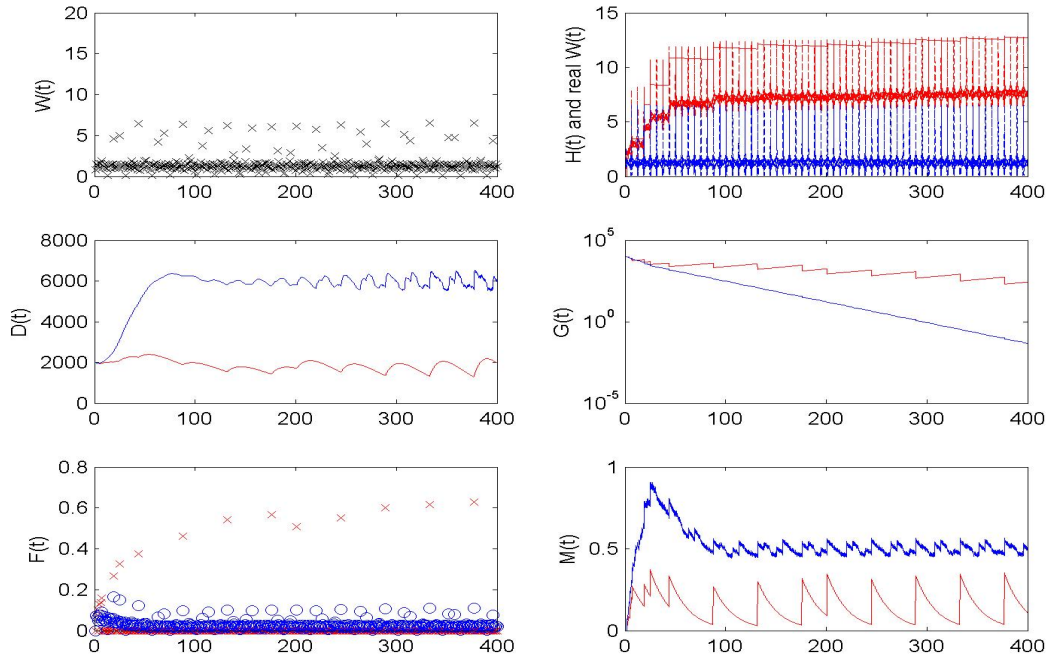
$$W_2(t) = \max\{0, \gamma_1 \sin^2(kt\pi) + \gamma_2\}$$

and

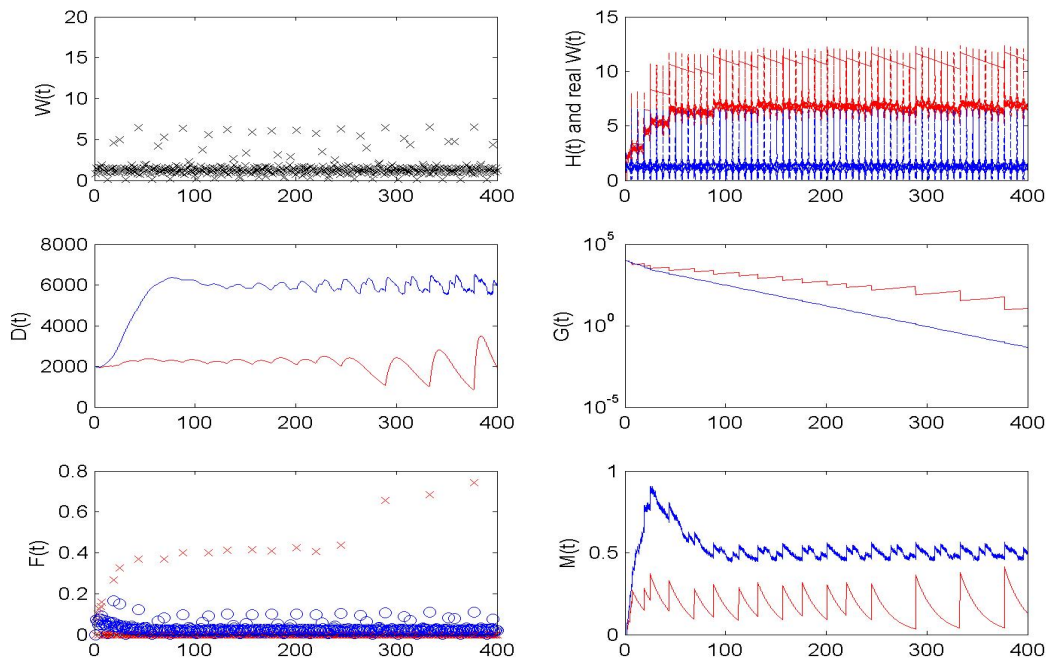
$$W_3(t) = 0.5 \sum_{j=1}^{10} \cos(jt) + 1.5.$$

In Figures (4.7)-(4.10) the results are plotted for  $W_2$ , whereas the results for  $W_3$  are shown in Figures (4.11)-(4.14). It has to be mentioned that these are the results of the uncontrolled model, which means that the two control variables  $u$  and  $v$  are held constant. Like in the previous simulations, we look at the four cases with  $H_0 = 0, 3, 5,$  and  $10$ , therefore, exponentially growing, constant, or exponentially falling heights of the levees occur.

All these figures deliver rather similar results. The distance  $D$  grows very fast to a high value of about 60000 m, but because of this great distance, the economy hardly benefits from the economic effects due to the proximity of the river. Therefore, the size of



(a) Low  $\kappa_T = 0.0003$

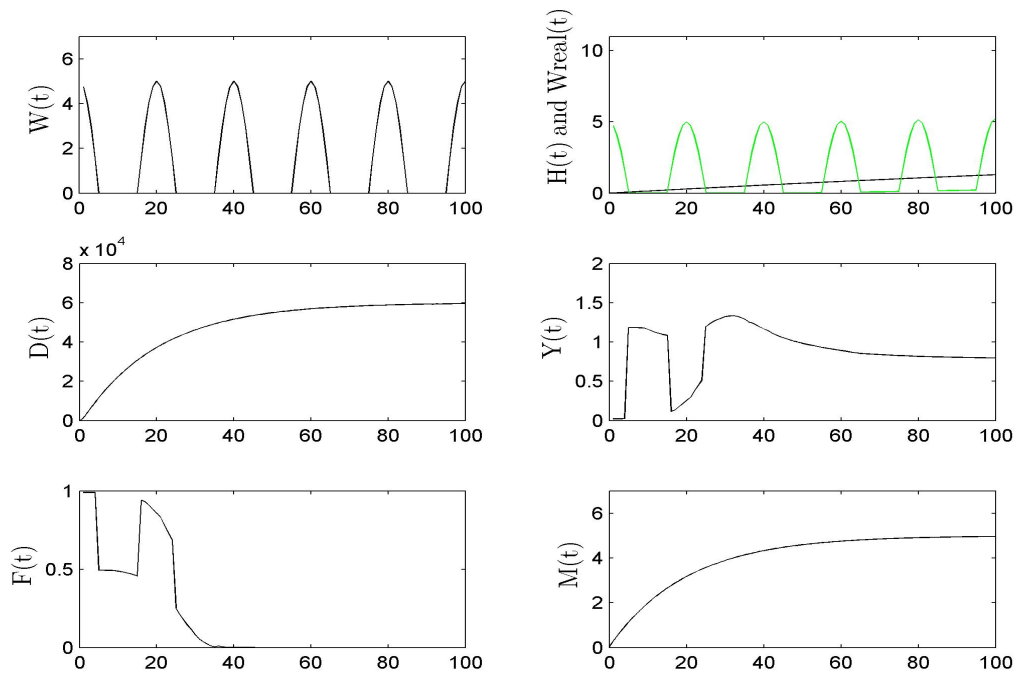


(b) High  $\kappa_T = 0.003$

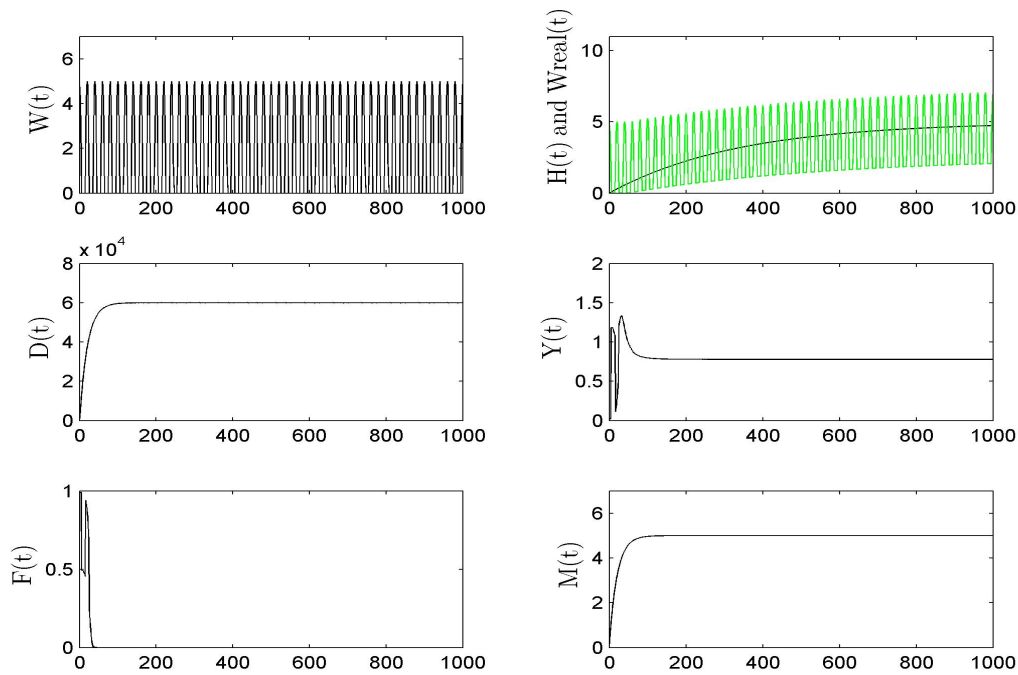
Figure 4.6: The simulations with  $W_3(t) = 0.5 \sum_{j=1}^{10} \cos(jt) + 1.5$

the city converges to a low level of about 0.8 after some ups and downs in the beginning. A positive aspect is that this behaviour of living far away from the river leads to very low damage due to flooding. In all cases, the graph of  $F$  is not even visible after some periods, because it is too low. The memory  $M$  reaches a quite high level of about 5.

With the chosen parameters, the height of the levees always converges to 5 m, independently of the starting value  $H_0$  and the fluctuations of the water levels. If we consider the restriction of constant control variables, it is no surprise that the results do not show a remarkable reaction due to fluctuating water levels. Like in the simulations we presented in Chapter 3, the fluctuations in the variables due to the fluctuating water levels can only be seen within a small range.

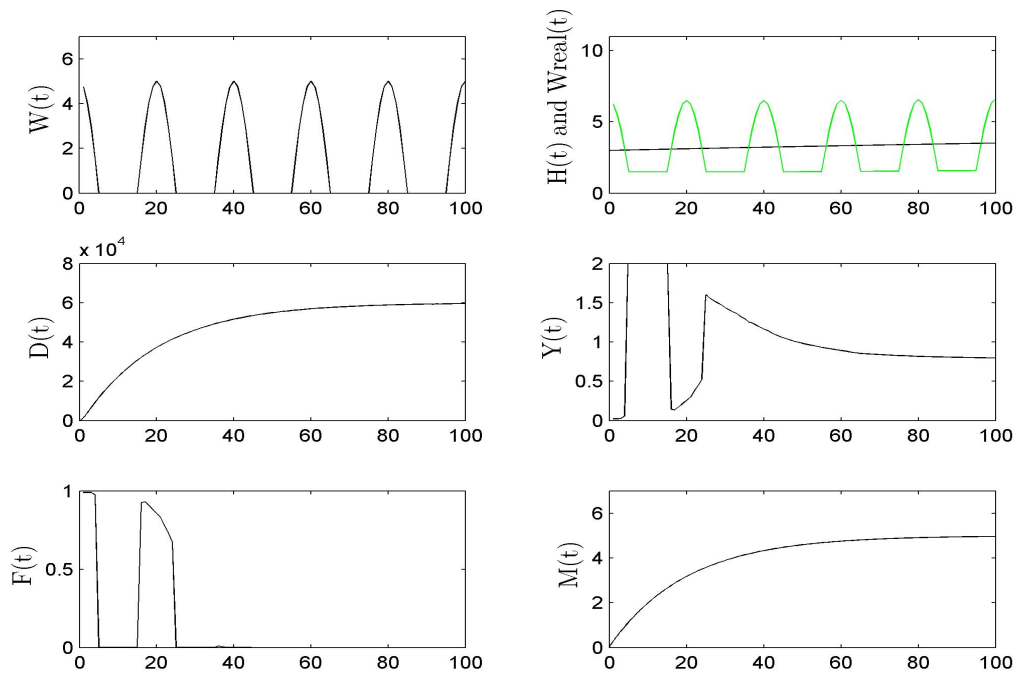


(a) Short run  $t \in (0, 100)$

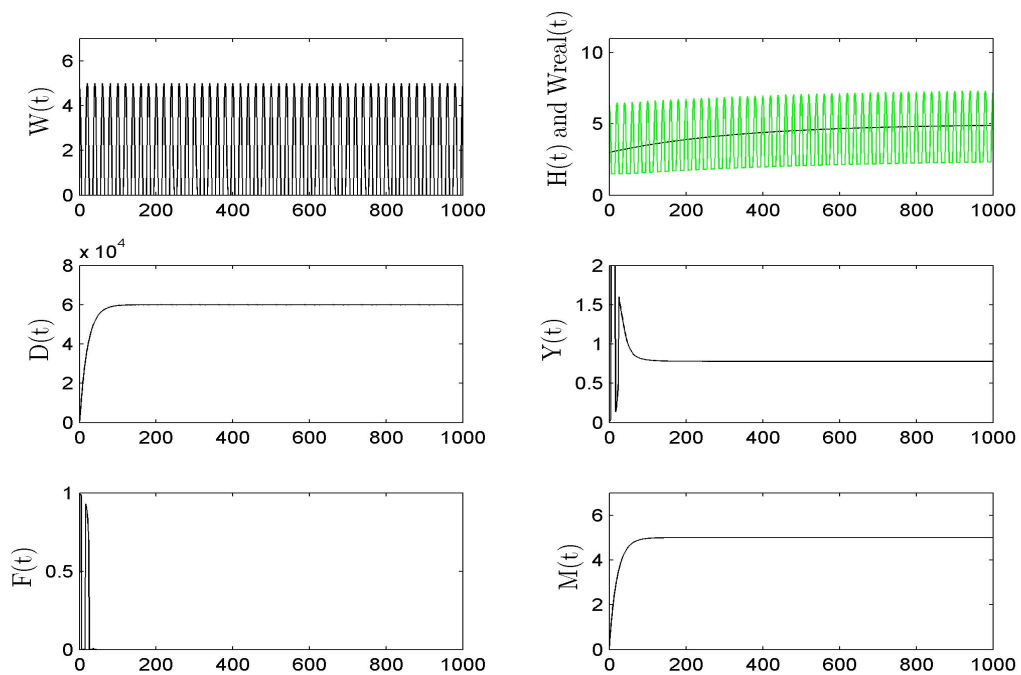


(b) Long run  $t \in (0, 1000)$

Figure 4.7: The simulations of the uncontrolled system for  $(D_0, M_0, H_0) = (1, 0, 0)$  for  $W_2(t) = \max\{0, \gamma_1 \sin^2(kt\pi) + \gamma_2\}$

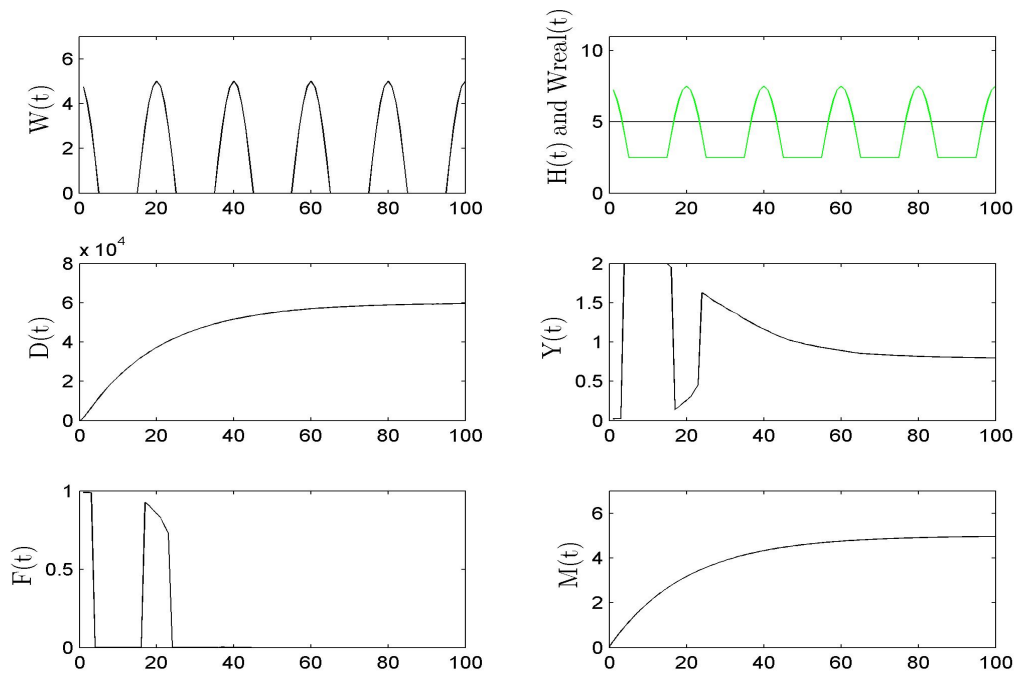


(a) Short run  $t \in (0, 100)$

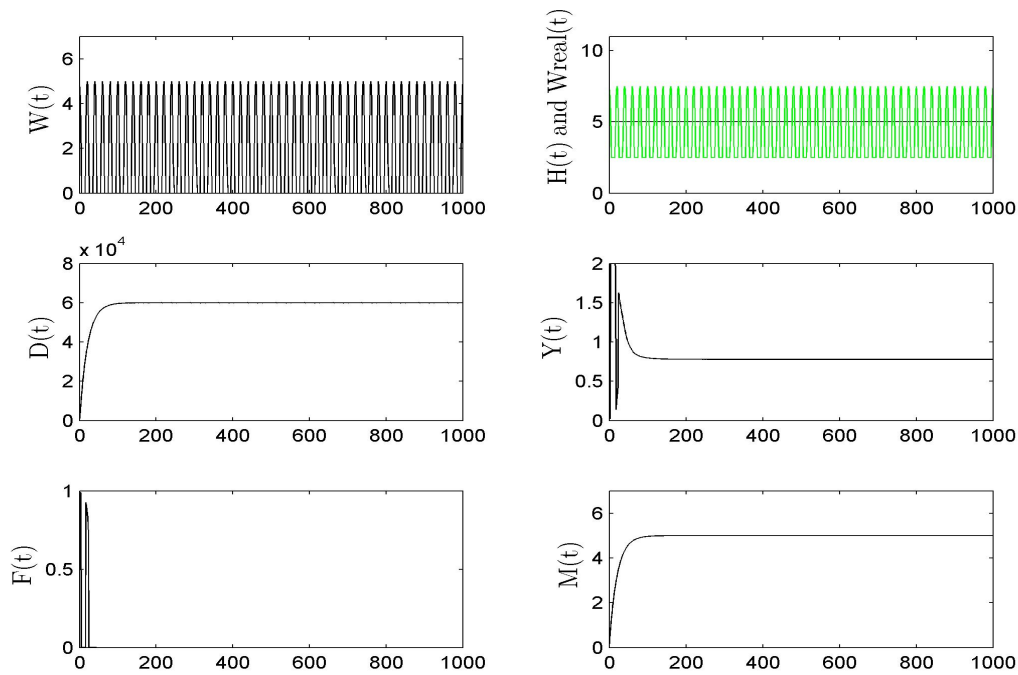


(b) Long run  $t \in (0, 1000)$

Figure 4.8: The simulations of the uncontrolled system for  $(D_0, M_0, H_0) = (1, 0, 3)$  for  $W_2(t) = \max\{0, \gamma_1 \sin^2(kt\pi) + \gamma_2\}$

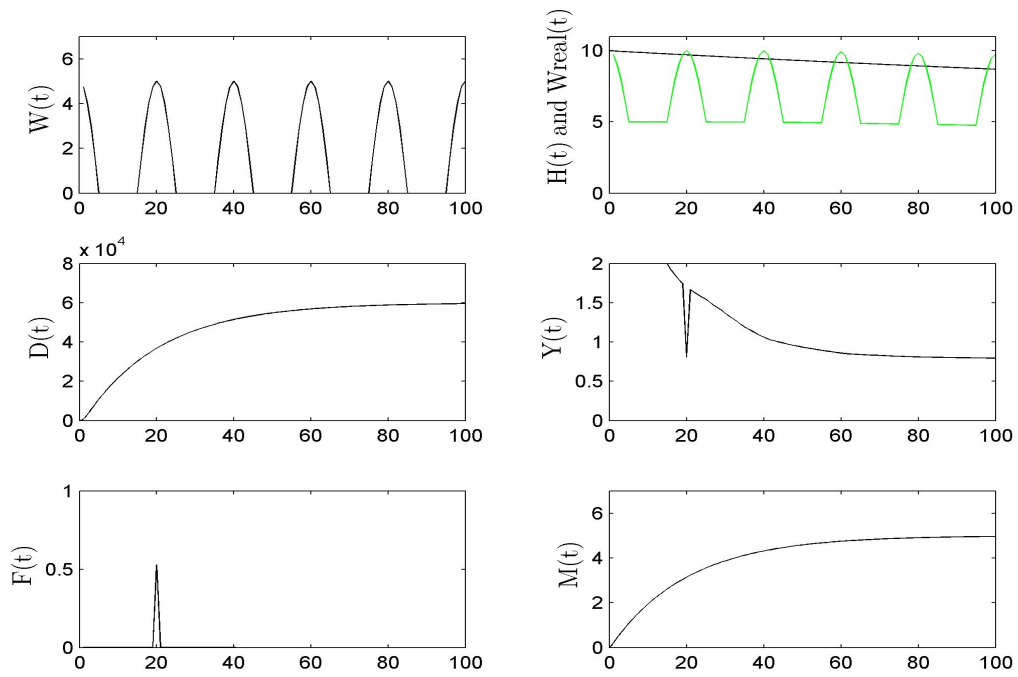


(a) Short run  $t \in (0, 100)$

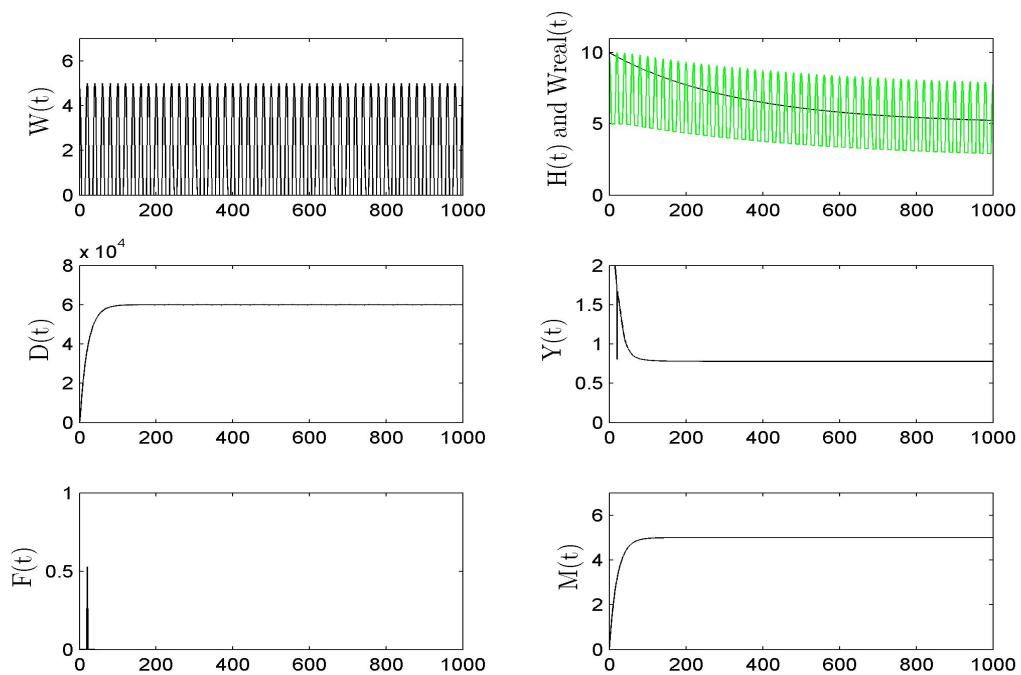


(b) Long run  $t \in (0, 1000)$

Figure 4.9: The simulations of the uncontrolled system for  $(D_0, M_0, H_0) = (1, 0, 5)$  for  $W_2(t) = \max\{0, \gamma_1 \sin^2(kt\pi) + \gamma_2\}$

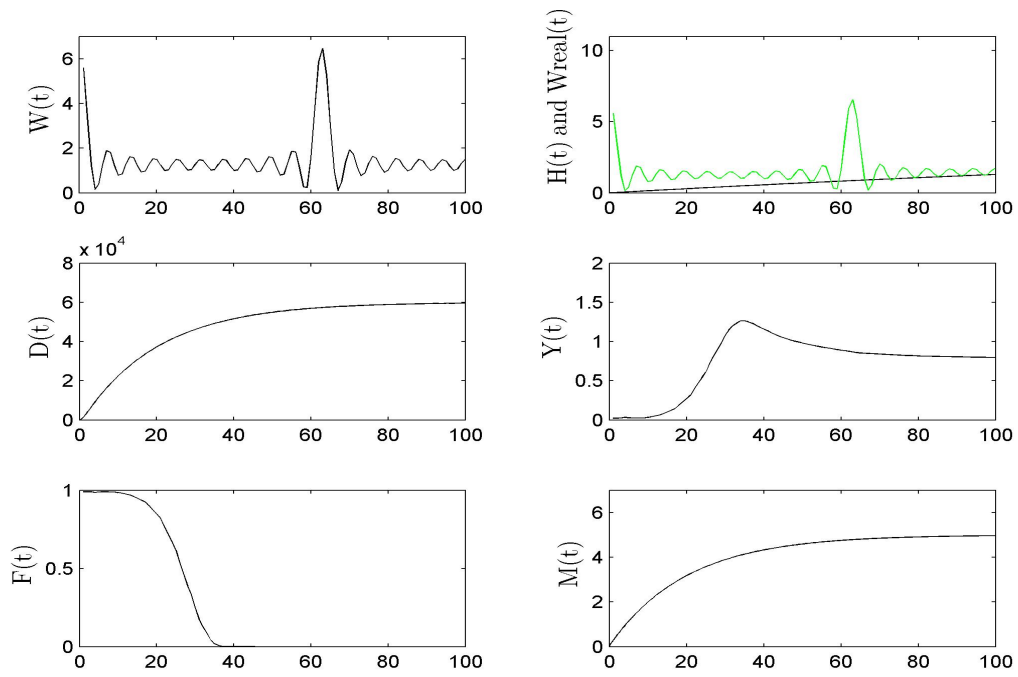


(a) Short run  $t \in (0, 100)$

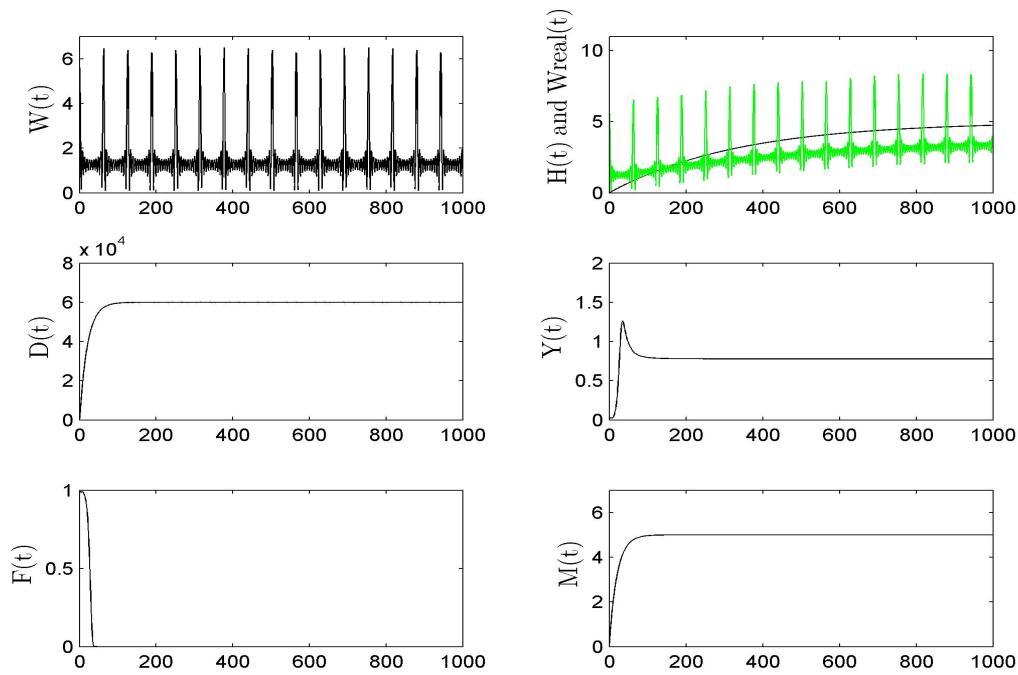


(b) Long run  $t \in (0, 1000)$

Figure 4.10: The simulations of the uncontrolled system for  $(D_0, M_0, H_0) = (1, 0, 10)$  for  $W_2(t) = \max\{0, \gamma_1 \sin^2(kt\pi) + \gamma_2\}$

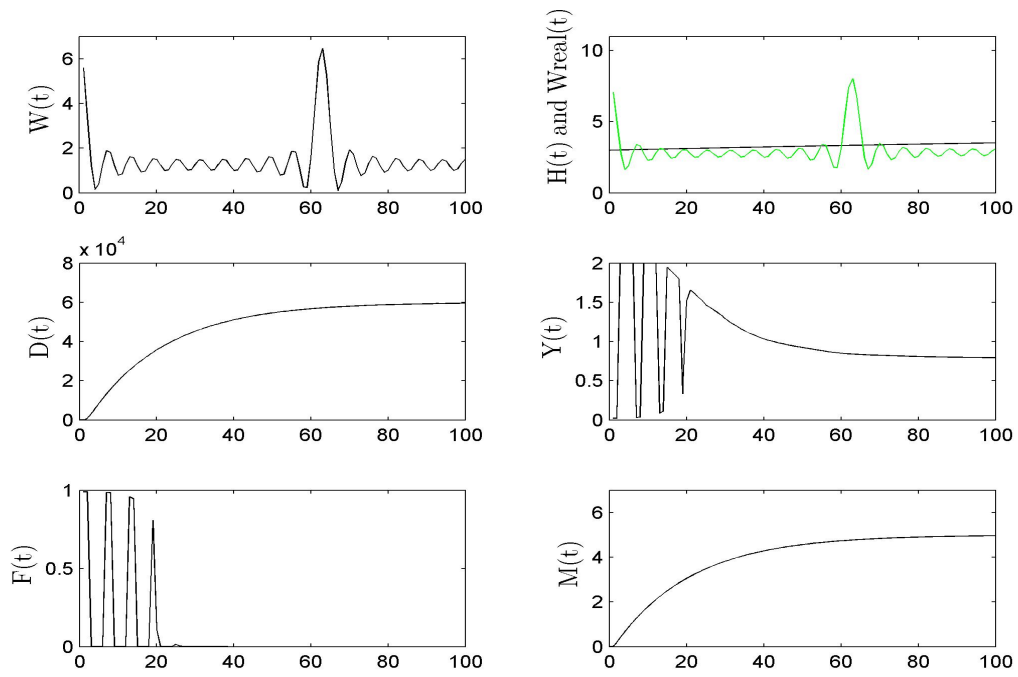


(a) Short run  $t \in (0, 100)$

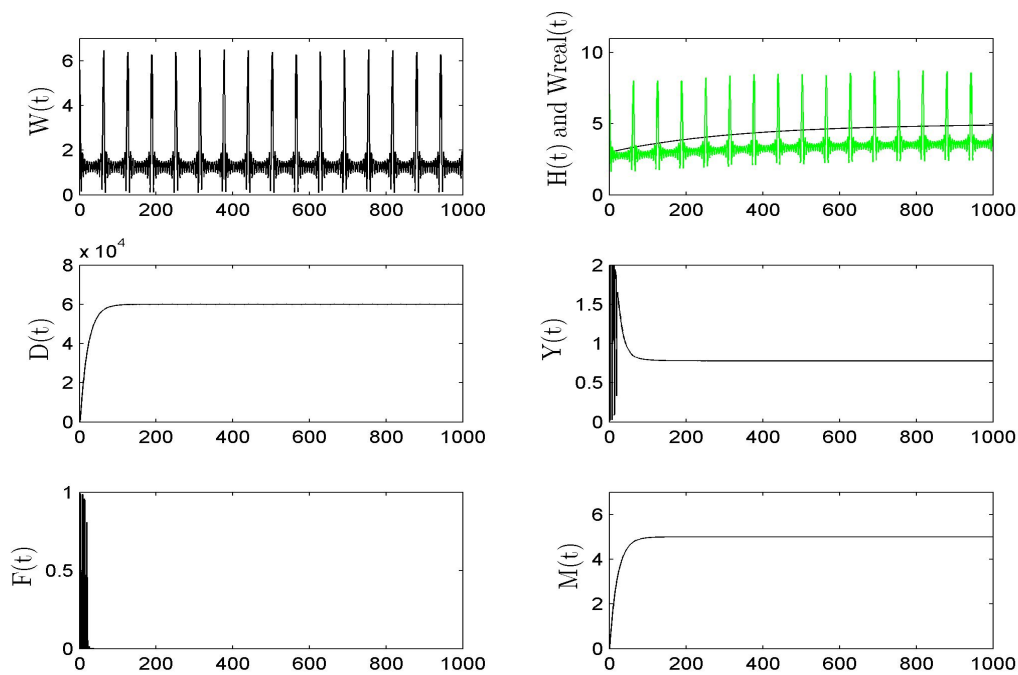


(b) Long run  $t \in (0, 1000)$

Figure 4.11: The simulations of the uncontrolled system for  $(D_0, M_0, H_0) = (1, 0, 0)$  for  $W_3(t) = 0.5 \sum_{j=1}^{10} \cos(jt) + 1.5$

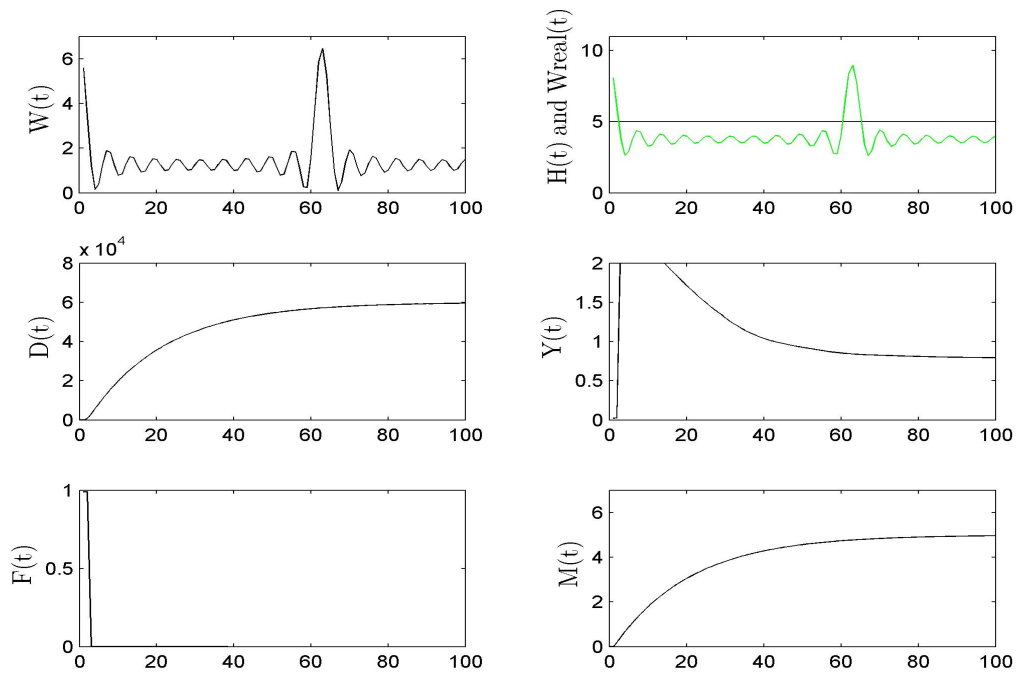


(a) Short run  $t \in (0, 100)$

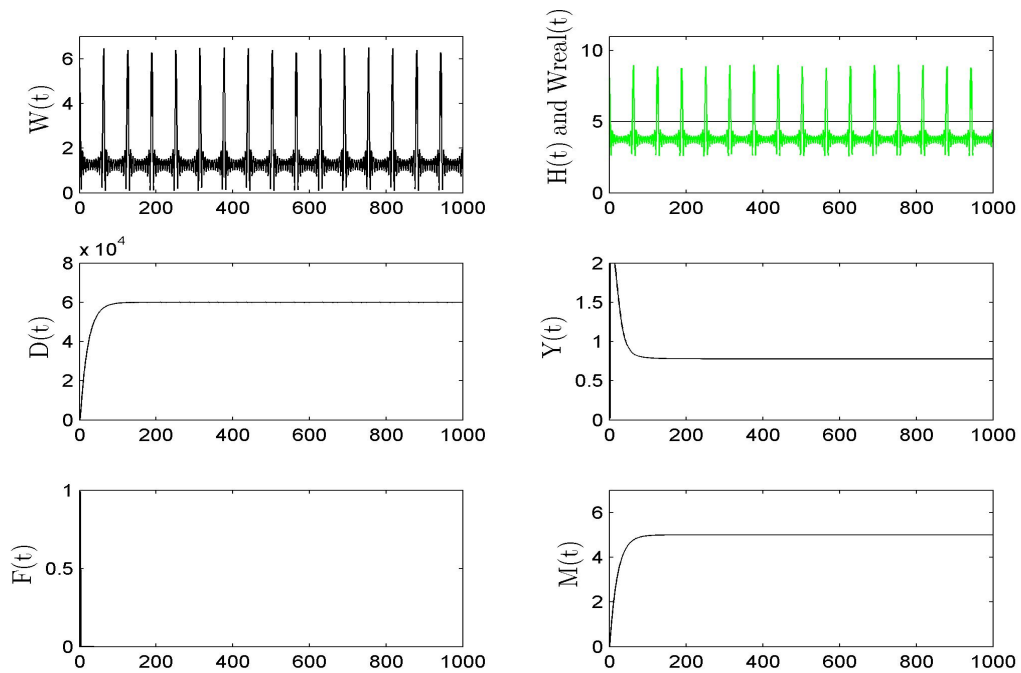


(b) Long run  $t \in (0, 1000)$

Figure 4.12: The simulations of the uncontrolled system for  $(D_0, M_0, H_0) = (1, 0, 3)$  for  $W_3(t) = 0.5 \sum_{j=1}^{10} \cos(jt) + 1.5$

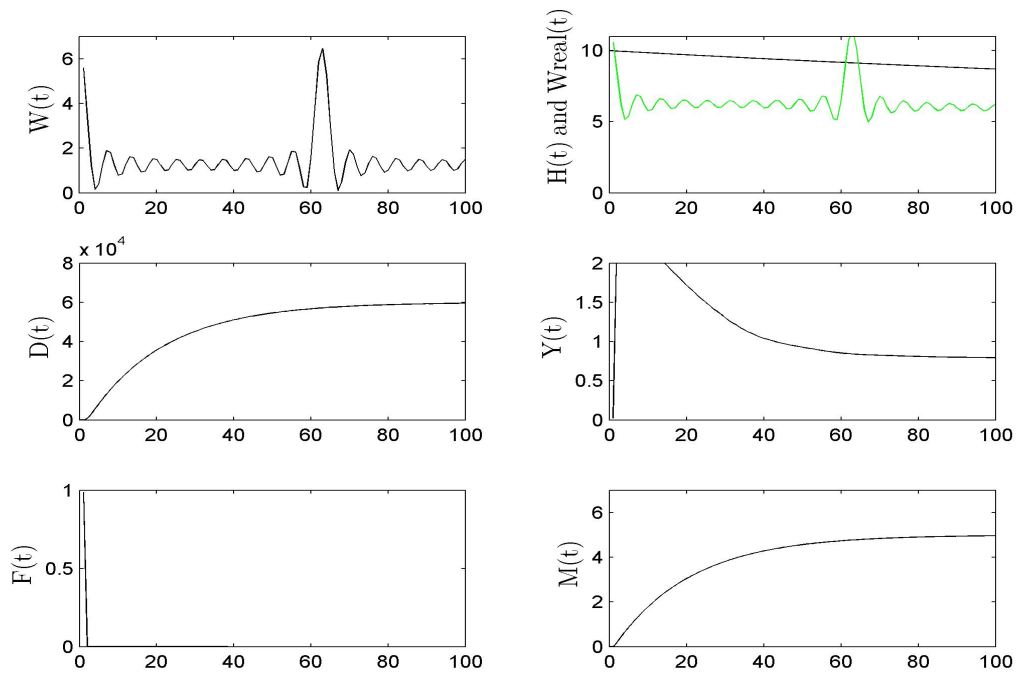


(a) Short run  $t \in (0, 100)$

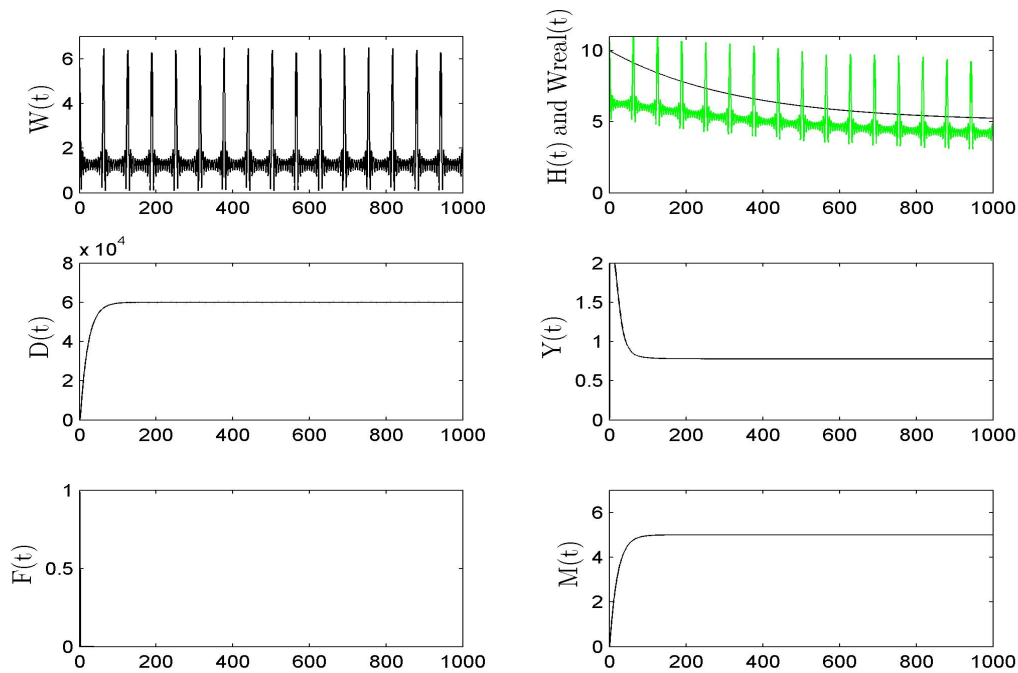


(b) Long run  $t \in (0, 1000)$

Figure 4.13: The simulations of the uncontrolled system for  $(D_0, M_0, H_0) = (1, 0, 5)$  for  $W_3(t) = 0.5 \sum_{j=1}^{10} \cos(jt) + 1.5$



(a) Short run  $t \in (0, 100)$



(b) Long run  $t \in (0, 1000)$

Figure 4.14: The simulations of the uncontrolled system for  $(D_0, M_0, H_0) = (1, 0, 10)$  for  $W_3(t) = 0.5 \sum_{j=1}^{10} \cos(jt) + 1.5$

# Chapter 5

## Preliminary Steps for Optimal Control

In this chapter we give the results of some preliminary steps to optimization for this model. The optimal control model we developed in Chapter 3 is described by

$$\min_{u,v} \int_0^{\infty} e^{-rt} (\rho F(W, H, D) + C(H, v)) dt$$

$$\begin{aligned} \text{s.t.} \quad \dot{D} &= \left(M - \frac{D}{u}\right) \frac{\varphi_p}{\sqrt{Y}}, \\ \dot{M} &= \alpha F - \mu_M M, \\ \dot{H} &= v - \mu_H H \end{aligned}$$

with

$$\begin{aligned} F(W, H, D) = F_2(W, H, D) &= \left(\frac{1}{2} + \frac{1}{\pi} \arctan(500(W - (1 - \xi_H)H))\right) \exp(-\alpha_H D), \\ Y &= (1 - \beta F) \left(\frac{D}{\lambda_E}\right)^{-\alpha_Y}, \\ C(H, v) = C_3(H, v) &= 2Hv + 10v + v^2 \end{aligned}$$

and the two water level functions

$$\begin{aligned} W_2(t) &= \max\{0, \gamma_1 \sin^2(kt\pi) + \gamma_2\}, \\ W_3(t) &= 0.5 \sum_{j=1}^{10} \cos(jt) + 1.5. \end{aligned}$$

Where possible, we used the same parameters as in the previous simulations, which are

summarized in Table (5.1).

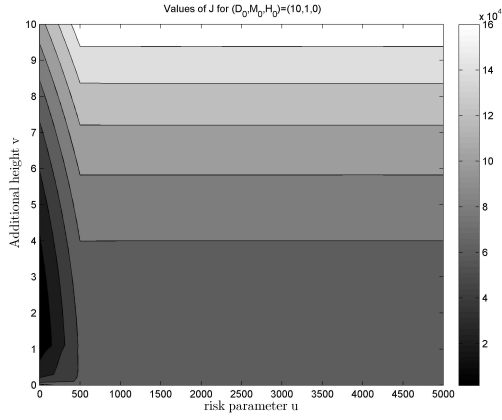
Table 5.1: Model parameters

Parameter	Value
$\varphi_P$	10000
$\beta$	1
$\zeta_H$	0.5
$\lambda_E$	5000
$\alpha_Y$	0.1
$\alpha$	0.5
$\alpha_H$	0.01
$\mu_M$	0.05
$\mu_H$	0.003
$\gamma_1$	10
$\gamma_2$	-5
$k$	0.05
$r$	0.04
$\rho$	5000, 10000

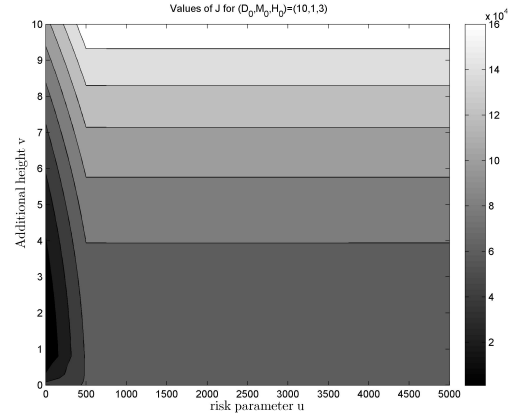
Firstly, we want to calculate the best constant pair of  $(u, v)$  chosen at  $t = 0$ , so that  $J = \int_0^{100} e^{-rt} (\rho F(W, H, D) + C(H, v)) dt$  is minimized. We look at values for the additional height of the levees  $v$  within a range from 0 m to 10 m with steps of 0.1 m. The risk parameter  $u$  is located within  $[0.01; 5000]$  with steps of 500. This range has to be chosen because in the differential equation (3.8) the risk parameter is in the denominator, so  $u \neq 0$  has to hold. For all these pairs of  $(u, v)$  we calculate the finite integral in the objective function, assuming the control variables to be constant over the first 100 years.

The resulting contour plots for these values are presented both for  $W_2$  in Figures (5.1) and (5.2), and for  $W_3$  in Figures (5.3) and (5.4), respectively. In both cases we start with  $D_0 = 10$ ,  $M_0 = 1$ , and  $H_0$  varying from 0 to 10 while distinguishing between  $\rho = 5000$  and  $\rho = 10000$ . Note that the risk parameter  $u$  is only a critical factor for the objective function up to a certain value. For bigger values of the risk parameter  $u$  the objective function does not show any further remarkable reaction. There is great sensitivity of the value of the objective function with respect to the additional height  $v$ . There seems to be a minimizing pair  $(u^*, v^*)$ , where  $u^*$  is at a very low level and  $v^*$  is somewhere in the range between 0 m and 3 m. We calculate the optimal pair  $(u^*, v^*)$  and summarize the results in Table (5.2) for  $W_2$  and in Table (5.3) for  $W_3$ , respectively.

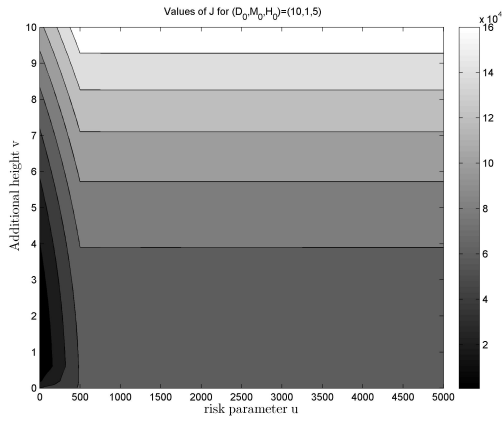
Analyzing these tables, two results can be concluded. Firstly, the objective function gets higher when  $H_0$  is lower. This is obviously due to the fact that the costs are higher if



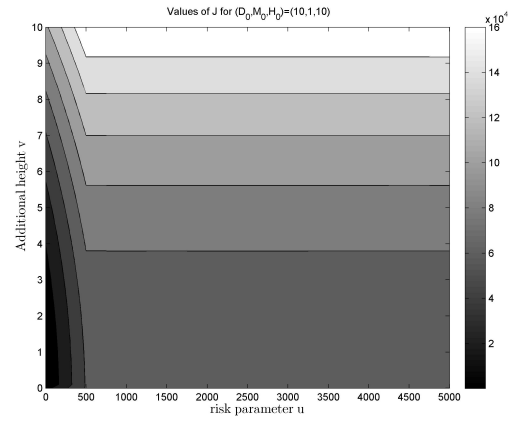
(a)  $(D_0, M_0, H_0) = (10, 1, 0)$



(b)  $(D_0, M_0, H_0) = (10, 1, 3)$

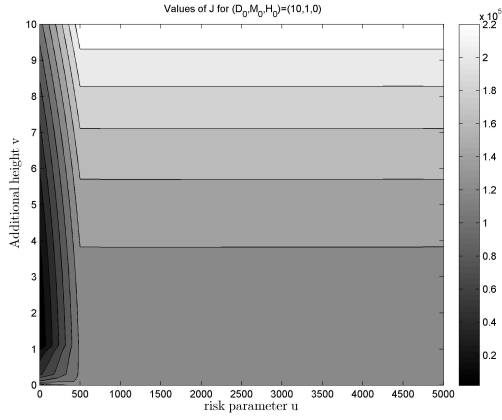


(c)  $(D_0, M_0, H_0) = (10, 1, 5)$

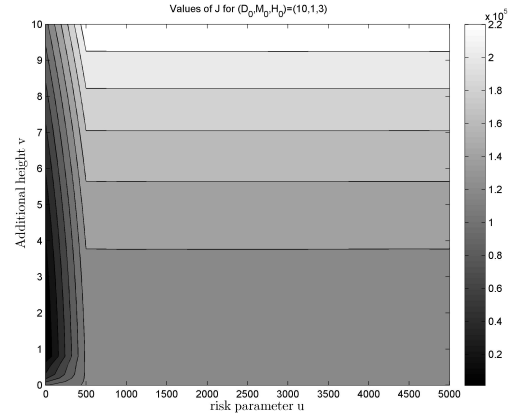


(d)  $(D_0, M_0, H_0) = (10, 1, 10)$

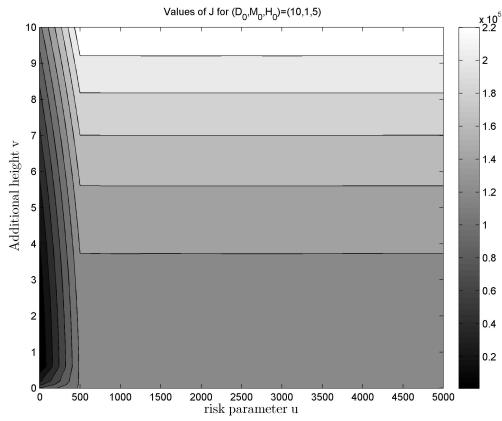
Figure 5.1: Values of  $J = \int_0^{100} e^{-rt} (\rho F(W, H, D) + C(H, v)) dt$  for  $W_2(t) = \max \{0, \gamma_1 \sin^2(kt\pi) + \gamma_2\}$  and  $\rho = 5000$



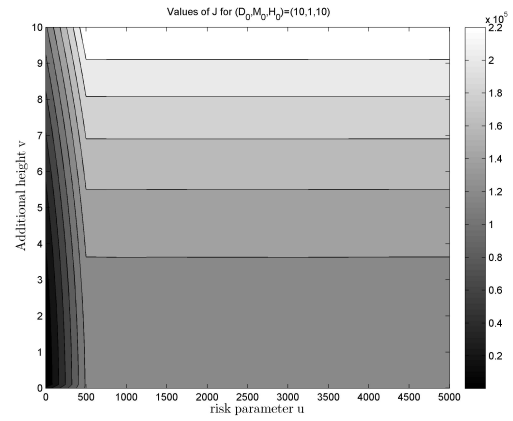
(a)  $(D_0, M_0, H_0) = (10, 1, 0)$



(b)  $(D_0, M_0, H_0) = (10, 1, 3)$

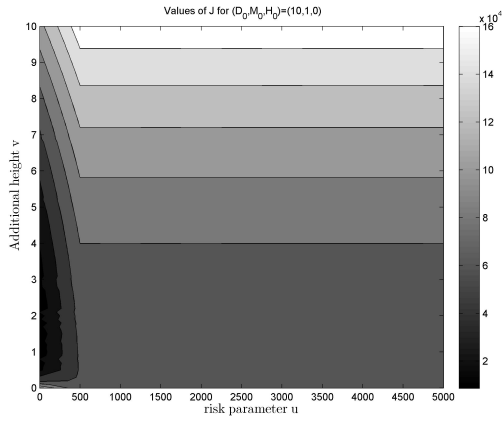


(c)  $(D_0, M_0, H_0) = (10, 1, 5)$

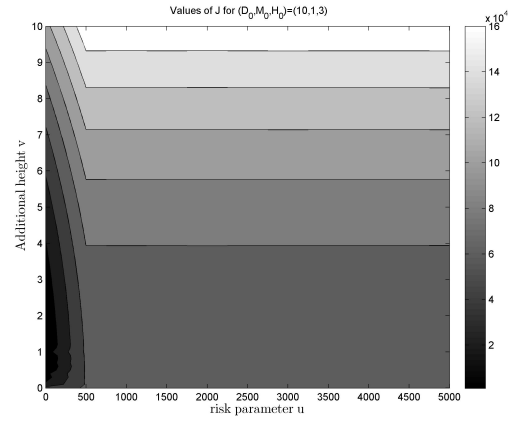


(d)  $(D_0, M_0, H_0) = (10, 1, 10)$

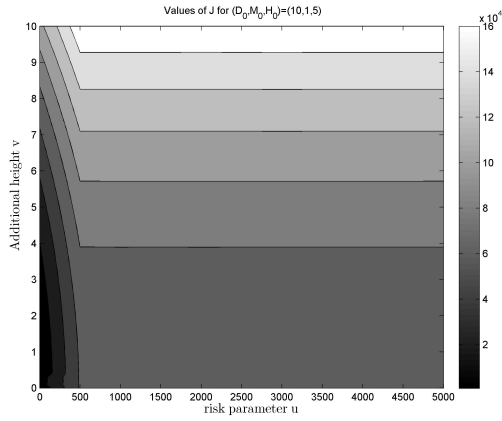
Figure 5.2: Values of  $J = \int_0^{100} e^{-rt} (\rho F(W, H, D) + C(H, v)) dt$  for  $W_2(t) = \max \{0, \gamma_1 \sin^2(kt\pi) + \gamma_2\}$  and  $\rho = 10000$



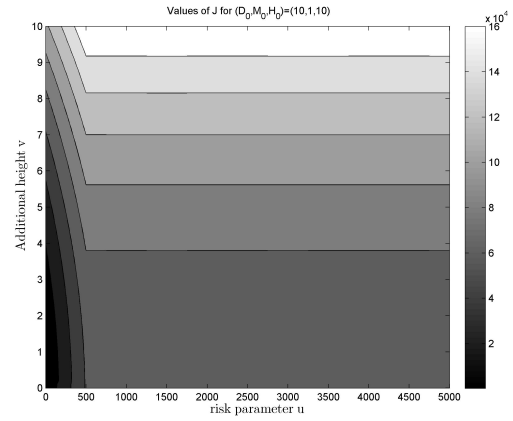
(a)  $(D_0, M_0, H_0) = (10, 1, 0)$



(b)  $(D_0, M_0, H_0) = (10, 1, 3)$

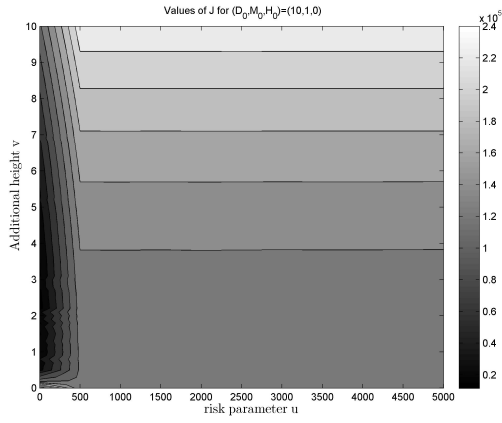


(c)  $(D_0, M_0, H_0) = (10, 1, 5)$

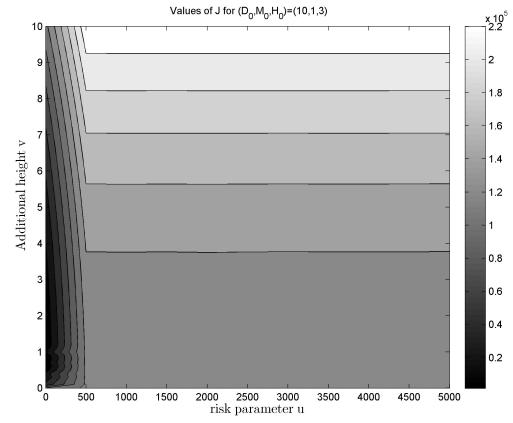


(d)  $(D_0, M_0, H_0) = (10, 1, 10)$

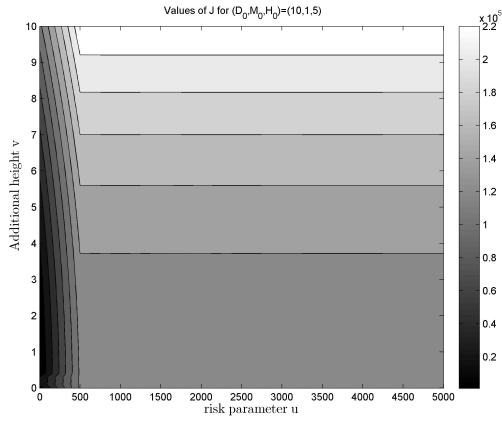
Figure 5.3: Values of  $J = \int_0^{100} e^{-rt} (\rho F(W, H, D) + C(H, v)) dt$  for  $W_3(t) = 0.5 \sum_{j=1}^{10} \cos(jt) + 1.5$  and  $\rho = 5000$



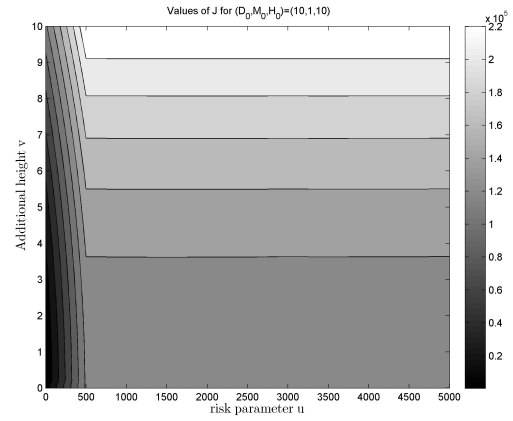
(a)  $(D_0, M_0, H_0) = (10, 1, 0)$



(b)  $(D_0, M_0, H_0) = (10, 1, 3)$



(c)  $(D_0, M_0, H_0) = (10, 1, 5)$



(d)  $(D_0, M_0, H_0) = (10, 1, 10)$

Figure 5.4: Values of  $J = \int_0^{100} e^{-rt} (\rho F(W, H, D) + C(H, v)) dt$  for  $W_3(t) = 0.5 \sum_{j=1}^{10} \cos(jt) + 1.5$  and  $\rho = 10000$

Table 5.2: Optimal decision for  $(u^*, v^*)$  if chosen at  $t = 0$ , using  $W_2$  (large-meshed)

$\rho = 5000$	$J^*$	$u^*$	$v^*$
$(D_0, M_0, H_0) = (10, 1, 0)$	1676	0.01	1.1
$(D_0, M_0, H_0) = (10, 1, 3)$	1045	0.01	0.8
$(D_0, M_0, H_0) = (10, 1, 5)$	716	0.01	0.6
$(D_0, M_0, H_0) = (10, 1, 10)$	121	0.01	0.1
$\rho = 10000$	$J^*$	$u^*$	$v^*$
$(D_0, M_0, H_0) = (10, 1, 0)$	1763	0.01	1.1
$(D_0, M_0, H_0) = (10, 1, 3)$	1084	0.01	0.8
$(D_0, M_0, H_0) = (10, 1, 5)$	754	0.01	0.6
$(D_0, M_0, H_0) = (10, 1, 10)$	162	0.01	0.1

Table 5.3: Optimal decision for  $(u^*, v^*)$  if chosen at  $t = 0$ , using  $W_3$  (large-meshed)

$\rho = 5000$	$J^*$	$u^*$	$v^*$
$(D_0, M_0, H_0) = (10, 1, 0)$	8639	0.01	2.2
$(D_0, M_0, H_0) = (10, 1, 3)$	1005	0.01	0.6
$(D_0, M_0, H_0) = (10, 1, 5)$	738	0.01	0.5
$(D_0, M_0, H_0) = (10, 1, 10)$	228	0.01	0.2
$\rho = 10000$	$J^*$	$u^*$	$v^*$
$(D_0, M_0, H_0) = (10, 1, 0)$	11459	0.01	2.2
$(D_0, M_0, H_0) = (10, 1, 3)$	1388	0.01	0.6
$(D_0, M_0, H_0) = (10, 1, 5)$	964	0.01	0.5
$(D_0, M_0, H_0) = (10, 1, 10)$	272	0.01	0.2

people have to build up the levees first. The second observation is that  $u^* = 0.01$  always holds, which is the bottom border of the range we examined for  $u$ . So the question arises if there is an optimal decision at all because maybe the best decision would be to choose  $u$  as low as possible but it must not be 0.

To obtain insights into the way, how the values of the finite integral depend on small changes in  $u$ , we repeat the calculations from before, but for a more accurate range for the additional height  $v$  from 0 to 10 m with steps of 0.01 m. Additionally, we let the risk parameter  $u$  range from 0.001 to 0.030 with steps of 0.001. A summary of these results can be found in Table (5.4) and Table (5.5), where we can find hints that  $J^*$  does not always decrease if  $u$  decreases. Nevertheless, we interpret these values  $(u^*, v^*)$  as optimal and continue with investigating the impact of the starting values.

In what follows, we compare the results not only for four cases of starting values  $(D_0, M_0, H_0)$  but rather for a wider range. In particular, we set  $M_0 = 1$  and calculate  $J^*$ , if we vary the starting height  $H_0$  between 0 and 10 m with steps of 0.5 m and the starting distance

Table 5.4: Optimal decision for  $(u^*, v^*)$  if chosen at  $t = 0$ , using  $W_2$  (fine-meshed)

$\rho = 5000$	$J^*$	$u^*$	$v^*$
$(D_0, M_0, H_0) = (10, 1, 0)$	1355	0.020	0.96
$(D_0, M_0, H_0) = (10, 1, 3)$	697	0.013	0.60
$(D_0, M_0, H_0) = (10, 1, 5)$	477	0.013	0.43
$(D_0, M_0, H_0) = (10, 1, 10)$	77	0.013	0.04
$\rho = 10000$	$J^*$	$u^*$	$v^*$
$(D_0, M_0, H_0) = (10, 1, 0)$	1469	0.020	0.96
$(D_0, M_0, H_0) = (10, 1, 3)$	771	0.013	0.60
$(D_0, M_0, H_0) = (10, 1, 5)$	538	0.006	0.45
$(D_0, M_0, H_0) = (10, 1, 10)$	118	0.013	0.05

Table 5.5: Optimal decision for  $(u^*, v^*)$  if chosen at  $t = 0$ , using  $W_3$  (fine-meshed)

$\rho = 5000$	$J^*$	$u^*$	$v^*$
$(D_0, M_0, H_0) = (10, 1, 0)$	8099	0.011	2.05
$(D_0, M_0, H_0) = (10, 1, 3)$	786	0.004	0.55
$(D_0, M_0, H_0) = (10, 1, 5)$	321	0.003	0.25
$(D_0, M_0, H_0) = (10, 1, 10)$	137	0.010	0.11
$\rho = 10000$	$J^*$	$u^*$	$v^*$
$(D_0, M_0, H_0) = (10, 1, 0)$	11111	0.011	2.05
$(D_0, M_0, H_0) = (10, 1, 3)$	1030	0.004	0.55
$(D_0, M_0, H_0) = (10, 1, 5)$	453	0.003	0.26
$(D_0, M_0, H_0) = (10, 1, 10)$	183	0.010	0.11

$D_0$  between 0 and 100000 m with steps of 5000 m. Both  $\rho = 5000$  and  $\rho = 10000$  bring qualitatively the same results, so we concentrate on the first one, see Figure (5.5).

In this figure we can see that in general values for  $J^*$  decrease when  $H_0$  is higher. This reinforces the assumption made by looking at the tables from above. However, there is an interesting fact in this figure, namely that  $J^*$  does hardly show differences when  $D_0$  varies. If we look at a fixed value for  $H_0$  and vary  $D_0$ , we do not see a monotone reaction in  $J^*$ , although there are two areas with strong local deviations. This is an interesting point, because one of the most important assumptions in this field in general is the fact, that the distance of the settlement to the river affects the economic situation of the people crucially. But our result is that, at least with constant controls for  $t = 100$ , initial distance does not affect the objective function significantly.

Finally, we want to consider the relation  $\frac{\hat{J}-J^*}{J^*}$ , if not the optimal pair of constant controls is chosen, but a pair  $(\hat{u}, \hat{v})$  with  $\hat{u} \in \{0.9u^*, 1.0u^*, 1.1u^*\}$  and  $\hat{v} \in \{0.9v^*, 1.0v^*, 1.1v^*\}$ , respectively. For each of these possible combinations we calculate the percentual changes

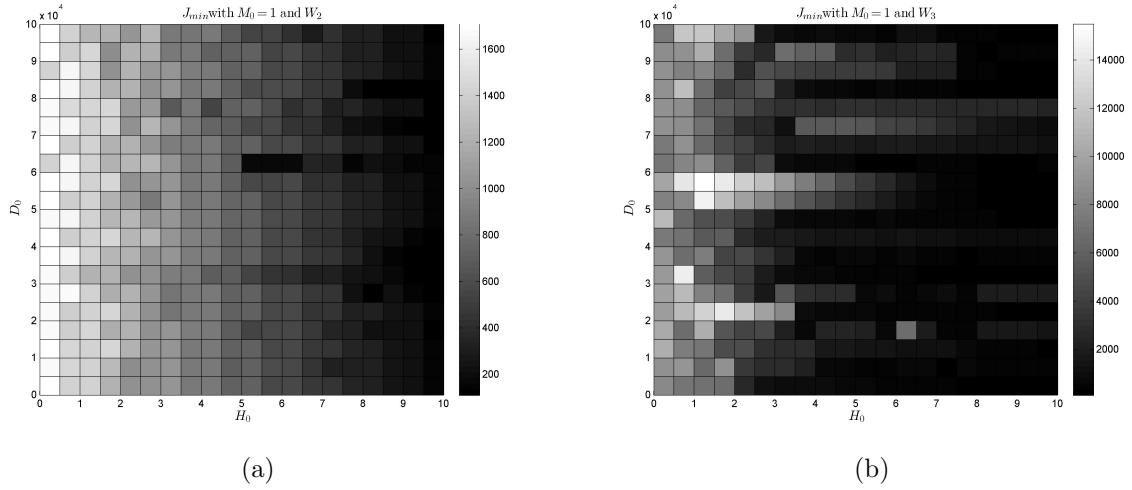


Figure 5.5: Best value for the objective function with constant controls

of the values of the objective function. We present the results for varying  $\rho$  for  $W_2$  in Tables (5.6) and (5.7), and for  $W_3$  in Tables (5.8) and (5.9), respectively.

Table 5.6: Percentual Changes  $100 \cdot \frac{\hat{J}-J^*}{J^*}$  for  $W_2 = \max\{0, \gamma_1 \sin^2(kt\pi) + \gamma_2\}$  and  $\rho = 5000$

(10, 1, 0)	$0.9v^*$	$1.0v^*$	$1.1v^*$	(10, 1, 3)	$0.9v^*$	$1.0v^*$	$1.1v^*$
$0.9u^*$	1019	755	20	$0.9u^*$	1965	1656	1283
$1.0u^*$	1017	0	296	$1.0u^*$	1964	0	1283
$1.1u^*$	1015	749	16	$1.1u^*$	1967	1656	1280
(10, 1, 5)	$0.9v^*$	$1.0v^*$	$1.1v^*$	(10, 1, 10)	$0.9v^*$	$1.0v^*$	$1.1v^*$
$0.9u^*$	2425	2049	1584	$0.9u^*$	26	16	19
$1.0u^*$	2435	0	1578	$1.0u^*$	4	0	-1
$1.1u^*$	2428	2045	1581	$1.1u^*$	21	18	18

Table 5.7: Percentual Changes  $100 \cdot \frac{\hat{J}-J^*}{J^*}$  for  $W_2 = \max\{0, \gamma_1 \sin^2(kt\pi) + \gamma_2\}$  and  $\rho = 10000$

(10, 1, 0)	$0.9v^*$	$1.0v^*$	$1.1v^*$	(10, 1, 3)	$0.9v^*$	$1.0v^*$	$1.1v^*$
$0.9u^*$	1894	1392	20	$0.9u^*$	3565	2995	2307
$1.0u^*$	1891	0	531	$1.0u^*$	3564	0	2306
$1.1u^*$	1888	1383	14	$1.1u^*$	3570	2994	2301
(10, 1, 5)	$0.9v^*$	$1.0v^*$	$1.1v^*$	(10, 1, 10)	$0.9v^*$	$1.0v^*$	$1.1v^*$
$0.9u^*$	4029	3269	2268	$0.9u^*$	28	25	24
$1.0u^*$	4036	0	11	$1.0u^*$	1	0	1
$1.1u^*$	4053	3272	2256	$1.1u^*$	24	27	27

Table 5.8: Percentual Changes  $100 \cdot \frac{j-J^*}{J^*}$  for  $W_3 = 0.5 \sum_{j=1}^{10} \cos(jt) + 1.5$  and  $\rho = 5000$

(10, 1, 0)	$0.9v^*$	$1.0v^*$	$1.1v^*$	(10, 1, 3)	$0.9v^*$	$1.0v^*$	$1.1v^*$
$0.9u^*$	90	31	139	$0.9u^*$	184	194	217
$1.0u^*$	27	0	25	$1.0u^*$	200	0	225
$1.1u^*$	120	138	71	$1.1u^*$	125	160	158
(10, 1, 5)	$0.9v^*$	$1.0v^*$	$1.1v^*$	(10, 1, 10)	$0.9v^*$	$1.0v^*$	$1.1v^*$
$0.9u^*$	950	1967	8	$0.9u^*$	5692	5372	5705
$1.0u^*$	1589	0	5	$1.0u^*$	3312	0	7
$1.1u^*$	368	3799	3455	$1.1u^*$	7135	6747	3165

Table 5.9: Percentual Changes  $100 \cdot \frac{j-J^*}{J^*}$  for  $W_3 = 0.5 \sum_{j=1}^{10} \cos(jt) + 1.5$  and  $\rho = 10000$

(10, 1, 0)	$0.9v^*$	$1.0v^*$	$1.1v^*$	(10, 1, 3)	$0.9v^*$	$1.0v^*$	$1.1v^*$
$0.9u^*$	140	45	193	$0.9u^*$	289	296	322
$1.0u^*$	48	0	28	$1.0u^*$	313	0	334
$1.1u^*$	183	200	94	$1.1u^*$	198	244	231
(10, 1, 5)	$0.9v^*$	$1.0v^*$	$1.1v^*$	(10, 1, 10)	$0.9v^*$	$1.0v^*$	$1.1v^*$
$0.9u^*$	2767	2866	11	$0.9u^*$	8524	8578	8533
$1.0u^*$	109	0	3018	$1.0u^*$	4962	0	5
$1.1u^*$	3923	5001	10	$1.1u^*$	10684	10097	4731

Looking at these tables we observe rather high numbers in most cases. Looking, for example, at Table (5.6) in the case with  $(D_0, M_0, H_0) = (10, 1, 3)$  we see that the best value for the objective function is 13 to 20 times higher if we choose the different pairs of  $(\hat{u}, \hat{v})$ . For  $(D_0, M_0, H_0) = (10, 1, 5)$  we even get values for the different objective function up to 25 times the values for the pair  $(u^*, v^*)$ . This means that in most cases the optimal value of the objective function is very sensitive to changes in the control variables. A possible explanation is that since the control variables have to be chosen constantly for 100 years, the changes of  $J^*$  take on a dramatic scale if  $u^*$  and  $v^*$  are varied. Interestingly, one negative value occurs in Table (5.6), which is obviously the result of the too large grid used for the initial conditions and makes clear that  $(u^*, v^*)$  are only close to the truly optimal levels.

Comparing the results for  $W_2$  and  $W_3$ , we see that in the first case the sensitivity of  $J^*$  increases, when  $H_0$  rises from 0 to 5, but in the case of  $H_0 = 10$  the relative differences are much smaller than in the other cases. Starting with high levees, it lasts a few years of decay of the levees until the first possible occurrence of a flooding event. This is a possible reason for the lower sensitivity in this case. A big fraction of the 100 years the additional height  $v^*$  only affects the cost function, but has no impact on the damage function because in these years there is no damage anyway. The results for  $W_3$

are different. In this case the sensitivity of  $J^*$  increases if  $H_0$  does.

Another difference in the results for the two water functions concerns  $v^*$ .  $J^*$  is more sensitive when  $v^*$  is chosen too low rather than too high in the case of  $W_2$ , whereas we do not see a unique reaction looking at  $W_3$ . Moreover, for neither water level function a unique reaction concerning the magnitude of relative differences can be observed, if  $u^*$  is chosen 10% too low or too high.

# Chapter 6

## Summary and Possible Extensions

The goal of this thesis was to analyze the mutual implications and dependences of a river and people living close to this river. For this purpose, we developed an optimal control model, based on the model by Di Baldassarre et al. in [1]. Firstly, we want to sum up the results obtained in the previous chapters.

### 6.1 Summary

In the first part of this thesis the main results and simulations of [1] by Di Baldassarre et al. were discussed. Given a stochastic time series for the water levels, functions for the damage due to floods, the additional height in that case, and a psychological shock were defined. The dynamics were given by four differential equations for the size of the city, the distance to the river, the height of the levees, and the awareness of floods. Finally, the authors provided results in the form of several simulations, which we also carried out, but with the programme MATLAB instead of R.

Based on this model, we defined an optimal control model, where the objective function contains the damage due to floods and the costs of building levees. The water level function was changed from a stochastic formulation to a deterministic one. We reduced the number of differential equations to three by defining the wealth of the community explicitly instead of in the form of a differential equation. So finally, this optimal control model consisted of the two control variables, describing the additional height of the levees and a risk parameter, and three differential equations for the state variables, namely the distance to the river, the awareness of floods, and the height of the levees.

We next carried out simulations and compared the qualitative results of using the dynamics and functions of [1] on the one hand, and using the dynamics and functions of

the optimal control model, on the other hand. In the next part we tried to improve the model by providing two new functions for the water levels, and a new function for the damage, since the steepness of the first function in the inflection point was not sufficiently high. Then again we carried out the simulations to analyze the development of our model.

Finally, we presented some preliminary steps for optimal control. A pair of control variables was calculated, which is the best constant pair until  $t = 100$ , chosen at  $t = 0$ . For each of the different water level functions, we presented the results and calculated the optimal values with varying accuracy, looking at a few different triples of starting values  $(D_0, M_0, H_0)$ . The next step was to compare the optimal values of the objective function, varying these starting values. For this purpose, we kept  $M_0$  fixed and varied the other two in certain ranges, for which we calculated the minimized objective function. Finally, we analyzed situations, in which not the optimal pair of control variables was chosen, but a pair, where both of the variables were 10% too high or too low, respectively. In these calculations, a very strong sensitivity of the objective function could be observed.

## 6.2 Possible Extensions

Although we achieved several improvements within this thesis, there seem to be many highly interesting issues, which should be taken into account in future work. We want to conclude this thesis by proposing some possible extensions:

- Obviously, the most important extension would be to actually look at the optimal control model, since we only calculated constant controls for a finite time horizon of 100 years.
- In this thesis, we mostly worked with the parameters, which Di Baldassarre et al. used in [1], because we wanted to compare the results of the two models. In future work, however, one should go through all these parameter values and see if for example the fluctuations of the water levels can have a stronger influence on the model.
- In the last chapter, where we made preliminary steps for optimal control, we concluded that the value of the objective function did not show remarkable changes, when we looked at different starting distances  $D_0$ . As already mentioned, one of the crucial assumptions in this field is the economic advantage due to the proximity to the river. Thus,  $D_0$  should play a bigger role in the model than it seemed to play throughout our simulations.

- A solution to that issue and also a possible extension could be to redefine the objective function by letting the production  $Y$  be of more importance. On the one hand, we did not consider a budget constraint, which implies unrestricted costs. On the other hand, the production  $Y$  is not considered in the objective function directly. Thus, it would be a good idea to change the objective function in this direction.

# List of Figures

1.1	The river Nile at night with Cairo at the top . . . . .	1
1.2	Levees for high water levels in Grein (Austria) in 2013 . . . . .	2
2.1	Levee building (from [8]) . . . . .	4
2.2	Additional height due to levees (from [8]) . . . . .	5
2.3	Loop diagram of the dynamics of the model in [1] . . . . .	7
2.4	The simulations in [1] with data set <i>Wevents.txt</i> . . . . .	10
3.1	Water levels $W(t)$ for $k = 0.1, 0.2, 0.3$ for two different sets of minimum and maximum water levels . . . . .	14
3.2	Damage $F(W)$ for $(\alpha_H, \zeta_H) = (0.01, 0.5)$ for $H = 1$ and $H = 5$ for different values of $D$ . . . . .	17
3.3	Damage $F(t)$ for different sets of parameters . . . . .	18
3.4	Adding height $v$ to the levees . . . . .	19
3.5	The evolution of $H(t)$ . . . . .	23
3.6	The simulations with $W(t) = \gamma_1 \sin^2(kt\pi) + \gamma_2$ and $\kappa_T = 0.003$ . . . . .	27
3.7	The simulations with $W(t) = \gamma_1 \sin^2(kt\pi) + \gamma_2$ and $\kappa_T = 0.0003$ . . . . .	28
3.8	Simulations of the system of differential equations for $(D_0, M_0, H_0) = (1, 0, 0)$	30
3.9	Simulations of the system of differential equations for $(D_0, M_0, H_0) = (1, 0, 3)$	31
3.10	Simulations of the system of differential equations for $(D_0, M_0, H_0) = (1, 0, 5)$	32
3.11	Simulations of the system of differential equations for $(D_0, M_0, H_0) = (1, 0, 10)$ . . . . .	33
4.1	$W_2(t) = \max \{0, \gamma_1 \sin^2(kt\pi) + \gamma_2\}$ . . . . .	37
4.2	$W_3(t) = 0.5 \sum_{j=1}^{10} \cos(jt) + 1.5$ . . . . .	38
4.3	Damage function $F_2(W, H, D)$ for $\zeta_H = 0.5$ , $\alpha_H = 0.01$ , $D = 10$ , and different values for $c$ and $H$ . . . . .	40
4.4	The simulations with $W_2(t) = \max \{0, \gamma_1 \sin^2(kt\pi) + \gamma_2\}$ and $\kappa_T = 0.0003$	42
4.5	The simulations with $W_2(t) = \max \{0, \gamma_1 \sin^2(kt\pi) + \gamma_2\}$ and $\kappa_T = 0.003$ .	43
4.6	The simulations with $W_3(t) = 0.5 \sum_{j=1}^{10} \cos(jt) + 1.5$ . . . . .	45
4.7	The simulations of the uncontrolled system for $(D_0, M_0, H_0) = (1, 0, 0)$ for $W_2(t) = \max \{0, \gamma_1 \sin^2(kt\pi) + \gamma_2\}$ . . . . .	47
4.8	The simulations of the uncontrolled system for $(D_0, M_0, H_0) = (1, 0, 3)$ for $W_2(t) = \max \{0, \gamma_1 \sin^2(kt\pi) + \gamma_2\}$ . . . . .	48
4.9	The simulations of the uncontrolled system for $(D_0, M_0, H_0) = (1, 0, 5)$ for $W_2(t) = \max \{0, \gamma_1 \sin^2(kt\pi) + \gamma_2\}$ . . . . .	49
4.10	The simulations of the uncontrolled system for $(D_0, M_0, H_0) = (1, 0, 10)$ for $W_2(t) = \max \{0, \gamma_1 \sin^2(kt\pi) + \gamma_2\}$ . . . . .	50

4.11	The simulations of the uncontrolled system for $(D_0, M_0, H_0) = (1, 0, 0)$ for $W_3(t) = 0.5 \sum_{j=1}^{10} \cos(jt) + 1.5$ . . . . .	51
4.12	The simulations of the uncontrolled system for $(D_0, M_0, H_0) = (1, 0, 3)$ for $W_3(t) = 0.5 \sum_{j=1}^{10} \cos(jt) + 1.5$ . . . . .	52
4.13	The simulations of the uncontrolled system for $(D_0, M_0, H_0) = (1, 0, 5)$ for $W_3(t) = 0.5 \sum_{j=1}^{10} \cos(jt) + 1.5$ . . . . .	53
4.14	The simulations of the uncontrolled system for $(D_0, M_0, H_0) = (1, 0, 10)$ for $W_3(t) = 0.5 \sum_{j=1}^{10} \cos(jt) + 1.5$ . . . . .	54
5.1	Values of $J = \int_0^{100} e^{-rt} (\rho F(W, H, D) + C(H, v)) dt$ for $W_2(t) = \max \{0, \gamma_1 \sin^2(kt\pi) + \gamma_2\}$ and $\rho = 5000$ . . . . .	57
5.2	Values of $J = \int_0^{100} e^{-rt} (\rho F(W, H, D) + C(H, v)) dt$ for $W_2(t) = \max \{0, \gamma_1 \sin^2(kt\pi) + \gamma_2\}$ and $\rho = 10000$ . . . . .	58
5.3	Values of $J = \int_0^{100} e^{-rt} (\rho F(W, H, D) + C(H, v)) dt$ for $W_3(t) = 0.5 \sum_{j=1}^{10} \cos(jt) + 1.5$ and $\rho = 5000$ . . . . .	59
5.4	Values of $J = \int_0^{100} e^{-rt} (\rho F(W, H, D) + C(H, v)) dt$ for $W_3(t) = 0.5 \sum_{j=1}^{10} \cos(jt) + 1.5$ and $\rho = 10000$ . . . . .	60
5.5	Best value for the objective function with constant controls . . . . .	63

# List of Tables

2.1	Model parameters in [1] . . . . .	9
2.2	Data-set <i>Wevents.txt</i> . . . . .	11
3.1	Model parameters for Chapter 3 . . . . .	34
5.1	Model parameters . . . . .	56
5.2	Optimal decision for $(u^*, v^*)$ if chosen at $t = 0$ , using $W_2$ (large-meshed) .	61
5.3	Optimal decision for $(u^*, v^*)$ if chosen at $t = 0$ , using $W_3$ (large-meshed) .	61
5.4	Optimal decision for $(u^*, v^*)$ if chosen at $t = 0$ , using $W_2$ (fine-meshed) .	62
5.5	Optimal decision for $(u^*, v^*)$ if chosen at $t = 0$ , using $W_3$ (fine-meshed) .	62
5.6	Percentual Changes $100 \cdot \frac{\hat{j}-J^*}{J^*}$ for $W_2 = \max \{0, \gamma_1 \sin^2(kt\pi) + \gamma_2\}$ and $\rho = 5000$ . . . . .	63
5.7	Percentual Changes $100 \cdot \frac{\hat{j}-J^*}{J^*}$ for $W_2 = \max \{0, \gamma_1 \sin^2(kt\pi) + \gamma_2\}$ and $\rho = 10000$ . . . . .	63
5.8	Percentual Changes $100 \cdot \frac{\hat{j}-J^*}{J^*}$ for $W_3 = 0.5 \sum_{j=1}^{10} \cos(jt) + 1.5$ and $\rho = 5000$	64
5.9	Percentual Changes $100 \cdot \frac{\hat{j}-J^*}{J^*}$ for $W_3 = 0.5 \sum_{j=1}^{10} \cos(jt) + 1.5$ and $\rho = 10000$	64

# References

- [1] Di Baldassarre G., Viglione A., Carr G., Kuil L., Salinas J.L. and Blöschl G. *Socio-hydrology: conceptualising human-flood interactions*. *Hydrology and Earth System Sciences*, 17(8):3234–3244, 2013.
- [2] Schultz J. and Elliot J. *Natural disasters and local demographic change in the United States*. *Population and Environment*, 34(3):293–312, 2012.
- [3] White, G.F. *Human Adjustment to Floods: A Geographical Approach to the Flood Problem in the United States*. Research paper. University of Chicago, 1945.
- [4] Di Baldassarre G., Castellarin A. and Brath A. *Analysis on the effects of levee heightening on flood propagation: Example of the River Po, Italy*. *Hydrological Sciences Journal*, 54(6):1007–1017, 2009.
- [5] Remo J., Megan C. and Pinter N. *Hydraulic and flood-loss modeling of levee, floodplain, and river management strategies, Middle Mississippi River, USA*. *Natural Hazards*, 61(2):551–575, 2012.
- [6] Heine R. and Pinter N. *Levee effects upon flood levels: an empirical assessment*. *Hydrological Processes*, 26(21):3225–3240, 2012.
- [7] Sivapalan M., Savenije H.H. and Blöschl G. *Socio-Hydrology: a new science of people and water*. *Hydrological Processes*, 26(8):1270–1276, 2012.
- [8] Di Baldassarre G., Kooy M., Kemerink J.S. and Brandimarte L. *Towards understanding the dynamics behaviour of floodplains as human-water systems*. *Hydrology and Earth System Sciences*, 17(6):3255–3303, 2013.
- [9] Werner B. and McNamara D. *Dynamics of coupled human-landscape systems*. *Geomorphology*, 91(3-4):393–407, 2007.
- [10] Chahim M., Brekelmans R., den Hertog D. and Kort P. *An impulse control approach to dike height optimization*. *Optimization Methods and Software*, 28(3):458–477, 2013.